JAERI - M
90-046

EVALUATION REPORT ON SCTF CORE-III TEST S3-9

(INVESTIGATION OF CCTF COUPLING TEST RESULTS UNDER AN EVALUATION MODEL CONDITION IN PWRS WITH COLD-LEG-INJECTION-TYPE ECCS)

March 1990

Tsutomu OKUBO, Tadashi IGUCHI, Takamichi IWAMURA
Hajime AKIMOTO, Akira OHNUKI, Yutaka ABE
Isao SAKAKI*, Hiromichi ADACHI and Yoshio MURAO

日本原子力研究所
Japan Atomic Energy Research Institute

JAERI-Mレポートは，日本原子力研究所が不定期に公刊している研究報告書です。
入手の問合わせは，日本原子力研究所技術情報部情報資料課（〒319-11茨城県那珂郡東海村）あて，お申しこしください。なお，このほかに財団法人原子力弘済会資料センター（〒319-11 茨城県那珂郡東海村日本原子力研究所内）で複写による実費頒布をおこなっております。

JAERI-M reports are issued irregularly.
Inquiries about availability of the reports should be addressed to Information Division, Department of Technical Information, Japan Atomic Energy Research Institute, Tokai-mura, Naka-gun, Ibaraki-ken 319-11, Japan.

編集兼発行　日本原子力研究所
印　　刷　㈱原子力資料サービス

JAERI-M 90-046

Evaluation Report on SCTF Core-III Test S3-9

(Investigation of CCTF Coupling Test Results under an Evaluation Model Condition in PWRs with Cold-leg-injection-type ECCS)

Tsutomu OKUBO, Tadashi IGUCHI, Takamichi IWAMURA
Hajime AKIMOTO, Akira OHNUKI, Yutaka ABE
Isao SAKAKI*, Hiromichi ADACHI and Yoshio MURAO

Department of Reactor Engineering
Tokai Research Establishment
Japan Atomic Energy Research Institute
Tokai-mura, Naka-gun, Ibaraki-ken

(Received February 5, 1990)

In order to obtain the data of the reflooding behavior in a wide core under an Evaluation Model (EM) condition for a Pressurized Water Rector (PWR) with a cold-leg-injection-type Emergency Core Cooling System (ECCS), a test was performed with the Slab Core Test Facility (SCTF) Core-III, which has the same radial width as the radius of a 1,000 MWe class PWR. The test was named Test S3-9. The experimental data of the present test were supposed to be used for an experimental coupling between the SCTF and the Upper Plenum Test Facility (UPTF) of FRG, which is a full scale facility but without the heated core, based on the 2D/3D Agreement, *i.e.* an international cooperation among FRG, the USA and Japan. Major core initial and boundary conditions for the test were determined based on the test results of Cylindrical Core Test Facility (CCTF) Test C2-4, which is the base case test for the CCTF test series and was performed under an EM condition for a PWR with a cold-leg-injection-type ECCS. Therefore, the present test is also a coupling test between the SCTF and the CCTF under an EM condition.

---

* Toshiba, Ltd.

In the present report, the difference in the reflooding behavior between the SCTF and the CCTF is mainly investigated by comparing the experimental data from those two tests. Major conclusions obtained are as in the following:

(1) Test S3-9 was successfully completed under an EM condition. Tie plate mass flow rate data were obtained and can be used for an experimental coupling with the UPTF.

(2) The overall core cooling behavior observed in Test S3-9 was nearly the same as that observed in CCTF Test C2-4.

(3) However, the core differential pressure characteristic observed in Test S3-9 was somewhat different from that observed in Test C2-4. Main reasons for the difference are almost explained to be different core inlet water subcooling between the two tests and the different effective core flow area between two facilities.

(4) The core two-dimensional behavior observed in Test S3-9 had the same characteristic as observed in the other tests with the SCTF Core-II.

Keywords: Reactor Safety, PWR, LOCA, ECCS, Reflood Experiments, Two-phase Flow, Heat Transfer, Thermo-hydrodynamics, SCTF

SCTF第3次炉心試験S3－9評価報告書
(コールドレグ注水型ECCS付PWRの評価モデル条件下でのCCTF結合試験結果の検討)

日本原子力研究所東海研究所原子炉工学部
大久保　努・井口　正・岩村　公道・秋本　肇
大貫　晃・阿部　豊・榊　勲*・安達　公道
村尾　良夫

（1990年2月5日受理）

コールドレグ注水型非常用炉心冷却系（ECCS）付加圧水型原子炉（PWR）に対する評価モデル（EM）条件下に於ける広い炉心内の再冠水データを得る為に，1000MWe級PWRの半径と同じ半径方向長さを有する平板炉心試験装置（SCTF）第3次炉心を用いて試験を実施した。本試験は試験S3－9と名付けられた。本試験のデータは，西ドイツ，アメリカ合衆国および日本の間の国際協力である2D／3D協定に基づき，SCTFと西ドイツの上部プレナム試験装置（UPTF）との間の実験的結合に用いられる事になっていた。本試験の炉心の主要な初期および境界条件は，円筒炉心試験装置（CCTF）による試験C2－4の試験結果に基づいて決定された。試験C2－4は，CCTF試験シリーズの基準試験であり，コールドレグ注水型ECCS付PWRに対するEM条件下で実施された試験である。従って，本試験はEM条件下におけるSCTFとCCTFの間の結合試験にもなっている。

本報告書では，この2つの試験の実験データの比較により，SCTFとCCTFの間の再冠水挙動の差を主として検討した。得られた主要な結論は以下の通りである。

(1) 試験S3－9はEM条件下で成功裏に実施された。これにより，タイプレート流量データが取得され，UPTFとの実験的結合に用いることが可能である。

(2) 試験S3－9でみられた全体的な炉心冷却挙動は，CCTF試験C2－4のそれとほぼ同一であった。

(3) しかし，試験S3－9でみられた炉心差圧の特徴は，試験C2－4でみられたものと多少異なっていた。この相違の理由は，両試験の間で炉心入口サブクーリングが異なっていた事と両試験装置の間で炉心の実効流路面積が異なっている事であるとしてほぼ説明できた。

(4) 試験S3－9でみられた炉心の2次元挙動は，SCTF第2次炉心でみられたのと同じ特徴を示していた。

東海研究所：〒319－11 茨城県那珂郡東海村白方字白根2－4
*（株）東芝

目　　次

Contents

List of Tables

List of Figures

1. Introduction

The Slab Core Test Facility (SCTF) test program is a part of the large scale reflood test program[1] together with the Cylindrical Core Test Facility (CCTF) test program, which are performed by Japan Atomic Energy Research Institute (JAERI) under a contract with Atomic Energy Bureau of Science and Technology Agency of Japan. The SCTF test program is also one of the research activities based on a trilateral agreement (*i.e.* 2D/3D Agreement) among JAERI, the United States Nuclear Regulatory Commission (USNRC) and the Federal Minister for Research and Technology (BMFT) of Federal Republic of Germany (FRG).

There are three test series (Core-I, -II and -III) in the SCTF test program. The SCTF Core-I[2] and Core-II[3] test series were already performed mainly to investigate two-dimensional thermal hydraulic behavior in the core during the reflood phase of a loss-of-coolant accident (LOCA) of a Westinghouse type pressurized water reactor (denoted US/J PWR) with the cold-leg-injection-type emergency core cooling system (ECCS). On the other hand, one of the major objectives of the SCTF Core-III[4] test series was to investigate the effectiveness of the combined-injection-type ECCS in a German type PWR (denoted GPWR). In addition, simulation tests for a US/J PWR were also performed with the SCTF Core-III.

In order to obtain the data for the reflood phenomena in the wide core of a US/J PWR, a test was conducted with the SCTF Core-III under an Evaluation Model (EM) condition. This test was named Test S3-9 (Run 713). The data of the test, especially the tie plate mass flow rates were supposed to be used for an experimental coupling with the Upper Plenum Test Facility (UPTF) in FRG based on the 2D/3D Agreement. Major core initial and boundary conditions of the test were determined based on the results of CCTF Test C2-4[5], which was also conducted under an EM condition. Therefore, the present test is also a coupling test between the SCTF and the CCTF under an EM condition.

This report describes the major results of the present test and the discussion on the difference between the SCTF and the CCTF. A brief description of the SCTF Core-III is presented in Appendix A. Also, some selected data obtained in Test S3-9 are presented in Appendix B for better understanding of the test.

Brief information on the test is presented in the following:

(1) Test name

US/J PWR simulation integral EM Test

where, US/J PWR : PWR of the USA and Japan with cold-leg-injection-type ECCS

EM : Evaluation model

(2) Test number

S3-9 (Run 713)

where, S : SCTF

3 : Core-III

9 : Sequential number of the main test

(3) Objectives of test

i) To investigate the difference in the reflooding phenomena between the SCTF and the CCTF under an EM condition of a US/J PWR

ii) To obtain data for experimental coupling with the UPTF of FRG

(4) Type of test

Refill and reflood integral test for a US/J PWR under an EM condition.

2. Test Description

2.1 Test Facility[4]

The SCTF was originally designed to study two-dimensional effects on thermal hydraulics during the reflood phase in the PWR core with full length radius[2],[3].

A flow diagram of the SCTF is shown in Fig. 2.1. The SCTF is simulating a 200% cold-leg-large-break with a simplified primary system and can be operated at the system pressure less than 0.6 MPa. It consists of a pressure vessel, a combined intact loop, a broken loop at the pressure vessel side, and a broken loop at the steam-water separator side.

Figure 2.2 shows a vertical cross section of the pressure vessel. The pressure vessel includes a simulated core, an upper plenum with its internals, a lower plenum, a core baffle region and a downcomer. The configurations of the upper plenum structure and the end box simulate those of a 1,300 MWe class GPWR as practically as possible.

The core is full-height, full-radius and one-bundle width one. The core flow area scaling ratio is 1/21.4 to a typical 1,000 MWe class US/J PWR. 1,888 electrical heater rods are installed in the core to simulate fuel rods. Dimensions of a heater rod is 10.7 mm in diameter and 3,613 mm in heated length, simulating those of PWRs. The maximum available power supplied to the core is 10 MW.

The heater rods are assembled in a 16 x 16 square array bundle being positioned with grid spacers. Eight bundles are installed in a row in the core, as shown in Fig. 2.2. In the SCTF, the leftmost bundle in the figure is named Bundle 1 and orderly to the right direction the bundles are named Bundle 2, 3, ..., 8. Since the downcomer and the hot leg are connected to the Bundle 8 side, the Bundle 1 and 8 sides are corresponding to the central and the peripheral sides of PWRs, respectively.

The ECC water can be injected into the lower plenum, the cold leg and the upper plenum in the SCTF. The core and the upper plenum are enveloped by honeycomb thermal insulators with wall plates to minimize the wall thermal effects. Description of the SCTF Core-III is presented more in detail in Appendix A.

2.2 Test Conditions and Sequence

Test conditions were selected to simulate the refill and reflood phenomena under an EM condition for a US/J PWR 200% cold-leg-large-break LOCA. The bases for the test conditions are mainly the results of CCTF Test C2-4[5], which is an integral test performed under an EM condition with the CCTF, and are summarized in Sec. 2.3. Table 2.1 shows the planned and the measured test conditions.

Figure 2.3 shows the conceptual initial set-up of the facility for Test S3-9. The ECC water was injected into the lower plenum instead of the cold leg. This is because the core flooding rate for the present test was intended to be the same as that in CCTF Test C2-4 as closely as possible.

Orifice diameters for the steam-water separator side broken cold leg, the intact cold leg and the pump simulator were 86.4, 179.9 and 173.7 mm, respectively, and were the same as in SCTF Core-I and II tests. No orifice was inserted in the pressure vessel side broken cold leg. Water in the steam-water separator was set to be drained to containment tank 2 to keep the maximum water level in steam-water separator at 1.1 m.

Figure 2.4 shows sequence of Test S3-9. In this figure, the time when the maximum clad temperature reached 700 ^{o}C is defined as 0 s. Pressure in the containment tank 2 was kept constant at 0.2 MPa by controlling discharge rate of steam through the blow valve to the atmosphere after 0 s. ECC water was started to be injected into the lower plenum 8 s before 0 s. Water temperature for this was set to be 80 ^{o}C up to 28 s and 120 ^{o}C thereafter. Core power was initially set at 9.35 MW and was decreased to simulate decay as shown in Fig. 2.4.

2.3 Bases for Test Conditions

Bases for test conditions are summarized in Table 2.2. A brief explanation is as follows:

(1) Pressure

Pressures in the pressure vessel and the containment tank 2 was initially set at 0.2 MPa and was intended to be kept constant during the reflood phase. They were selected to be the same pressure conditions as in CCTF Test C2-4.

(2) Initial core power

Initial total core power for the present test was determined to be the same as in CCTF Test C2-4 and was set to be 9.35 MW.

(3) Power profile

Radial power ratio in the present test was determined to simulate that in SCTF Core-II steep power profile test (Test S2-6[6]). They are 1.0 : 1.2 : 1.0 : 0.8 for Bundles 1 and 2, 3 and 4, 5 and 6, and 7 and 8.

(4) Initial clad temperature

Initial clad temperature of the present test was determined to simulate the same stored energy in rods as that in CCTF Test C2-4. The maximum clad temperature of Test C2-4 was 1073 K at reflood initiation (*i.e.* BOCREC). Since the radial and the axial peaking factors were 1.36 and 1.40 in the test, the average temperature at BOCREC was estimated as follows:

$$(1073 - 393)/1.36/1.40 + 393 = 750 \text{ (K)}$$

In order to simulate the same stored energy in the present test, a correction due to the difference in heater rod number (*i.e.* 1888 for SCTF *vs.* 1824 for CCTF) should be considered as follows:

$$(750 - 393) \times \frac{1824}{1888} + 393 = 738 \text{ (K)}$$

Taking account of the radial and the axial peaking factor for the present test, 1.20 and 1.40, respectively, the maximum clad temperature at BOCREC for the present test was obtained as follows:

$$(718 - 393) \times 1.2 \times 1.4 + 393 = 973 \text{ (K)}$$

(5) ECC injection rate and temperature

ECC water injection rate ($\dot{m}_{ECC}$) for the present test was intended to be set to achieve the same core flooding rate ($\dot{m}_F$) as that in CCTF Test C2-4. Since ECC water injection into the lower plenum accumulates in the downcomer as well as the core, ECC water injection rate was set to be larger than the aimed core flooding rate as follows:

(i) Period 1 (0 ~ 5 s)

In this period, steam binding effect is negligible, and hence,

core flooding rate is expected to be

$$\dot{m}_F = A_{core} / (A_{core} + A_{downcomer}) \times \dot{m}_{ECC}$$
$$= 0.6\ \dot{m}_{ECC} \quad (1)$$

(ii) Period 2 (5 s ~ time when the downcomer water level reaches the balanced level)

In this period, it was observed in the SCTF Core-II test that the ratio among core flooding rate ($\dot{m}_F$), water accumulation rates in the downcomer ($\dot{m}_{DC}$) and the core baffle region ($\dot{m}_{CB}$) was

$$\dot{m}_F : \dot{m}_{DC} : \dot{m}_{CB} = 4 : 3 : 1$$

In the SCTF Core-III, the downcomer flow area is larger by 30 % and a flow path between the bottom of the core baffle and the core was plugged. Therefore, the ratio was roughly expected to be

$$\dot{m}_F : \dot{m}_{DC} = 4 : (3 \times 1.3) \approx 1 : 1$$

Accordingly,

$$\dot{m}_F \approx 0.5\ \dot{m}_{ECC} \quad (2)$$

(iii) Period 3 (after downcomer water level reaches the balanced level)

$$\dot{m}_F \approx \dot{m}_{ECC} \quad (3)$$

By using above relation (Eqs. (1), (2), and (3)), the ECC water injection rate for the present test was determined and is plotted in Fig. 2.5 in comparison with the aimed core flooding rate, which is a simplified curve for Test C2-4.

(6) Initial water temperature and level in the lower plenum

Initial water temperature in the lower plenum was the saturation temperature (393 K) as in the almost CCTF and SCTF tests. Initial water level was determined considering that the saturated lower plenum water be delivered to the core during initial 20 s after BOCREC prior to the subsequent delivery of the subcooled ECC water to the core.

2.4 Measured Boundary Conditions

Major measured test conditions are listed in Table 2.1. Table 2.3 shows the chronology of events occurred during the test. Figures 2.6 to 2.9 show the measured boundary conditions of the test.

Table 2.1 Major conditions for Test S3-9

Item		Planned	Measured
Pressure (MPa)			
Containment		0.2	0.2∿0.22
Pressure vessl		0.2	0.2∿0.25
Power			
Initial value	(MW)	9.35	9.32
Decay curve		ANS×1.2+Actinide×1.1	
Radial profile		1.0:1.2:1.0:0.8	1.0:1.2:1.0:0.8
Peak clad temperature (K)			
At ECC injection initiation		933	959.1
At BOCREC		973	1018
ECC water injection			
Location		Lower plenum	
Injection rate	(kg/s)	37→3.75	40→4.28
Temperature	(K)	353→393	376∿390

Table 2.2 Summary of bases of test conditions

Item		Condition	Basis
1	Containment pressure	0.2 MPa	(*1)
2	Initial system pressure	0.2 MPa	(*1)
3	Initial metal wall temperature	393 K	(*1)
4	Loop orifice size Broken cold leg (PV side) Broken cold leg (S/W side) Intact cold leg Pump simulator	 No orifice 86.4 mm 179.9 mm 173.7 mm	The same as in SCTF-I and -II
5	Initial lower plenum water temperature	393 K	Saturation temperature (T_{sat})
6	Initial lower plenum water level	1.2 m	Delivery of T_{sat} water for initial 20 S
7	Initial total core power	9.35 MW	(*1)
8	Power decay curve	ANS×1.2+Actinide×1.1 (30 s after scram)	(*1)
9	Power profile	1.0:1.2:1.0:0.8	SCTF Test S2-06
10	Maximum clad temperature at reflood initiation	973 K	
11	ECC injection rate	Follow $\dot{m}_F$ (*2) and T_F (*3) of CCTF Test C2-4	(*1)

Notes: (*1) The same as in CCTF Test C2-4

(*2) $\dot{m}_F$: Core inlet mass flow rate

(*3) T_F : Core inlet fluid temperature

Table 2.3 Chronology of events for Test S3-9

Item	Time (s)
Core power "ON"	0
ECC water injection initiation	74
Core power decay initiation	82
BOCREC	83
Whole core quench	723

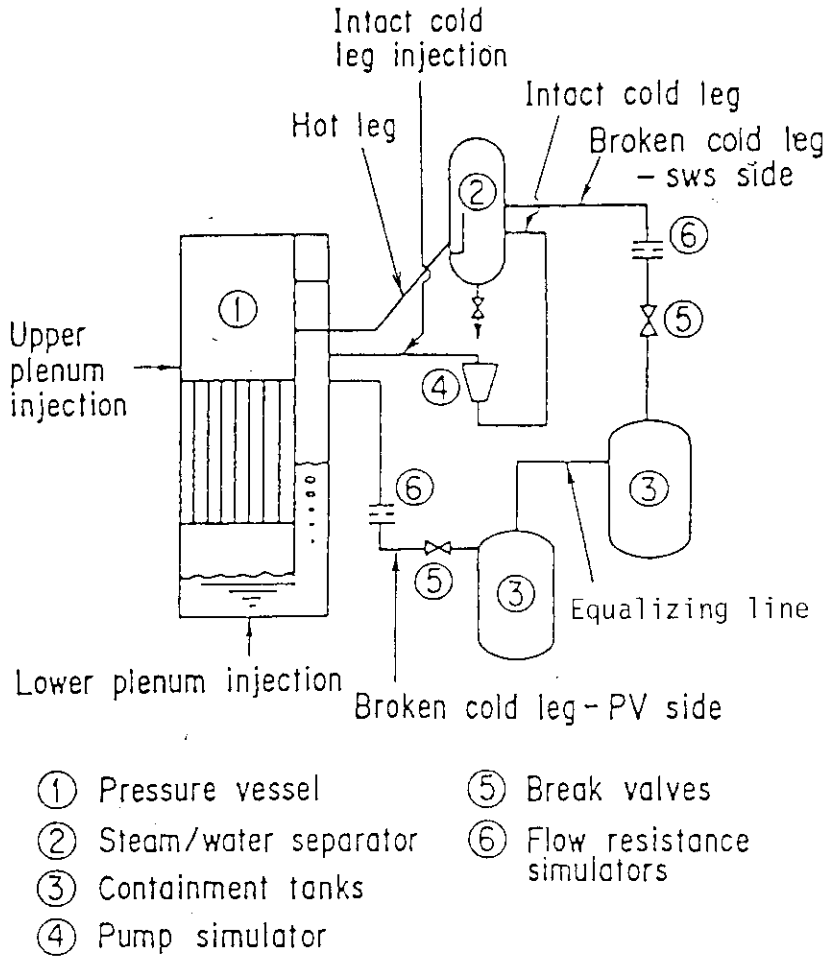

Fig. 2.1 Flow diagram of SCTF

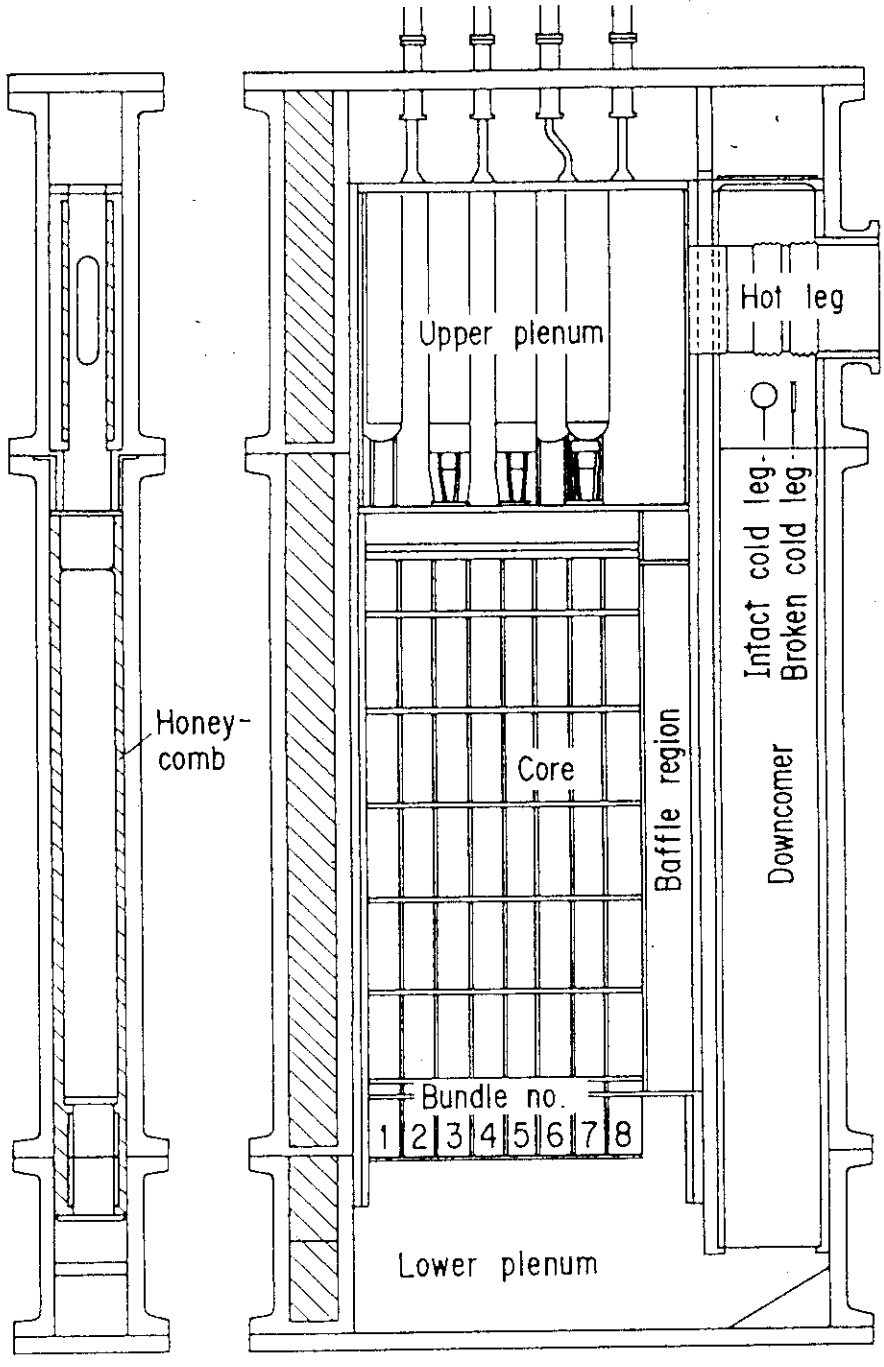

Fig. 2.2 Vertical cross section of pressure vessel

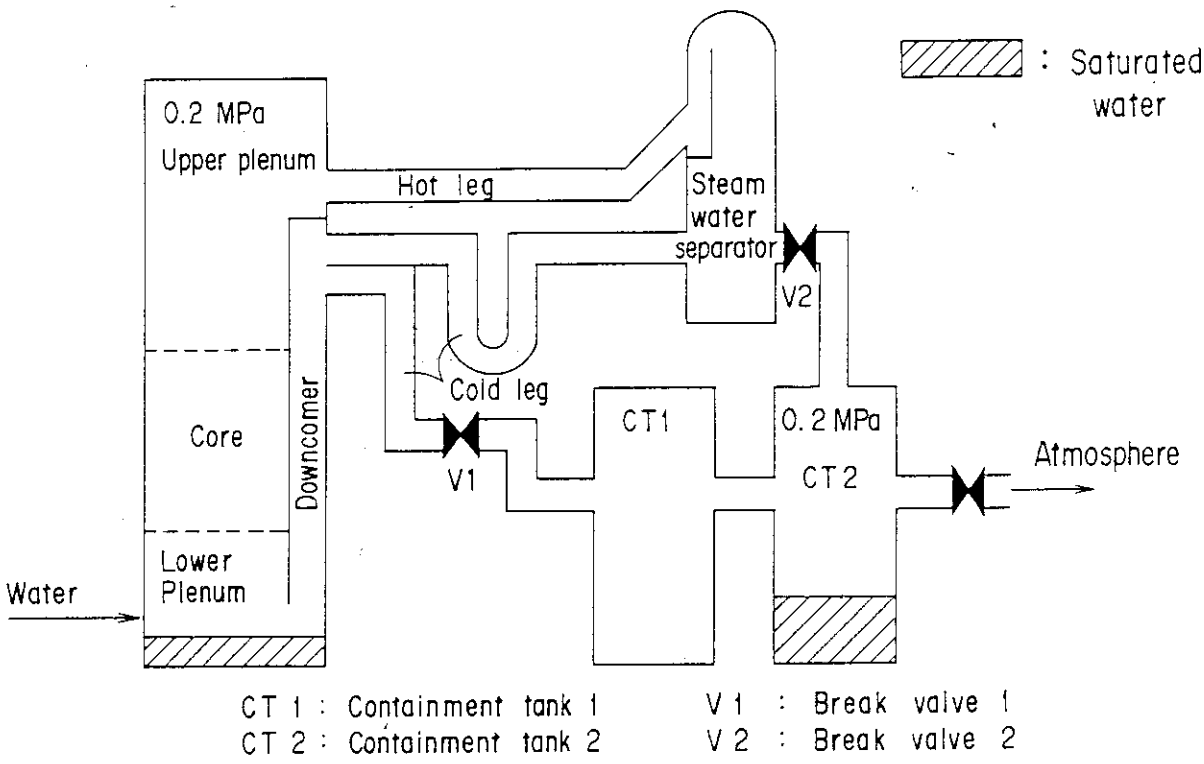

Fig. 2.3 Initial set-up of Test S3-9

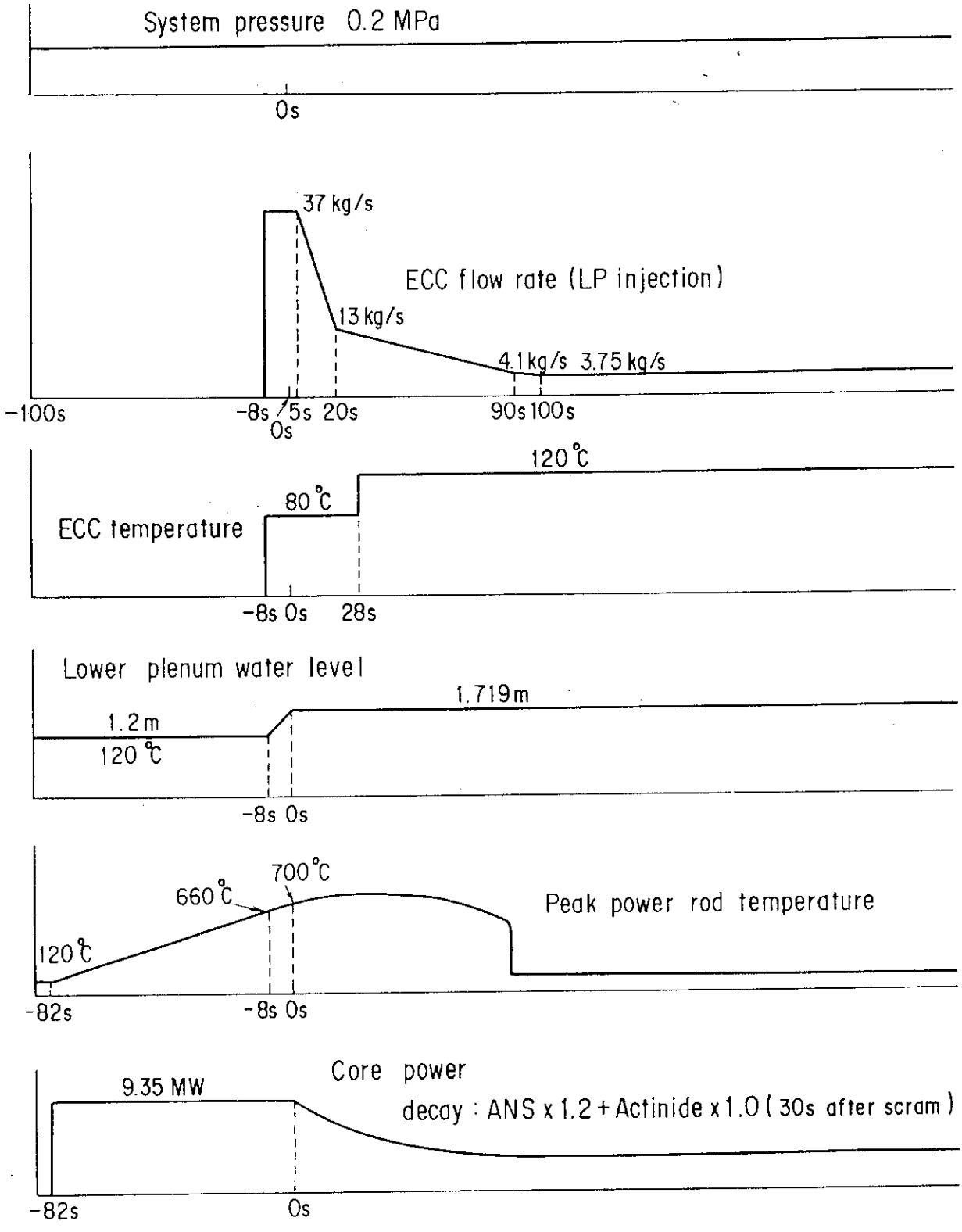

Fig. 2.4 Sequence for Test S3-9

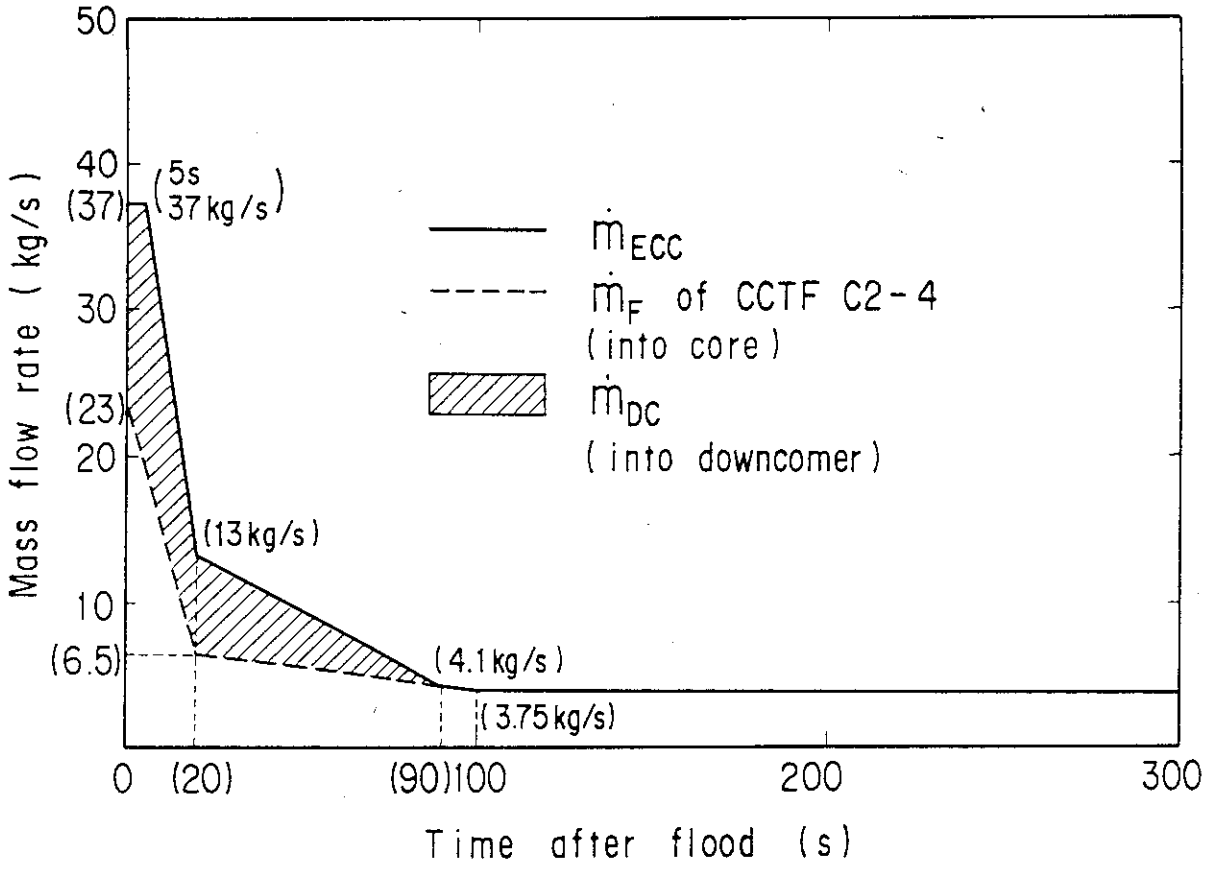

Fig. 2.5 Planned ECC water injection rate and core flooding rate

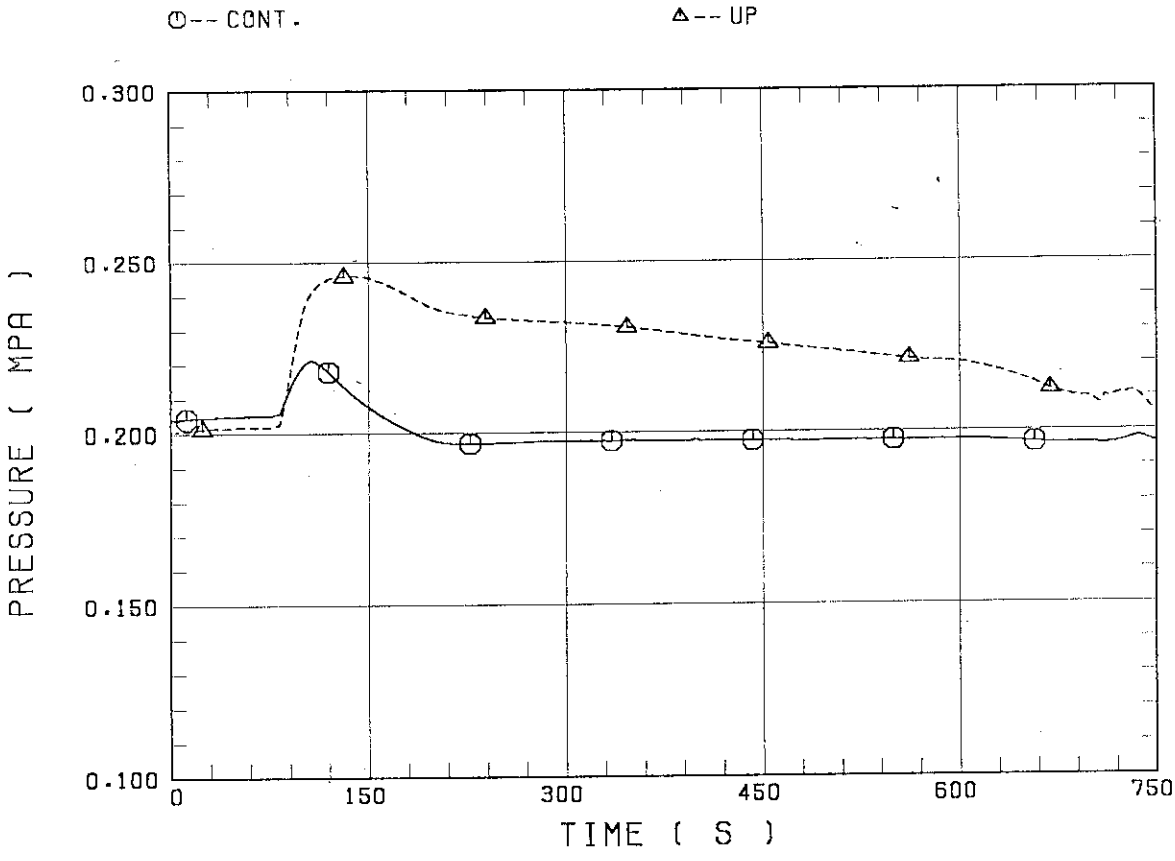

Fig. 2.6 Pressures of containment tank II and upper plenum

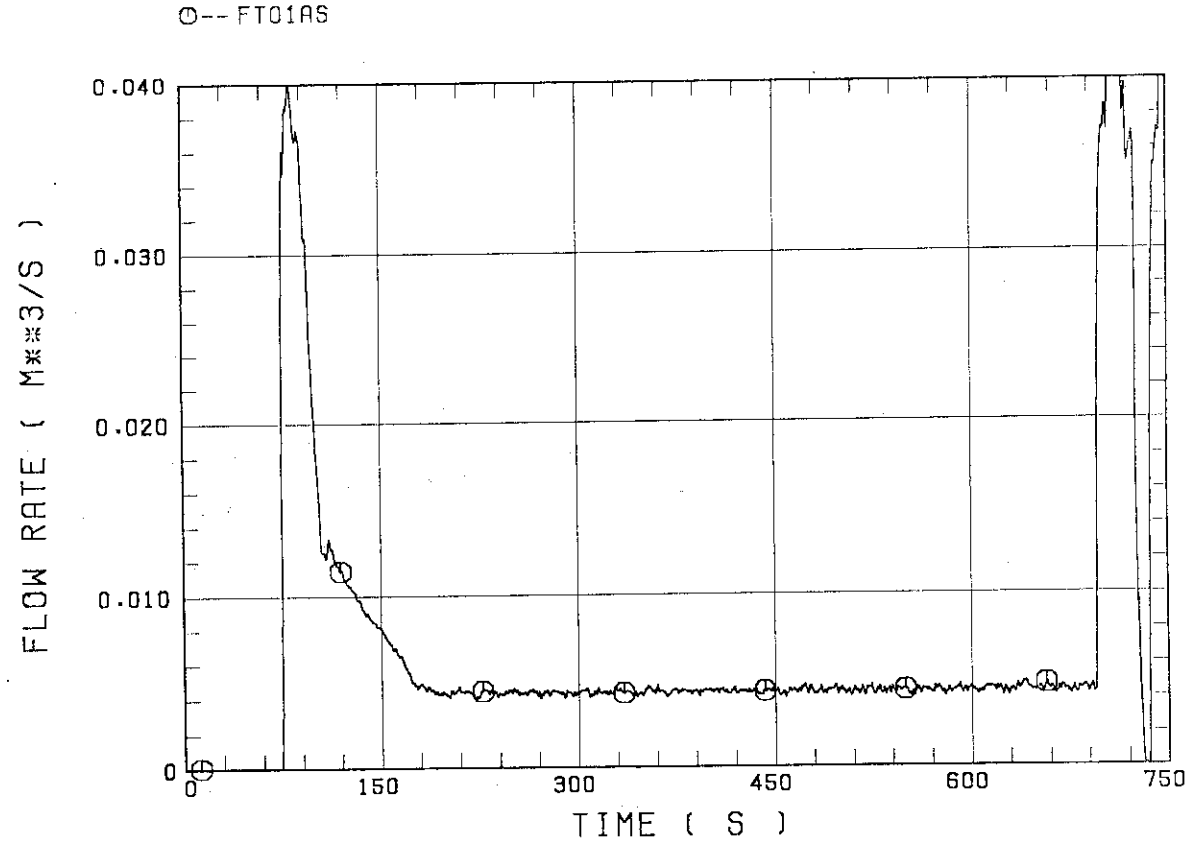

Fig. 2.7 ECC water injection rate into lower plenum

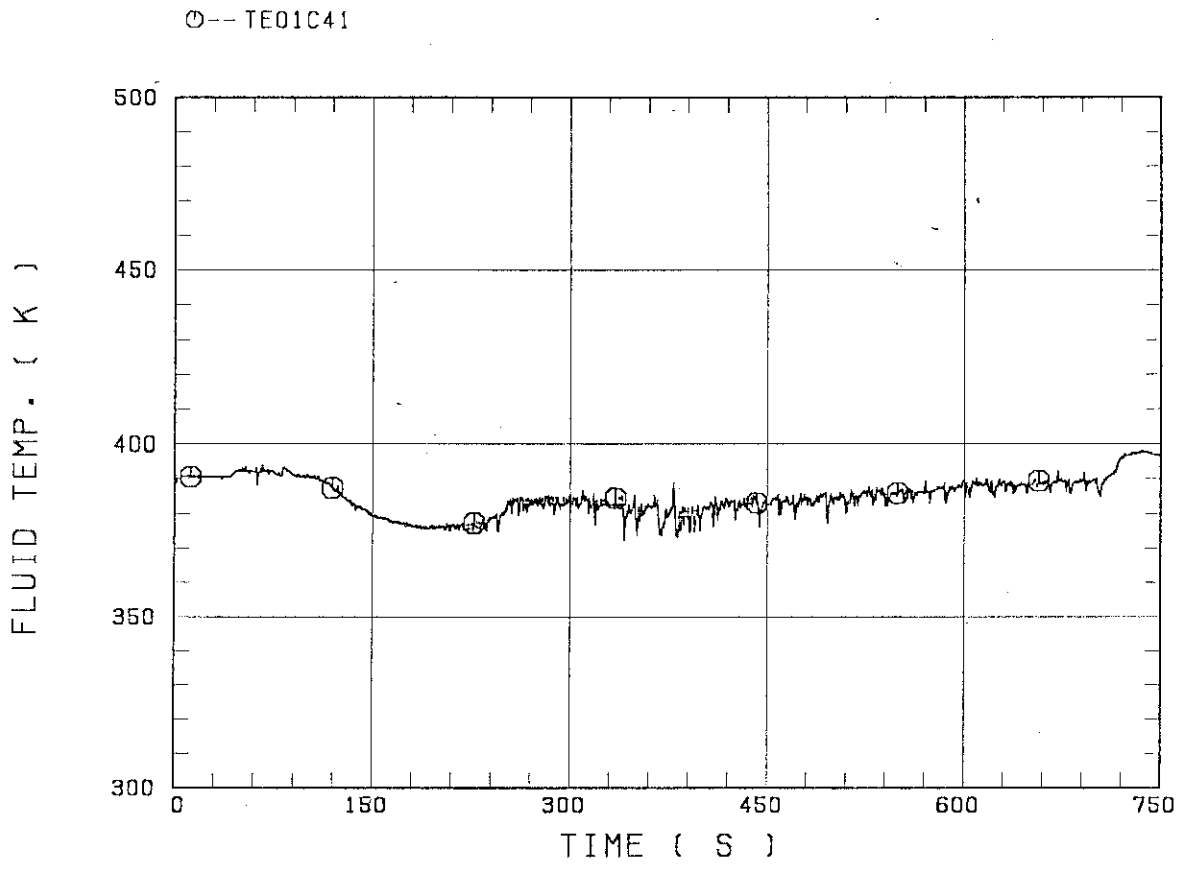

Fig. 2.8 Water temperature at core inlet

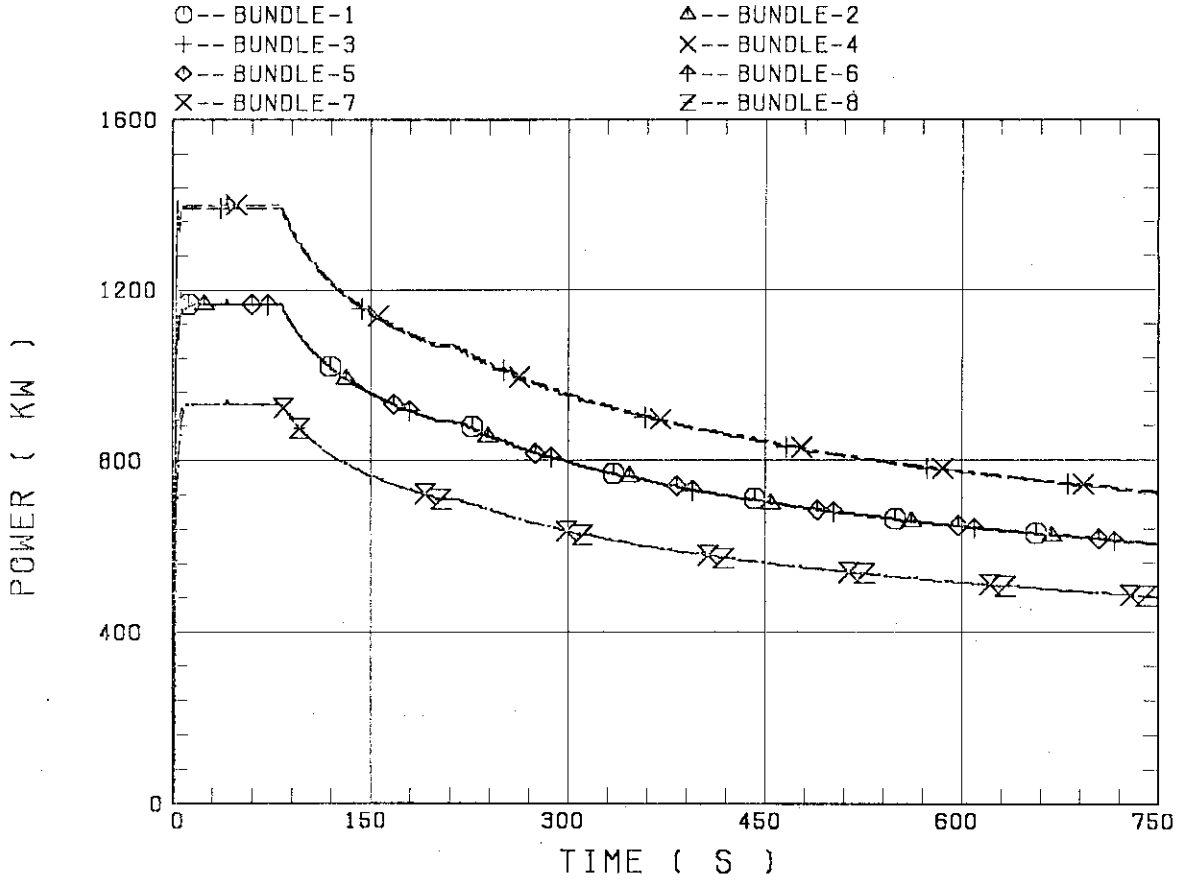

Fig. 2.9 Supplied core power for each bundle

3. Test Results and Discussion

3.1 Achieved Major Test Conditions

Since test conditions for the present test were determined to achieve the same core boundary conditions as those for CCTF Test C2-4[5] as closely as possible, it is important to review first the measured core boundary conditions. Boundary conditions such as the initial core power, the radial power profile, the initial clad temperature, the initial lower plenum water temperature and the initial lower plenum water level can be directly set and controlled by us, whereas the core flooding rate and the flooding water temperature can not. Therefore, these data are reviewed in the following.

Figure 3.1 shows a comparison of the core flooding rate between the achieved value and the planned. As shown in the figure, the achieved core flooding rate is satisfactorily in good agreement with the planned value. Core inlet water subcooling are compared in Fig. 3.2. The difference between them is within 20 K throughout the transient. The subcooling of the present test is larger by about 7 K after about 300 s.

3.2 Core Thermo-hydrodynamic Behavior

Figure 3.3(a) shows the core differential pressure compared with that for Test C2-4. It has been known[7] that the characteristic of the core differential pressure is somewhat different between the SCTF and the CCTF tests, and the comparison in the figure shows the same tendency as that. That is, the data for the present test are smaller up to about 250 s and becomes larger after that. Also, its increasing rate for the present test is smaller during the initial 50 s and becomes larger after 100 s.

One reason for this difference is considered to be the difference in the core inlet water subcooling between the tests shown in Fig. 3.2. In order to quantitatively investigate this effect on core differential pressure, two calculations were performed with REFLA-1D code[8], which can predict CCTF and SCTF test results well[9]. Figure 3.3(b) shows those calculational results. One is for Test C2-4 with its measured boundary conditions. The other is one obtained with the measured core inlet subcooling and pressure for Test S3-9 but with the same core flow area as the CCTF. The results show that the difference in the characteristics of the core differential pressure observed in Fig. 3.3(a) is qualitatively pre-

dicted except for the initial period.

Another reason for the difference is considered to be the existence of excess core flow area in the SCTF. In the SCTF, there is an additional core flow area between the heater rod assemblies and the vessel wall[4]. This is corresponding to the baffle region around the core. The flow area of the rod assemblies is calculated to be 0.25 m^2 (*i.e.* the same as in the CCTF), while there is the additional flow area of 0.07 ~ 0.10 m^2[4] in the SCTF. That is, in the SCTF, the effective core flow area where water can accumulate is 30 to 40 % larger than the real core flow area.

During the initial Acc injection period of reflooding, nearly the single phase water accumulates in the core and the core differential pressure increases rapidly. In this situation, core differential pressure is expected to be smaller in the SCTF under the same core inlet mass flow rate as for the CCTF because its effective core flow area is 1.3 ~ 1.4 times larger as mentioned above. In order to quantitatively investigate this effect on the core differential pressure, two calculations were also performed with the REFLA-1D code and the results are presented in Fig. 3.3(c). One is for Test C2-4. The other was obtained with the same core inlet subcooling as for Test S3-9 and with taking account of the geometrical effective core flow area (*i.e.* 1.4 times larger) only during the Acc period. That is, core flooding velocity was reduced by a factor of 1.4 during the Acc period. The results show that the characteristics observed in Fig. 3.3(a) is qualitatively predicted including the initial period. However, quantitative agreement in the later period is not enough in comparison with the difference of the measured values.

After the Acc period, the core is considered to be occupied with the two-phase mixture and its void fraction is determined mainly by steam velocity there. In this situation, the effective core flow area is only the area where steam can flow, being regardless of the geometrical value. The larger effective core flow area is expected to result in lower core void fraction due to its lower steam velocity (refer Wilson's correlation[10], for instance). If we take this effect into account, we may be able to qualitatively explain the larger increasing rate of core differential pressure in the SCTF after the Acc period. Although the effective core flow area where steam can flow is estimated to be only a little more (*i.e.* a few percent) than the real core flow area in the SCTF Core-III based on its design, some parametric calculations were performed with

REFLA-1D in order to know the magnitude of the influence of the effective core flow area on the core water accumulation characteristics. Figure 3.3(d) shows three of these results, *i.e.* results for the cases of the original core flow area and the 1.2 and 1.4 times larger effective core flow area. For the 1.4 times larger case, the effect of core flow area is much larger than the observed (see, Fig. 3.3(a)). For the 1.2 times larger case, the difference observed in Fig. 3.3(a) is well predicted. However, as mentioned above, the effective core flow area is expected to be a few percent at most and contradicts this value drawn from the calculation.

Two-dimensional flow behavior in the wide SCTF core may also affect the core differential pressure characteristics. That is, two-dimensional water flow from the periphery to the center of the core may increase water accumulation in the core. Furthermore, there may be an effect of flow from the side wall region to the central region of the core. However, they are not clarified yet and the quantitative investigation is not possible. Therefore, although the effects of the core inlet subcooling and the effective core flow area during the Acc period have been clarified at present, further investigation is necessary.

Figure 3.4 shows comparison of the quench front envelope for the heater rods with nearly identical average linear power density, *i.e.* 1.652 kW/m for SCTF *vs.* 1.674 kW/m for CCTF. This figure shows that the overall core cooling is close to each other. Comparisons of heater rod surface temperature and corresponding heat transfer coefficient are presented in Figs. 3.5 and 3.6, respectively. The data for the present test are taken at 2.33 m elevation and linear power density there is 2.17 kW/m, whereas those for Test C2-4 are taken at 2.44 m elevation and linear power density there is 2.12 kW/m. These data show that heat transfer for Test C2-4 is larger during the initial 60 s, and it becomes identical to that for the present test after that. The better heat transfer during the initial 60 s in Test C2-4 is attributed to the larger initial core differential pressure shown in Fig 3.3. Although quench times between the two tests are very close in these tests, it should be noted that the elevation is different and quench time at 2.33 m is earlier in Test C2-4 as shown in Fig. 3.4. According to the figure, quench time in Test C2-4 at 2.33 m is 386 s and is earlier than that in the present test by about 35 s.

3.3 Thermo-hydrodynamic Behavior in System

Figure 3.7 shows a comparison of the upper plenum pressure between the present test and Test C2-4. Although the initial pressure is the same, the pressure for the present test is lower by 0.025 ≈ 0.05 MPa during the transient. This is attributed to the lower pressure drop through the primary loop in the present test as presented in the following.

Figures 3.8 and 3.9 show comparisons of the pressure drop along the intact cold leg and the broken cold leg at the pressure vessel side, respectively. The upper plenum pressure is the summation of the containment pressure, the broken cold leg pressure drop and the intact cold leg pressure drop. Figure 3.8 shows that the intact cold leg differential pressure is lower by more than 0.02 MPa during the initial 50 s in the present test. Figure 3.9 shows that the broken cold leg differential pressure at the pressure vessel side is also lower by 0.01 ~ 0.03 MPa in the present test. There are two reasons for these lower differential pressures in the present test. One is the smaller intact loop flow resistance than a desired value. The other is that the single phase steam flows through the broken cold leg instead of the two-phase flow.

As shown in Fig. 3.10, the intact loop mass flow rate is lower in the present test. The reasons for this are considered to be the lower carry over from the core and the steam/water separation in the steam/water separator, which is used as a simulation of a steam generator in the SCTF. In order to compensate this expected lower intact loop mass flow rate in the SCTF, flow resistance of the intact loop is supposed to be adjusted with a couple of orifices. However, as seen above, this adjustment was not successful for the present test.

Figure 3.11 shows the downcomer water level and indicates the downcomer water level in the present test is much lower than the overflow level. This suggests that the single phase steam flowed through the broken cold leg in the present test because there was no cold leg ECC water injection. In Test C2-4, however, two-phase flow flowed through the broken cold leg, and hence, resulted in the large pressure drop[11] shown in Fig. 3.9.

Although our main concern is in the core cooling behavior and the system behavior is not focused in the present test, the upper plenum pres-

sure is known[12] to affect core cooling. That is, the higher is the upper plenum pressure, the better is the core cooling. Therefore, the core cooling in the present test is expected to be better under the same upper plenum pressure as in Test C2-4.

3.4 Two-dimensional Behavior in Core

It has been pointed out[6] that the core heat transfer is enhanced in the higher power region and degraded in the lower power region when there is a radial power distribution in the wide core. Figure 3.12 shows a comparison of the heat transfer coefficient plotted against distance from the quench front for three different power bundles. Bundle 2 is the average power bundle, Bundle 4 is the high power bundle and Bundle 8 is the low power bundle. As shown in the figure, the heat transfer coefficient for Bundle 8 is the lowest and that for Bundle 4 is the highest. This is exactly the same characteristic as observed in other SCTF experiments[6].

Figure 3.13 shows a comparison of the core void fraction in Bundles 2, 3 and 8 in the section of 1.365 ~ 1.905 m. Although data for Bundles 2 and 4 are almost the same, those for Bundle 8 are different from them. That is , Bundle 8 gives higher void fraction before 120 s, whereas it gives lower void fraction after 120 s. According to Fig. 3.4, quench front reaches 1.365 m elevation at about 120 s. Therefore, in Bundle 8, the void fraction is higher above the quench front, whereas lower below the quench front. This characteristic of void fraction is also the same as that observed in other SCTF tests[6].

3.5 Tie Plate Mass Flow Rate

There are four 'Flow Modules' at the tie plates in the SCTF Core-III. Flow Module is an advanced instrumentation for two-phase flow and consists of a drag body, a turbine flow meter, a DP-cell and a thermocouple. They are provided by the USNRC based on the 2D/3D Agreement for the experimental coupling between the SCTF Core-III and the UPTF. The same type of Flow Modules are also installed at the tie plates in the UPTF. By using Flow Modules we can measure the tie plate steam and water mass flow rates separately. For the experimental coupling between the SCTF Core-III and the UPTF, these tie plate mass flow rates of steam and water obtained in a SCTF Core-III experiment are supposed to be used as the boundary condi-

tions for steam and water mass flow rates at the tie plates of the UPTF. Since The UPTF does not have the heated core but a core simulator, from which steam and water are injected separately toward the upper plenum, the realistic steam and water mass flow rates from the heated core, such as of the SCTF, are necessary to determine its boundary conditions.

Although there are four Flow Modules in the SCTF Core-III and they are distributed above Bundles 1, 4, 5 and 8, one above Bundle 1 has found not to work well due to touch to the structure. Therefore, data from that Flow Module are not presented in the following. Figures 3.14(a), (b) and (c) show steam mass flow rates at the tie plates above Bundles 4, 5 and 8, respectively. As recognized from these data, the steam mass flow rate is higher above the lower power region, *i.e.* Bundle 8. The data above Bundle 8 give 0.5 ~ 0.6 kg/s, whereas around 0.4 kg/s above Bundle 4. Figures 3.15(a), (b) and (c) show water mass flow rates at tie plates above Bundles 4, 5 and 8, respectively. They all show water mass flow rate of nearly zero.

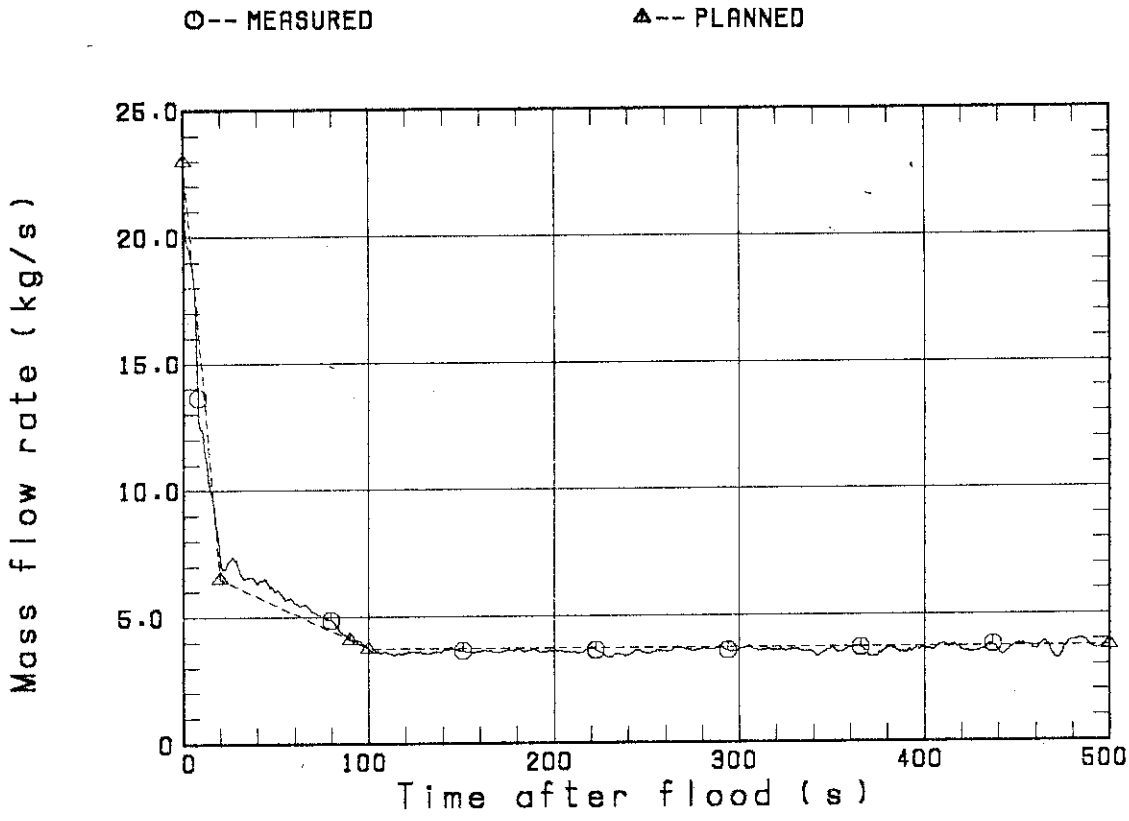

Fig. 3.1 Comparison of core inlet mass flow rate

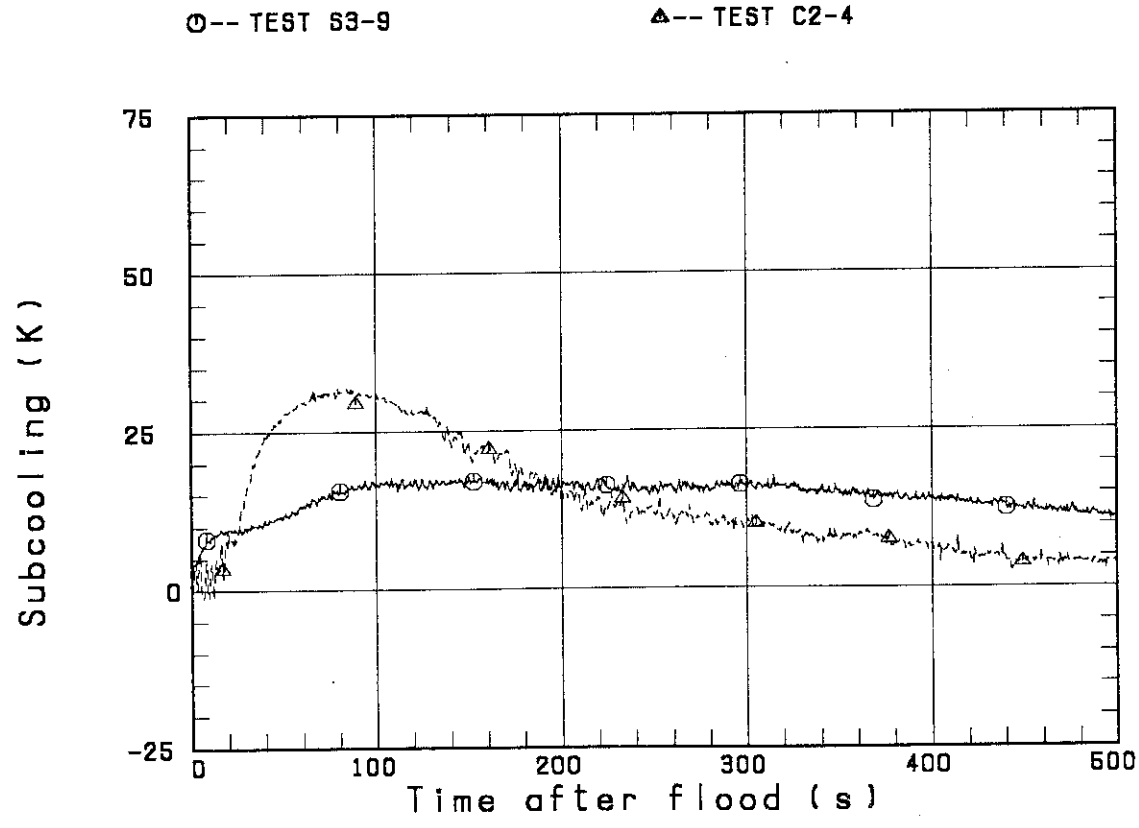

Fig. 3.2 Comparison of core inlet water subcooling

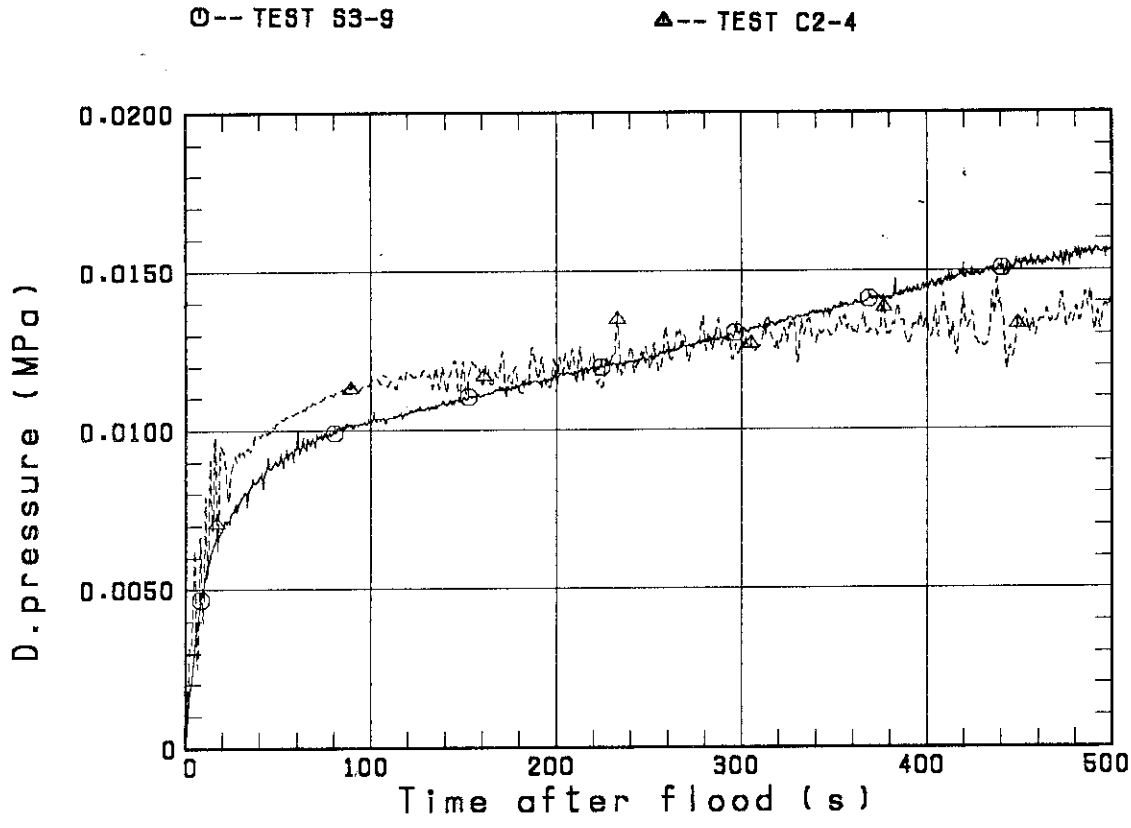

Fig. 3.3(a) Comparison of core differential pressure (measured values)

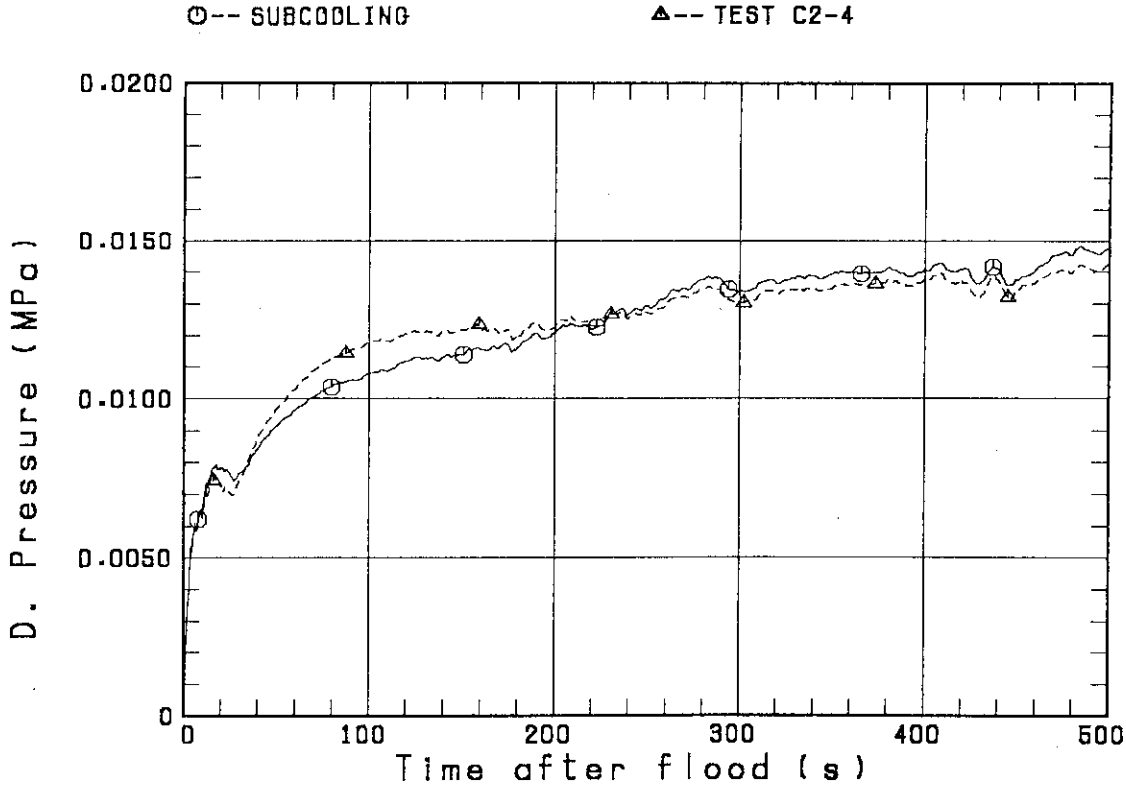

Fig. 3.3(b) Comparison of core differential pressure (calculated values ; effect of core inlet water subcooling)

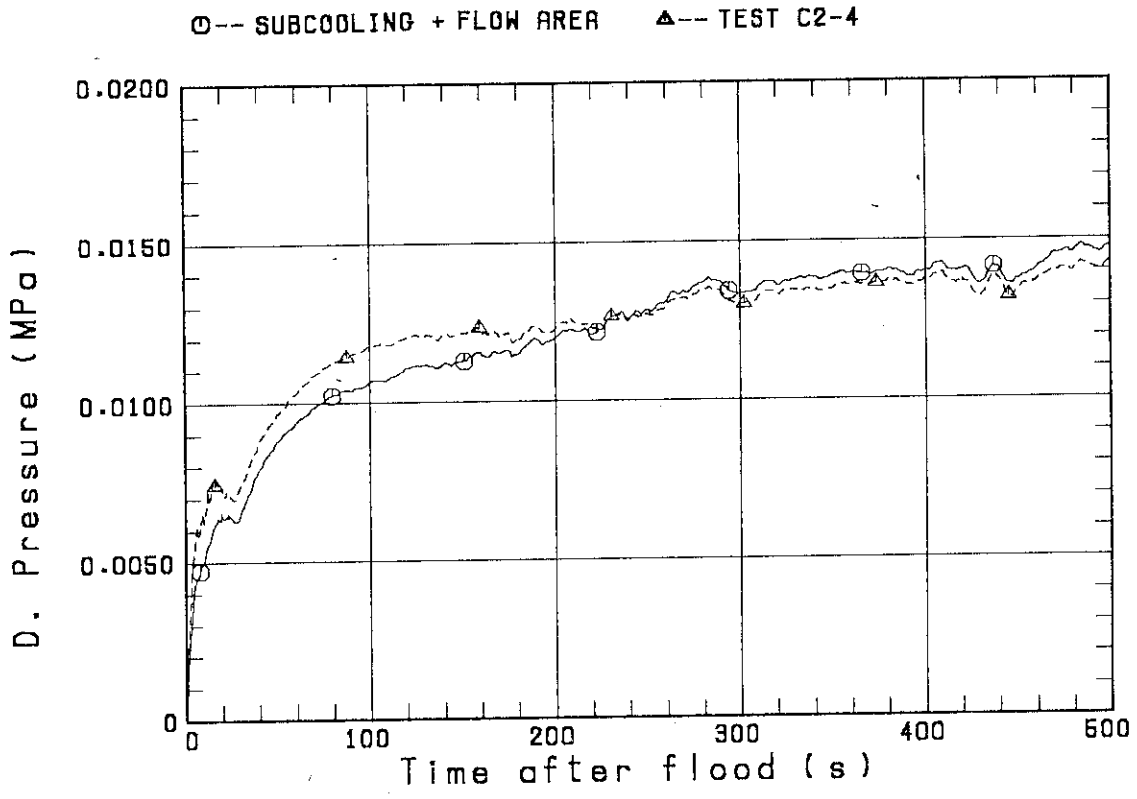

Fig. 3.3(c) Comparison of core differential pressure (calculated values ; effect of both core inlet water subcooling and core effective flow area during Acc period)

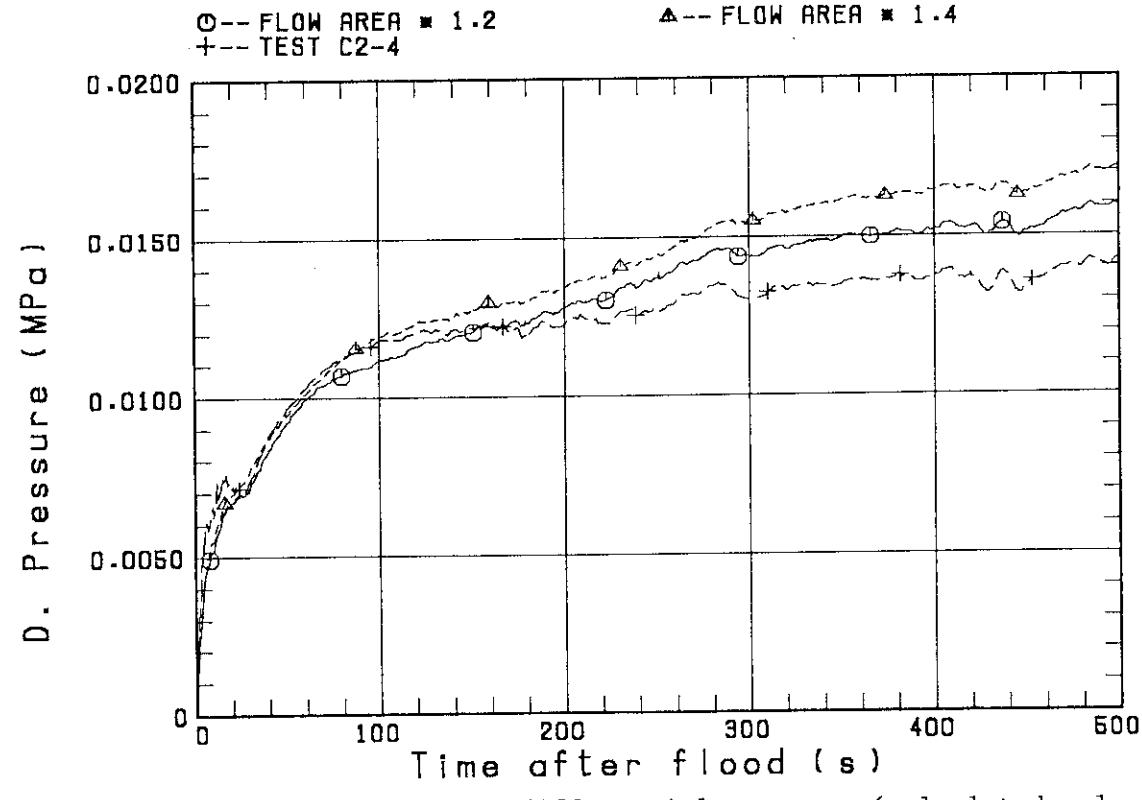

Fig. 3.3(d) Comparison of core differential pressure (calculated values ; effect of core effective flow area)

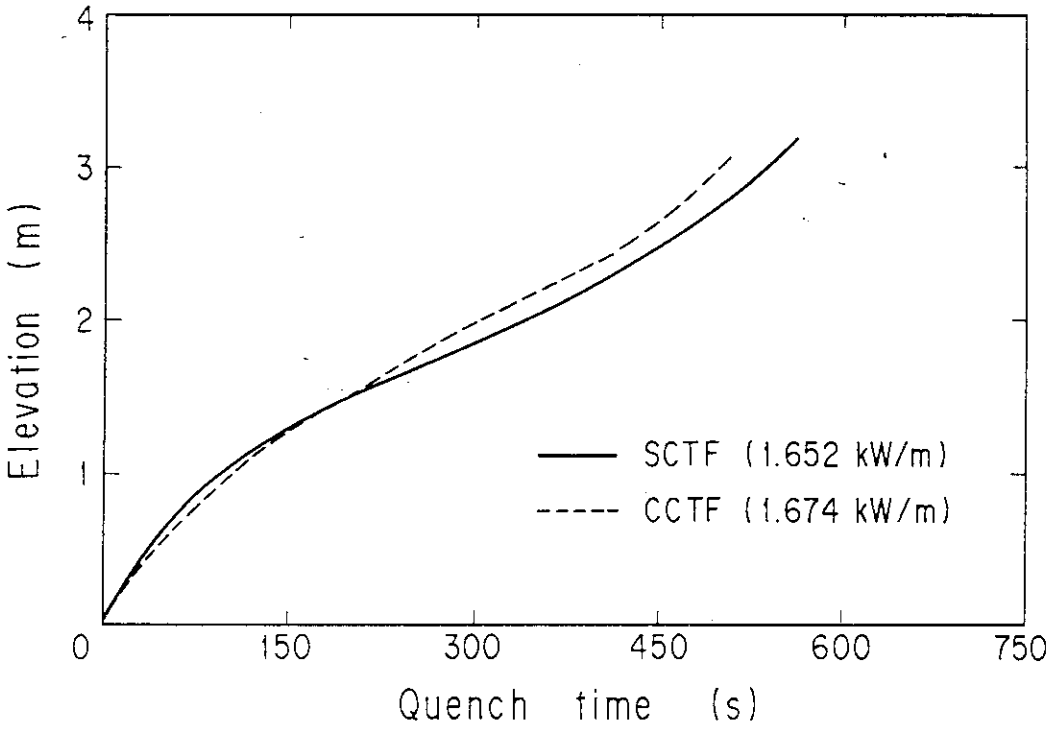

Fig. 3.4 Comparison of quench envelope

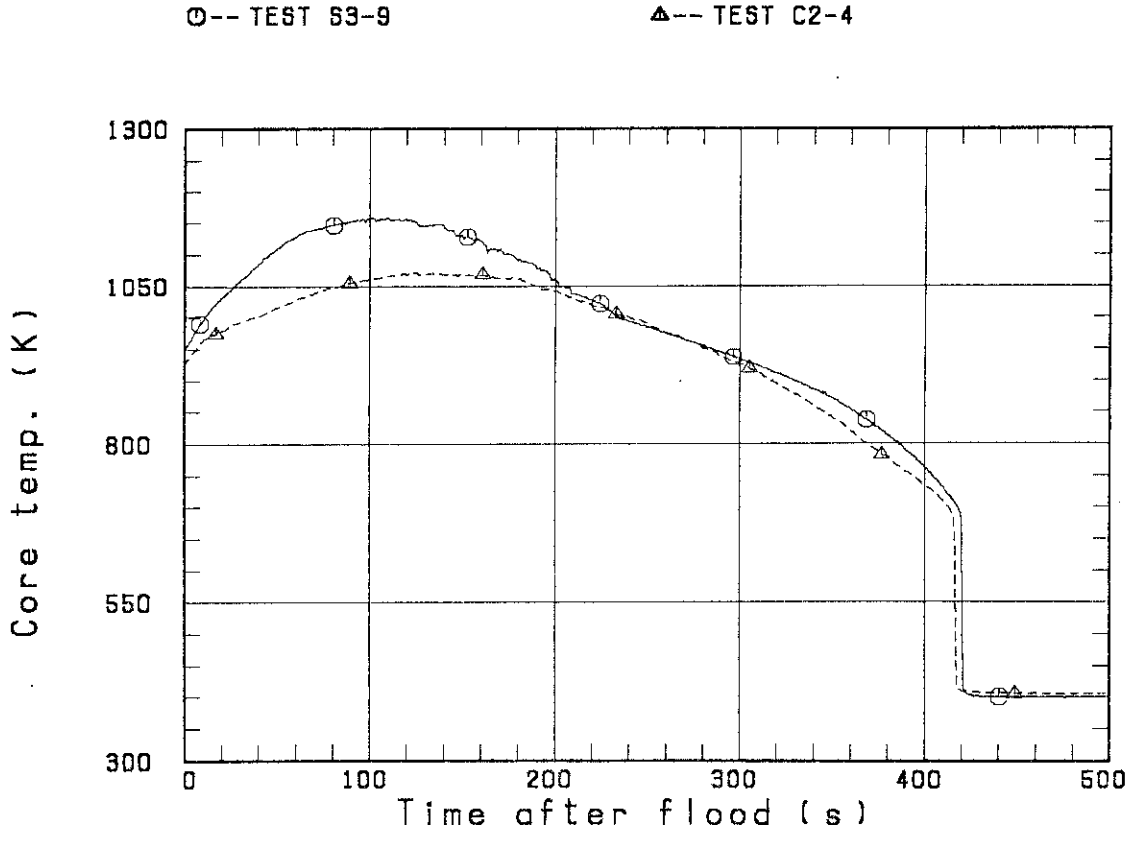

Fig. 3.5 Comparison of rod surface temperature at 2.33 m elevation

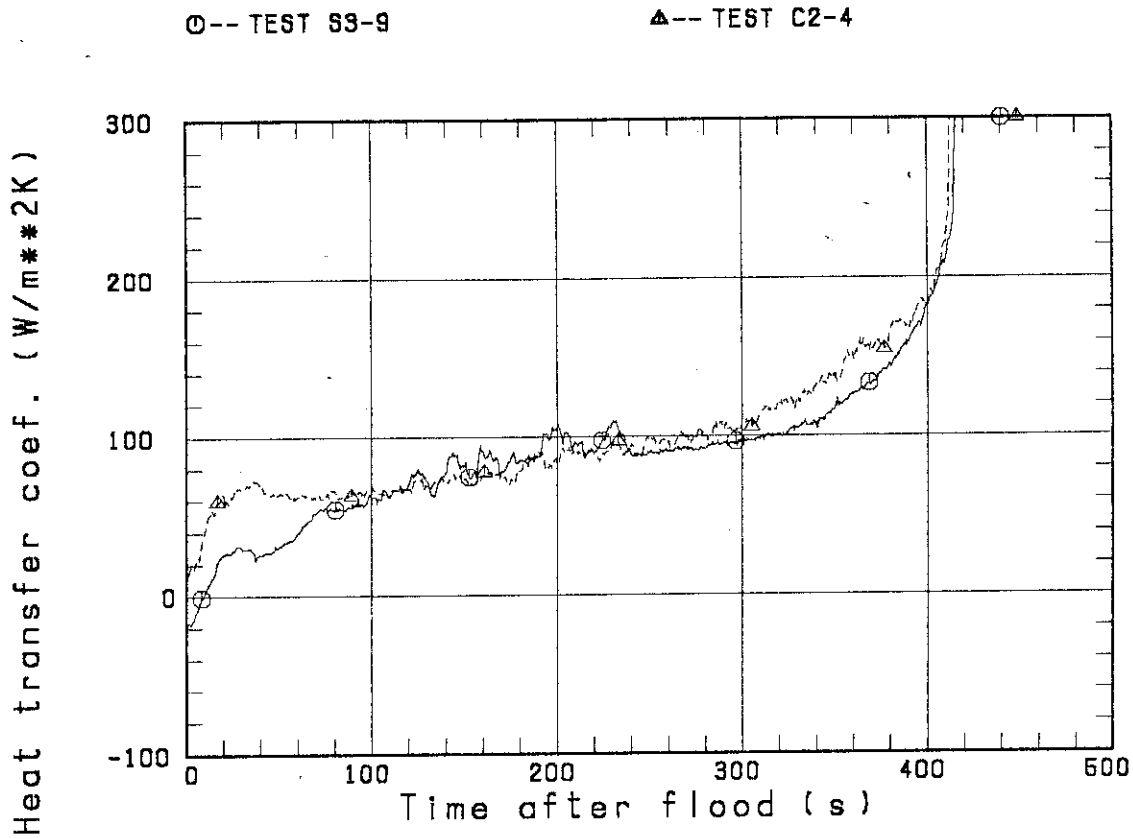

Fig. 3.6 Comparison of heat transfer coefficient at 2.33 m elevation

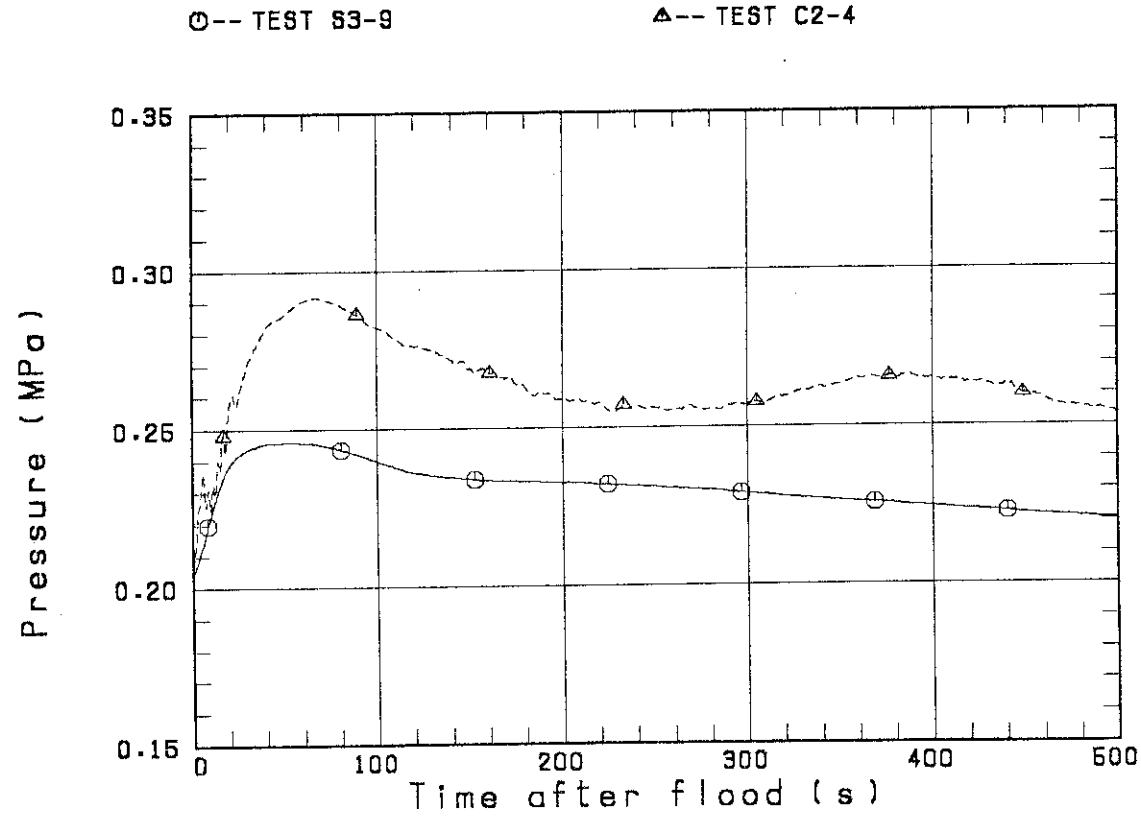

Fig. 3.7 Comparison of Upper plenum pressure

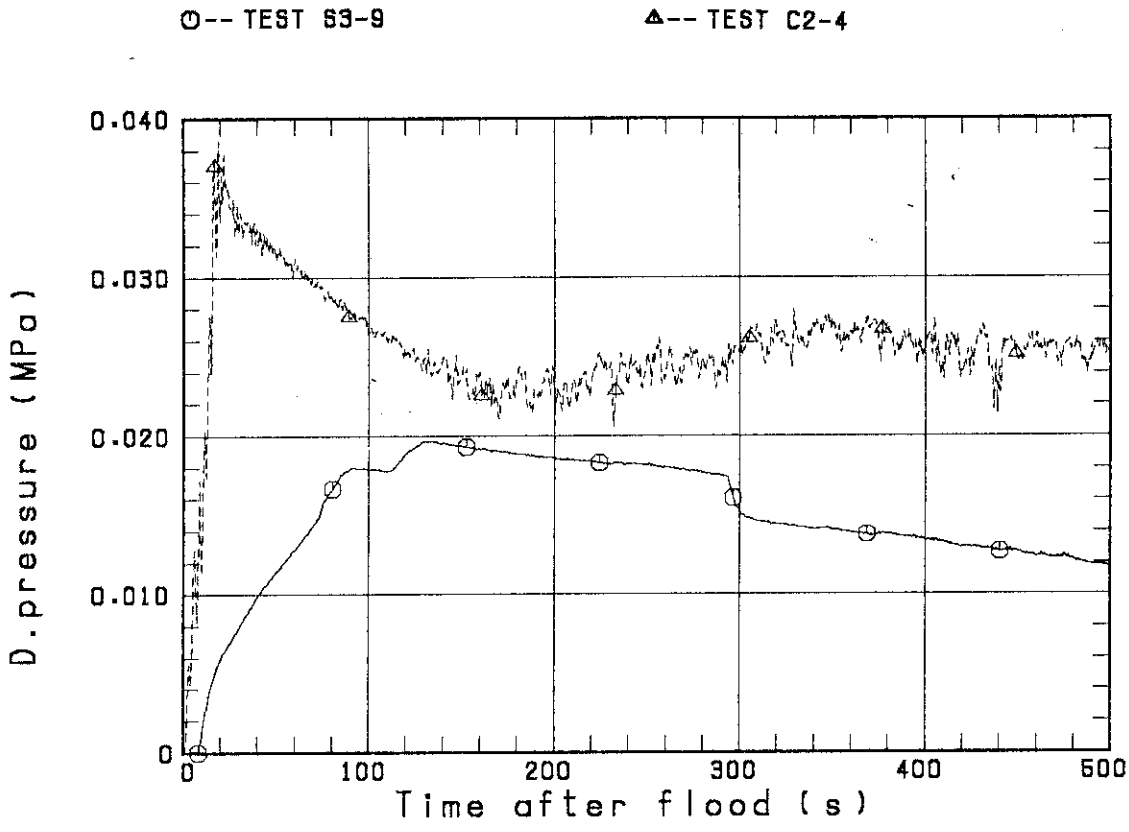

Fig. 3.8 Comparison of intact loop differential pressure

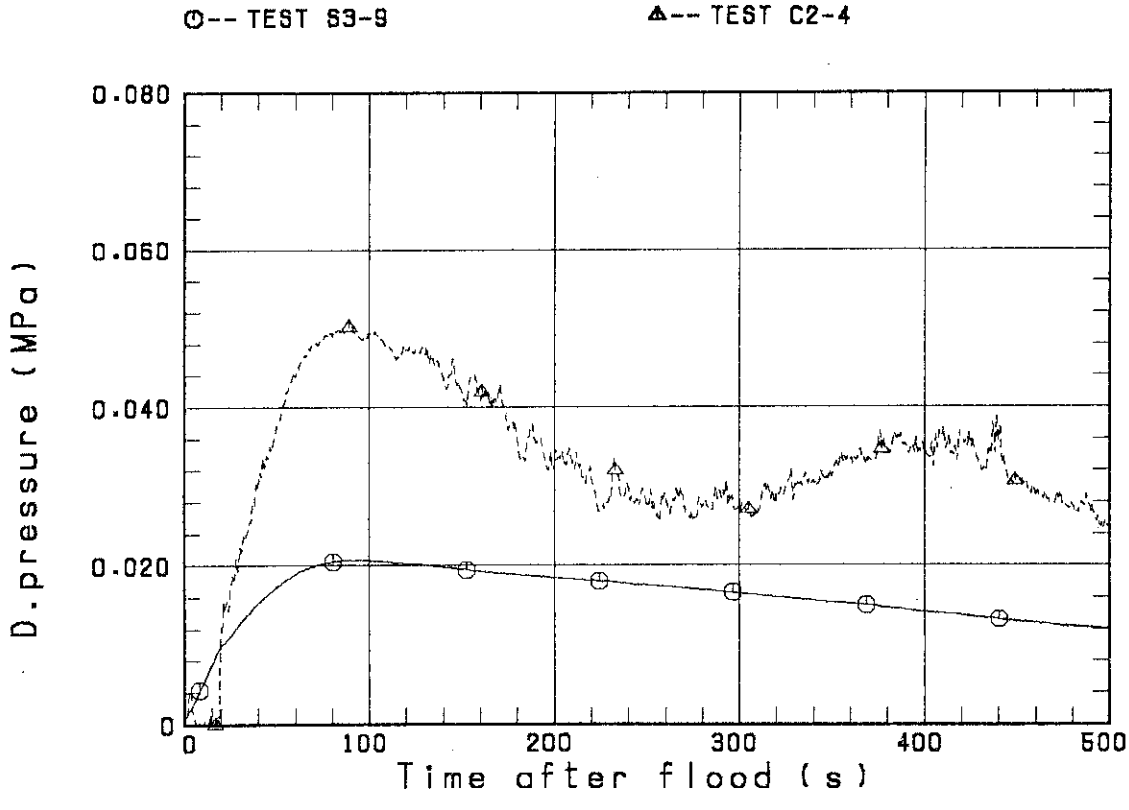

Fig. 3.9 Comparison of broken cold leg differential pressure at pressure vessel side

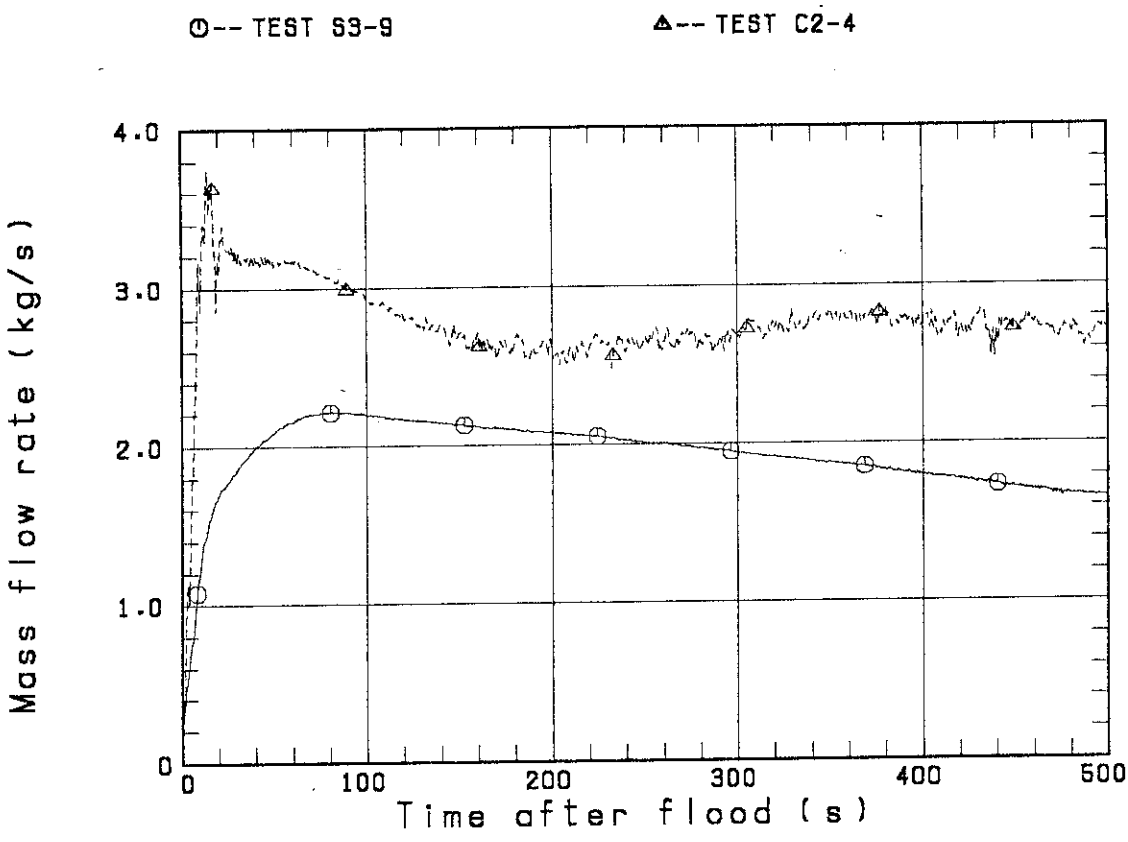

Fig. 3.10 Comparison of intact loop steam mass flow rate

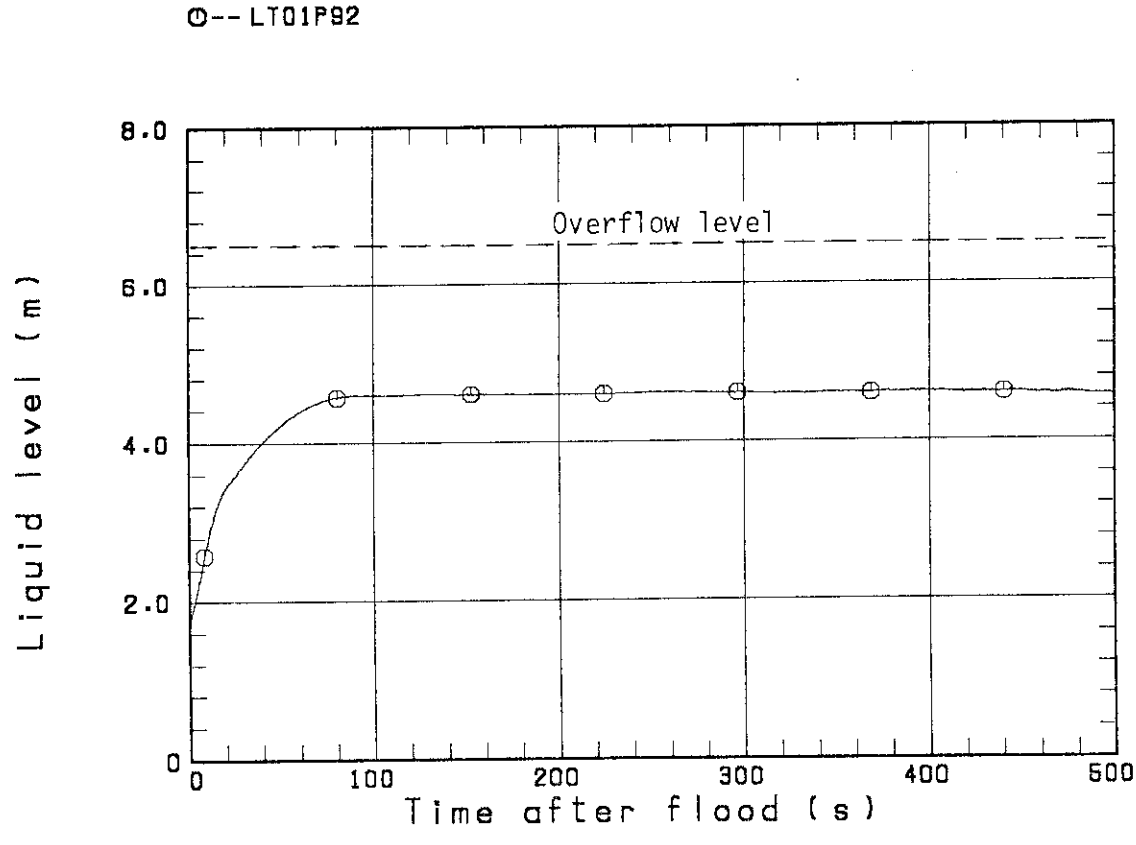

Fig. 3.11 Comparison of downcomer water level

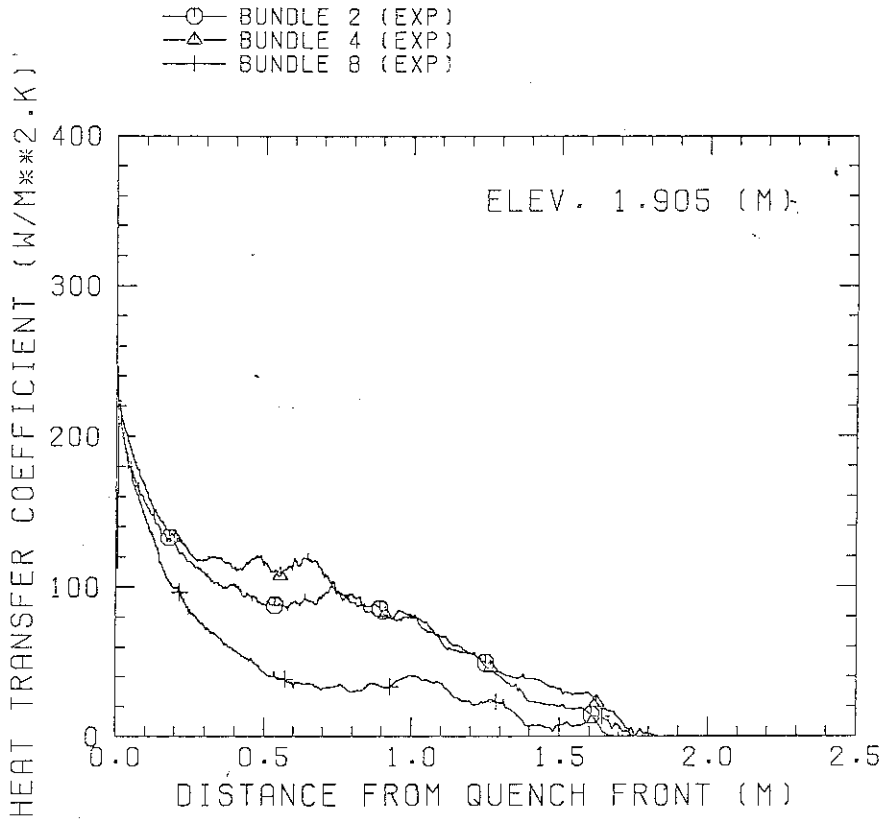

Fig. 3.12 Heat transfer coefficients at 1.905 m elevation

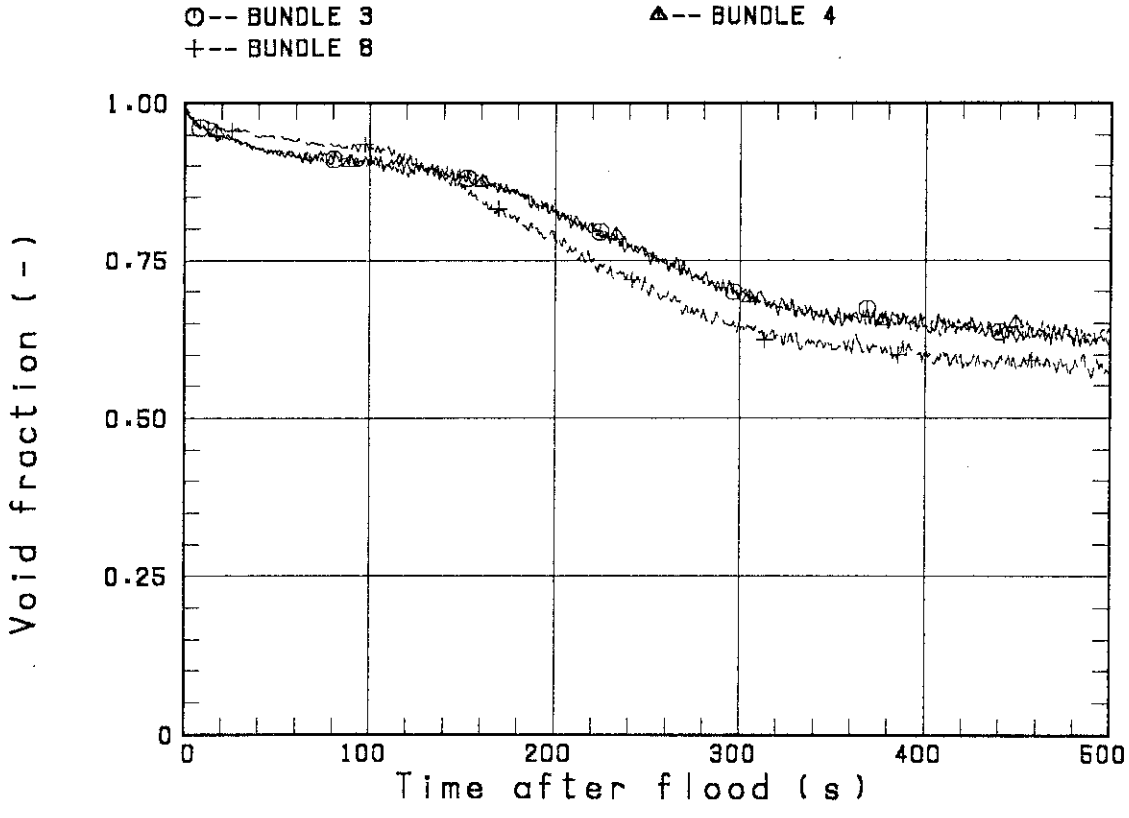

Fig. 3.13 Core void fractions between 1.365 m and 1.905 m elevation

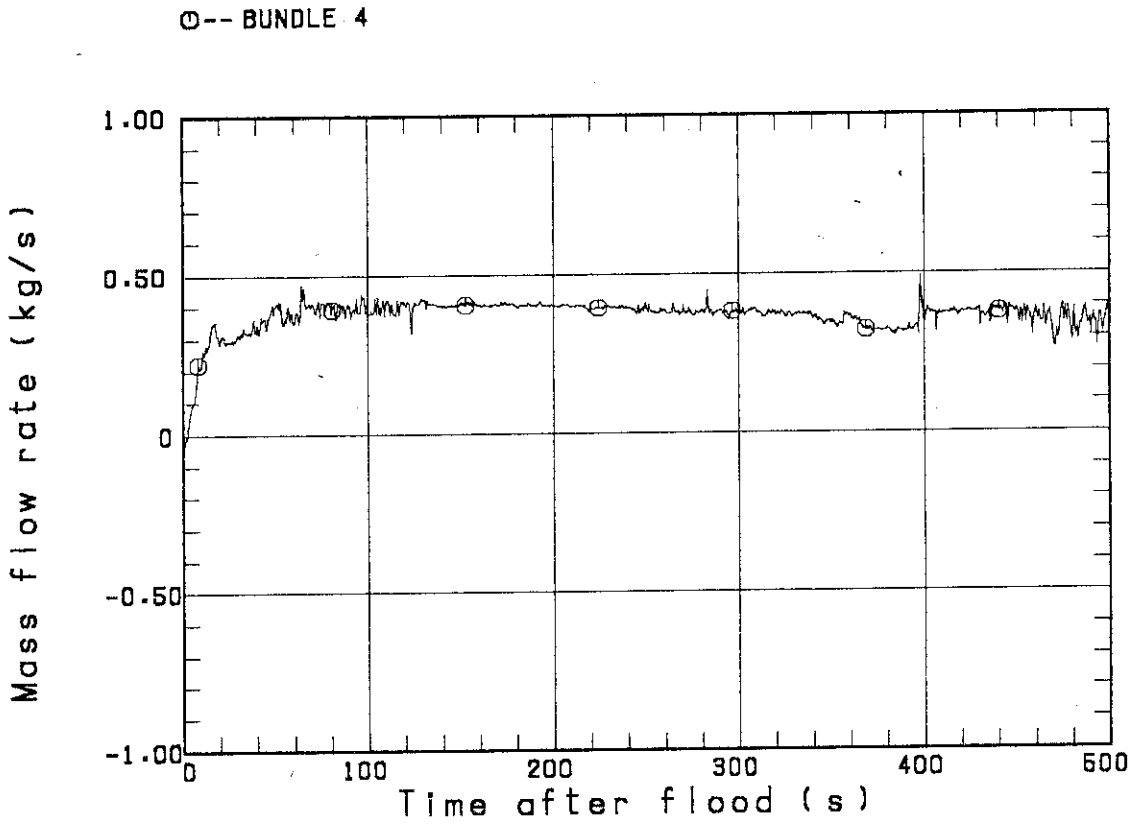

Fig. 3.14(a) Steam mass flow rate at tie plate above Bundle 4

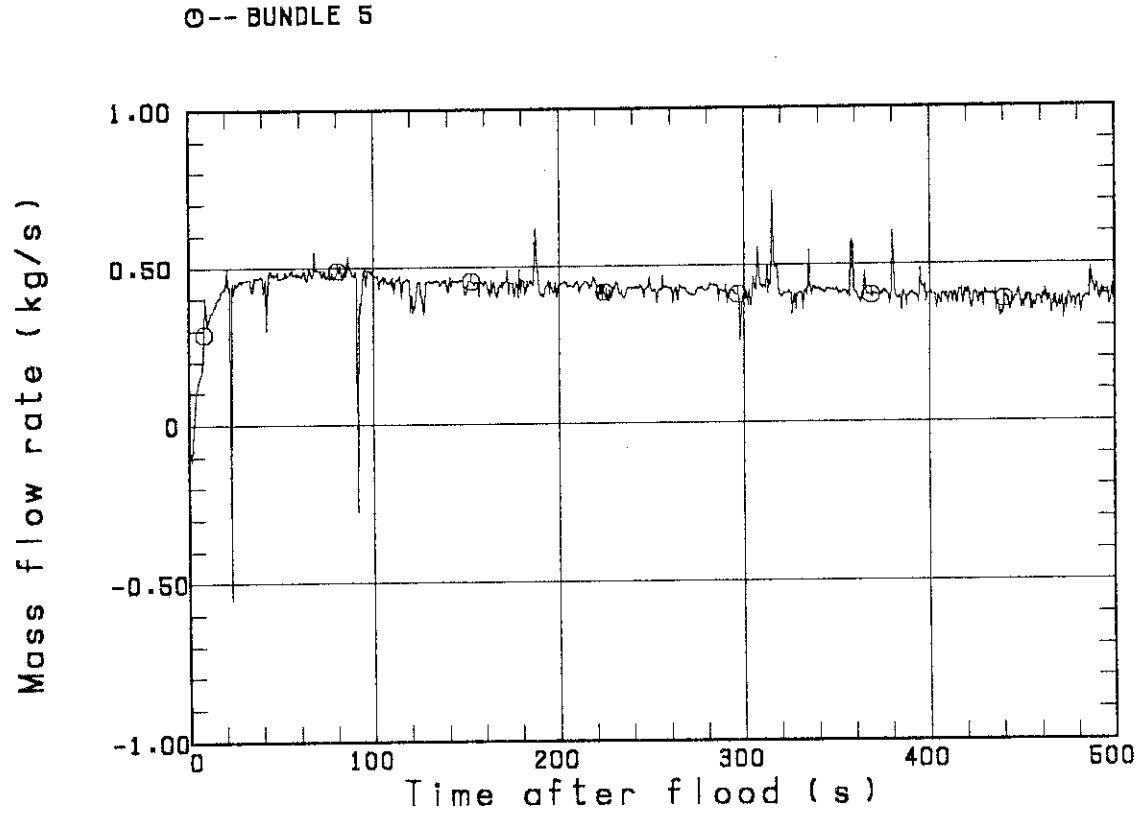

Fig. 3.14(b) Steam mass flow rate at tie plate above Bundle 5

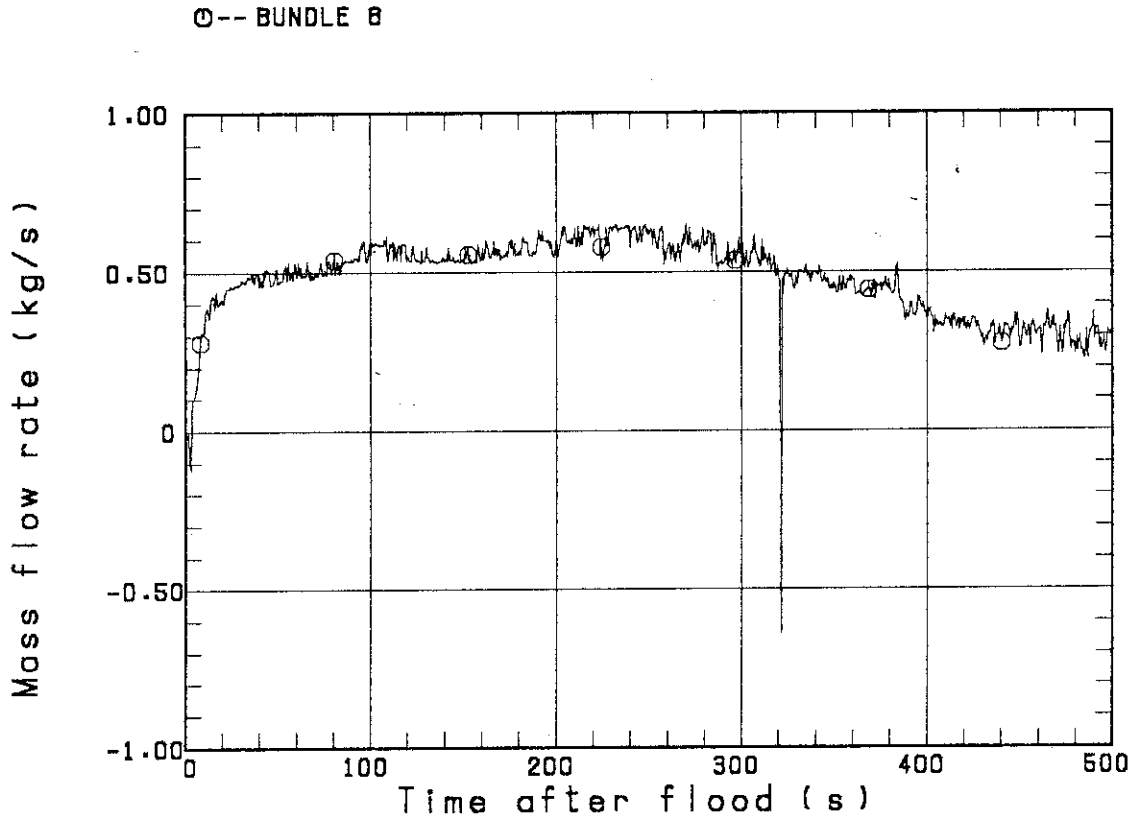

Fig. 3.14(c) Steam mass flow rate at tie plate above Bundle 8

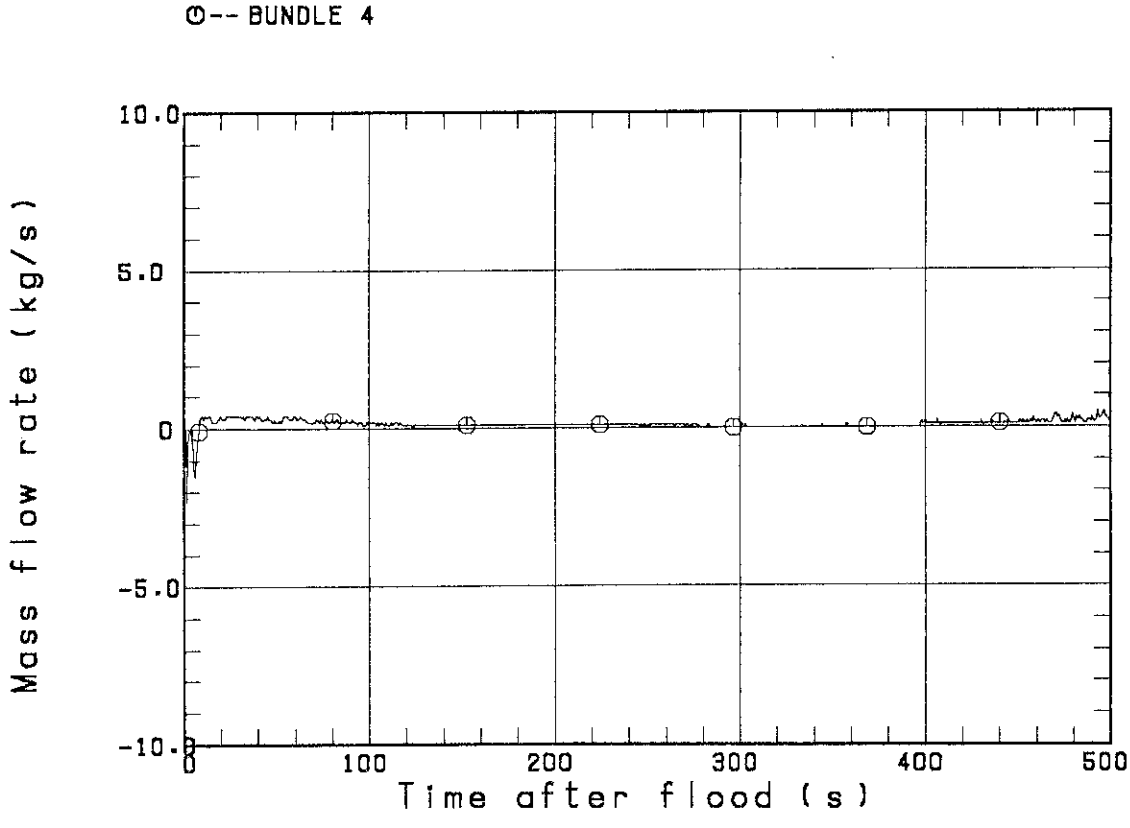

Fig. 3.15(a) Water mass flow rate at tie plate above Bundle 4

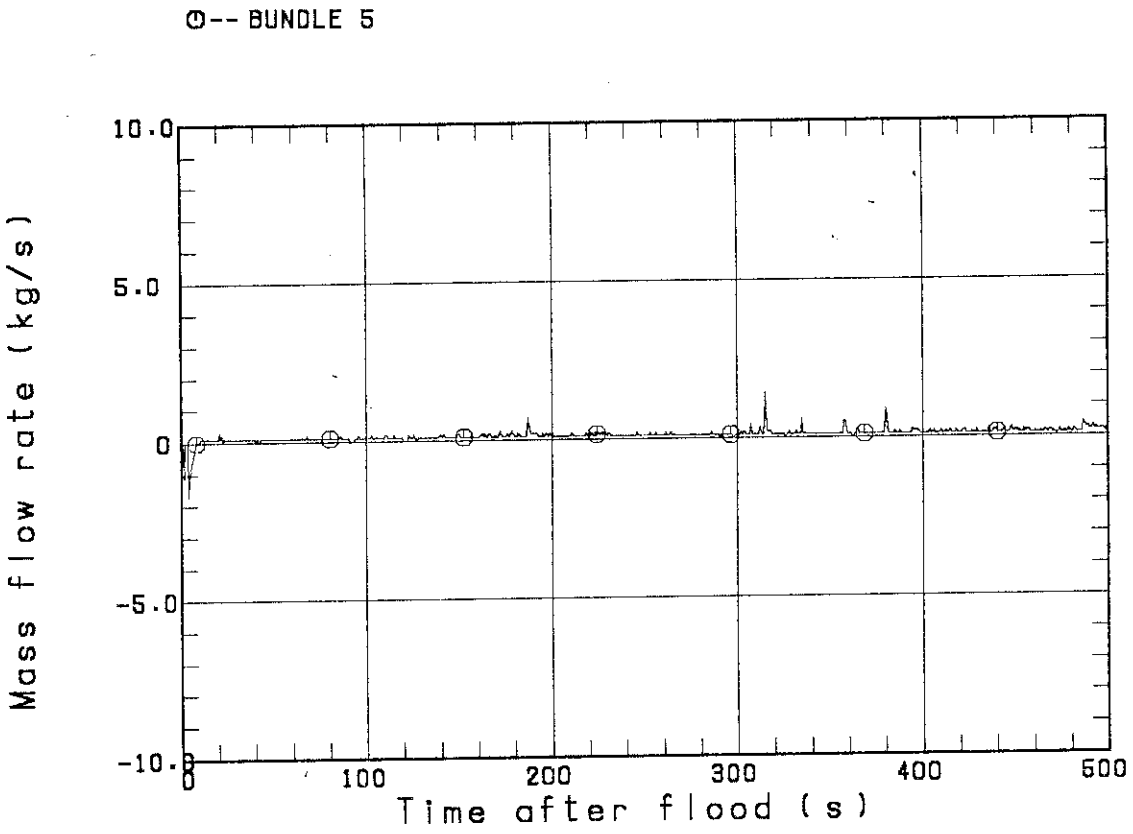

Fig. 3.15(b) Water mass flow rate at tie plate above Bundle 5

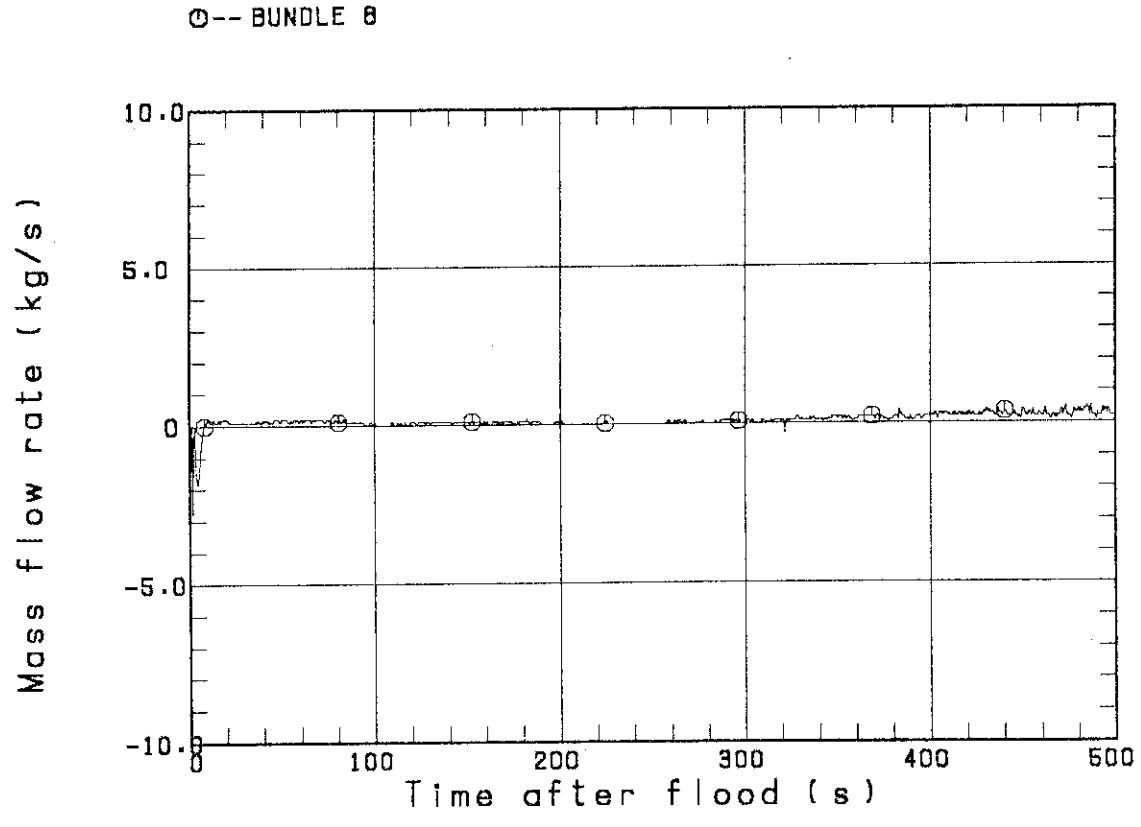

Fig. 3.15(c) Water mass flow rate at tie plate above Bundle 8

4. Conclusions

Analyzing data of Test S3-9 together with those of Test C2-4 and other SCTF tests, the following conclusions are obtained.

(1) Test S3-9 was successfully completed under an EM condition. The tie plate mass flow rate data were obtained and can be used for an experimental coupling with the UPTF.

(2) The overall core cooling behavior observed in Test S3-9 was nearly the same as that observed in CCTF Test C2-4.

(3) However, the core differential pressure characteristic observed in Test S3-9 was somewhat different from that observed in Test C2-4. Main reasons for the difference are almost explained to be different core inlet water subcooling between the two tests and the different effective core flow area between two facilities.

(4) The core two-dimensional behavior observed in Test S3-9 had the same characteristic as observed in the other tests with the SCTF Core-II.

Acknowledgments

The authors would like to express their appreciation to Messrs. A. Kamoshida, T. Oyama, Y. Niitsuma, K. Nakajima, T. Chiba, K. Komori, H. Sonobe and A. Owada for their contribution to the test conduction.

This work was performed under a contract with the Atomic Energy Bureau of Science and Technology Agency of Japan.

References

[1] Hirano, K. and Murao, Y.: "Large Scale Reflood Test", Nihon-Genshiryoku-Gakkai Shi (J. At. Energy Sco. Jpn.) [in Japanese], 22[10], 681(1980).

[2] Adachi, H. *et al.*: "Design of Slab Core test Facility (SCTF) in Large Scale Reflood Test Program, Part I: Core-I", JAERI-M 83-080 (1983).

[3] Sobajima, M. *et al.*: "Design of Slab Core Test Facility (SCTF) in Large Scale Reflood Test Program, Part II: Core-II", to be published as a JAERI-M report.

[4] Adachi, H. *et al.*: "Design of Slab Core Test Facility (SCTF) in Large Scale Reflood test Program, Part III: Core-III", to be published as a JAERI-M report.

[5] Okubo, T. *et al.*: "Evaluation Report on CCTF Core-II Reflood Test C2-4 (Run 62) -- Investigation of reproducibility -- ", JAERI-M 85-026 (1985).

[6] Iwamura, T. *et al.*: "Two-dimensional Thermal-hydraulic Behavior in Core in SCTF Core-II Cold Leg Injection Tests (Radial Power Profile Test Results)", JAERI-M 85-106 (1985).

[7] Okubo, T. *et al.*: "Analysys of SCTF/CCTF Counterpart Test Results", to be published as a JAERI-M report.

[8] Murao, Y. *et al.*: " REFLA-1D/MODE3: A Compuetr Code for Reflood Thermo-hydrodymanic Analysis during PWR-LOCA", JAERI-M 84-243 (1985).

[9] Okubo, T. and Murao, Y.: "Assessment of Core Thermo-hydrodynamic Models of REFLA-1D Code with CCTF Data for Reflood Phase of PWR-LOCA", J. Nucl. Sci. Technol., 22[12], 983 (1985).

Acknowledgments

The authors would like to express their appreciation to Messrs. A. Kamoshida, T. Oyama, Y. Niitsuma, K. Nakajima, T. Chiba, K. Komori, H. Sonobe and A. Owada for their contribution to the test conduction.

This work was performed under a contract with the Atomic Energy Bureau of Science and Technology Agency of Japan.

References

[1] Hirano, K. and Murao, Y.: "Large Scale Reflood Test", Nihon-Genshiryoku-Gakkai Shi (J. At. Energy Sco. Jpn.) [in Japanese], 22[10], 681(1980).

[2] Adachi, H. *et al.*: "Design of Slab Core test Facility (SCTF) in Large Scale Reflood Test Program, Part I: Core-I", JAERI-M 83-080 (1983).

[3] Sobajima, M. *et al.*: "Design of Slab Core Test Facility (SCTF) in Large Scale Reflood Test Program, Part II: Core-II", to be published as a JAERI-M report.

[4] Adachi, H. *et al.*: "Design of Slab Core Test Facility (SCTF) in Large Scale Reflood test Program, Part III: Core-III", to be published as a JAERI-M report.

[5] Okubo, T. *et al.*: "Evaluation Report on CCTF Core-II Reflood Test C2-4 (Run 62) -- Investigation of reproducibility -- ", JAERI-M 85-026 (1985).

[6] Iwamura, T. *et al.*: "Two-dimensional Thermal-hydraulic Behavior in Core in SCTF Core-II Cold Leg Injection Tests (Radial Power Profile Test Results)", JAERI-M 85-106 (1985).

[7] Okubo, T. *et al.*: "Analysys of SCTF/CCTF Counterpart Test Results", to be published as a JAERI-M report.

[8] Murao, Y. *et al.*: " REFLA-1D/MODE3: A Compuetr Code for Reflood Thermo-hydrodymanic Analysis during PWR-LOCA", JAERI-M 84-243 (1985).

[9] Okubo, T. and Murao, Y.: "Assessment of Core Thermo-hydrodynamic Models of REFLA-1D Code with CCTF Data for Reflood Phase of PWR-LOCA", J. Nucl. Sci. Technol., 22[12], 983 (1985).

[10] Wilson, J.F. *et al.*: "The Velocity of Rising Steam in a Bubling Two-Phase Mixture", Trans. Am. Nucl. Soc., 5, 151 (1962).

[11] Akimoto, H. *et al.*: "Pressure Drop through Broken Cold Leg during Reflood Phase of Loss-of-Coolant Accident of Pressurized Water Reactor", J. Nucl. Sci. Technol., 21[6], 450 (1984).

[12] Akimoto, H. *et al.*: "System Pressure Effect on System and Core Cooling Behavior during Reflood Phase of PWR LOCA", ibid., 24[4], 276 (1988).

Appendix A

Description of SCTF Core-III

A.1 Test Facility

The overall schematic diagram of SCTF is shown in Fig. A-1. The principal dimensions of the facility is shown in Table A-1, and the comparison of dimensions between SCTF and the reference PWR is shown in Fig. A-2.

A.1.1 Pressure Vessel

The pressure vessel is of slab geometry as shown in Fig. A-3. The height of the components in the pressure vessel is almost the same as the reference reactor's, and the flow area and the fluid volume of each component are scaled down based on the nominal core flow area scaling, 1/21.

The core consists of 8 bundles arranged in a row and each bundle includes heater rods and non-heated rods with 16×16 array. The core is enveloped by the honeycomb thermal insulator which is attached on the back surface of core wall plate.

The downcomer is located at one end of the pressure vessel which corresponds to the periphery of the actual reactor pressure vessel. The core baffle region located between the core and the downcomer is isolated for Core-III to minimize uncertainty in actual core flow. The cross sections of the pressure vessel at the upper head, upper plenum, core and lower plenum are shown in Fig. A-4.

A.1.2 Interface between Core and Upper Plenum

The interface between the core and the upper plenum consists of upper core support plate (UCSP), end box and various structures in the end box such as control rod spider which is paired with the control rod guid assembly (CRGA) and its support column bottom and special baffle plate spider which is paired with the hold-down bridge. These structures are exactly the same as those for a German PWR except some minor modifications.

Figure A-5 shows arrangement of the UCSP, the end box and the top grid spacer. The configuration of the end box is shown in Fig. A-6.

Detail of the end boxes with drag transducer device and other internals is shown in Fig. A-7. The UCSP shown in Fig. A-8 has two kinds of holes, i.e., the square holes correspond to the end boxes with control rod spider and the circular holes correspond to the end boxes with special baffle plate spider.

A.1.3 Upper Plenum and Upper Head

The vertical and horizontal cross sections of the upper plenum are shown in Figs. A-9 and A-4, respectively. In the SCTF Core-III, the slab cut of the upper plenum of a German (KWU) PWR is simulated. The splitted and staggered arrangement of the CRGA support columns was chosen to make good simulation of horizontal flow in the upper plenum.

As shown in Fig. A-10, there are three kinds of CRGA support column. Support column-1 is installed above Bundles 3 and 5 and connected to the CRGA support column bottom with the transition cone. Cross section of the CRGA support calumn changes from a circle to a half circle in this transition cone. Support column 2 is installed above Bundles 6 and 7 and the bottom is closed with the half conical bottom seal plate with many flow holes. Support column 3 is essentially the same as support column 2 but the edge of one side is cut off in order to install above Bundle 1. Each CRGA support column has ten or eleven baffle plates with flow holes. Top flow paths to the upper head bottom and to the upper plenum top are also provided.

Figure A-11 shows vertical cross section of the bottom part of the upper plenum and the interface between the core and the upper plenum. There are eight side flow injection nozzles and eight side flow extraction nozzles just at the opposite side of the upper plenum bottom, corresponding to each bundle.

The upper plenum is separated from the upper head by an upper support plate. Four top injection nozzles penetrate the upper head and open the top of upper plenum as shown in Fig. A-12. Outlet part of the top injection nozzle has a rectangular cross section and double mesh screen with 45 degree cross angle is attached at the mouth.

A.1.4 Simulated Core

The simulated core for the SCTF Core-III consists of 8 heater rod bundles arranged in a row. Each bundle has 236 electrically heated rods and 20 non-heated rods. The arrangement of rods in a bundle is shown in Fig. A-13. The dimensions of the heater rods are based on 15×15 fuel rods bundle for a PWR and the heated length and the outer diameter of each heater rod are 3.613 m and 10.7 mm, respectively. A heater rod consists of a nichrome heater element, boron nitride (BN) or magnesium oxide (MgO) depending on elevation in the heated zone and Nichrofer 7216 (equivalent to Inconel 600) sheath. The sheath thickness is about 1.0 mm and is thicker than the actual fuel cladding because of the requirements for thermocouple installation. The heater element is a helical coil and has a 17 step chopped cosine axial power profile as shown in Fig. A-14. The peaking factor is 1.4.

Non-heated rods are either pipes or solid rods of stainless steel with 13.8 mm O.D. The heater rods and non-heated rods are fixed at the top of the core allowing downward expansion. In Fig. A-15, relative elevation of rods and spacers is shown.

For better simulation of flow resistance in the lower plenum, the simulated fuel rods end in the lower plenum and do not penetrate through the bottom plate of the lower plenum as shown in Fig. A-15.

A.1.5 Primary Loops

Primary loops consist of a hot leg equivalent to four hot legs in area, a steam/water separator for simulating single steam phase flow downstream of the steam generator and for measuring flow rate of carry over water, an intact cold leg equivalent to three intact loops, a broken cold leg on the pressure vessel side and a broken cold leg on the steam/water separator side. These two broken cold legs are connected to two containment tanks through break valves, respectively. The arrangement of the primary loops is shown in Fig. A-16. The flow area of each loop is scaled down based on the core flow area scaling, 1/21. It should be emphasized that the cross section of the hot leg is an elongated circle with an actual height to realize proper flow pattern in the hot leg. The steam/water separator has a steam generator inlet plenum simulator to correctly simulate the flow

characteristics of carryover water into the U-tubes. The cross section of the hot leg and the configuration of the steam genrator inlet plenum simulator are shown in Fig. A-17.

A pump simulator and a loop seal part are provided for the intact cold leg. The arangement of the intact cold leg is shown in Fig. A-18. The pump simulator consists of the casing and duct simulators and an orifice plate as shown in Fig. A-19. The loop resistance is adjusted with the orifice plates attached to the intact cold leg, the steam/water separator side and pressure vessel side broken cold legs and the pump simulator.

A.1.6 ECC Water Injection System

Three kinds of ECCSs are provided, i.e., the accumulator injection system (Acc), low pressure coolant injection system (LPCI) and combined injection system. Available injection locations for the former two are the intact and broken cold legs, the hot leg, the lower plenum and the downcomer. On the other hand, those for the last one are the top and bottom-side of the upper plenum and the intact and broken cold legs.

A.1.7 Containment Tanks and Auxiliary System

Two containment tanks are provided to SCTF. The containment tank-I is connected with the downcomer through the pressure vessel side broken cold leg and the containment tank-II is connected with the steam/water separator through the steam/water separator side broken cold leg. Especially in the containment tank-I, carryover water from the downcomer is measured by the differentiation of the liquid level. These containment tanks and auxiliary system such as a pressurizer for injecting water from the Acc tanks, etc. are shared with CCTF.

A.2 Instrumentation

The instrumentation in SCTF has been provided both by JAERI and USNRC. The JAERI-provided instrumentation includes the measurement of temperatures, pressures, differential pressures, liquid levels, flow velocities, and heating powers. USNRC has provided film probes, impedance probes, string probes, liquid level detectors (LLDs), fluid distribution grids (FDGs), turbine meters, drag disks, densitometers, spool pieces, drag bodies, break through detectors and video optical probes. Locations of the JAERI-provided instruments are shown in Figs. A-20 through A-43.

Table A-1 Principal Dimensions of the SCTF

1.	Core Dimension	
	(1) Quantity of Bundle	8 Bundles
	(2) Bundle Array	1 × 8
	(3) Bundle Pitch	230 mm
	(4) Rod Array in a Bundle	16 × 16
	(5) Rod Pitch in a Bundle	14.3 mm
	(6) Quantity of Heater Rod in a Bundle	236 rods
	(7) Quantity of Non-Heated Rod in a Bundle	20 rods
	(8) Total Quantity of Heater Rods	236×8=1,888 rods
	(9) Total Quantity of Non-Heated Rods	20×8=160 rods
	(10) Effective Heated Length of Heater Rod	3613 mm
	(11) Diameter of Heater Rod	10.7 mm
	(12) Diameter of Non-Heated Rod	13.8 mm
2.	Flow Area & Fluid Volume	
	(1) Core Flow Area	0.25 m^2
	(2) Core Fluid Volume	0.903 m^3
	(3) Baffle Region Flow Area (isolated)	(0.096) m^2
	(4) Baffle Region Fluid Volume (nominal)	0.355 m^3
	(5) Cross-Sectional Area of Core Additional Fluid Volumes Including Gap between Core Barrel and Pressure Vessel Wall and Various Penetration Holes	0.07 m^2 ? 0.10 m^2
	(6) Downcomer Flow Area	0.158 m^2
	(7) Upper Annulus Flow Area	0.158 m^2
	(8) Upper Plenum Horizontal Flow Area (max.)	0.541 m^2
	(9) Upper Plenum Vertical Flow Area	0.525 m^2
	(10) Upper Plenum Fluid Volume	1.156 m^3
	(11) Upper Head Fluid Volume	0.86 m^3
	(12) Lower Plenum Fluid Volume (excluding below downcomer)	1.305 m^3
	(13) Steam Generator Inlet Plenum Simulator Flow Area	0.626 m^2
	(14) Steam Generator Inlet Plenum Simulator Fluid Volume	0.931 m^3
	(15) Steam Water Separator Fluid Volume	5.3 m^3
	(16) Flow Area at the Top Plate of Steam Generator Inlet Plenum Simulator	0.195 m^2
	(17) Hot Leg Flow Area	0.0826 m^2

Table A-1 (continue)

(18)	Intact Cold Leg Flow Area (Diameter = 297.9 mm) Inverted U-Tube with 0.0314 m^2 Cross-Sectional Area (Diameter = 200 mm) and 10 m Height from the Top of Steam Generator Inlet Plenum Simulator Can Be Added As an Option.	0.0697 m^2
(19)	Broken Cold Leg Flow Area (Diameter = 151.0 mm)	0.0197 m^2
(20)	Containment Tank-I Fluid Volume	30 m^3
(21)	Containment Tank-II Fluid Volume	50 m^3
(22)	Flow Area of Exhausted Steam Line from Containment Tank-II to the Atmosphere	see Fig. 3-63

3. Elevation & Height

(1)	Top Surface of Upper Core Support Plate (UCSP)	0 mm
(2)	Bottom Surface of UCSP	- 40 mm
(3)	Top of the Effective Heated Length of Heater Rod	- 444 mm
(4)	Bottom of the Effective Heated Length of Heater Rod	-4,057 mm
(5)	Bottom of the Skirt in the Lower Plenum	-5,270 mm
(6)	Bottom of Intact Cold Leg	+ 724 mm
(7)	Bottom of Hot Leg	+1,050 mm
(8)	Top of Upper Plenum	+2,200 mm
(9)	Bottom of Steam Generator Inlet Plenum Simulator	+1,933 mm
(10)	Centerline of Loop Seal Bottom	-2,281 mm
(11)	Bottom Surface of End Box	- 263 mm
(12)	Top of Upper Annulus of Downcomer	+2,234 mm
(13)	Height of Steam Generator Inlet Plenum Simulator	1,595 mm
(14)	Height of Loop Seal	3,140 mm
(15)	Inner Height of Hot Leg Pipe	737 mm
(16)	Bottom of Lower Plenum	-5,772 mm
(17)	Top of Upper Head	+2,887 mm

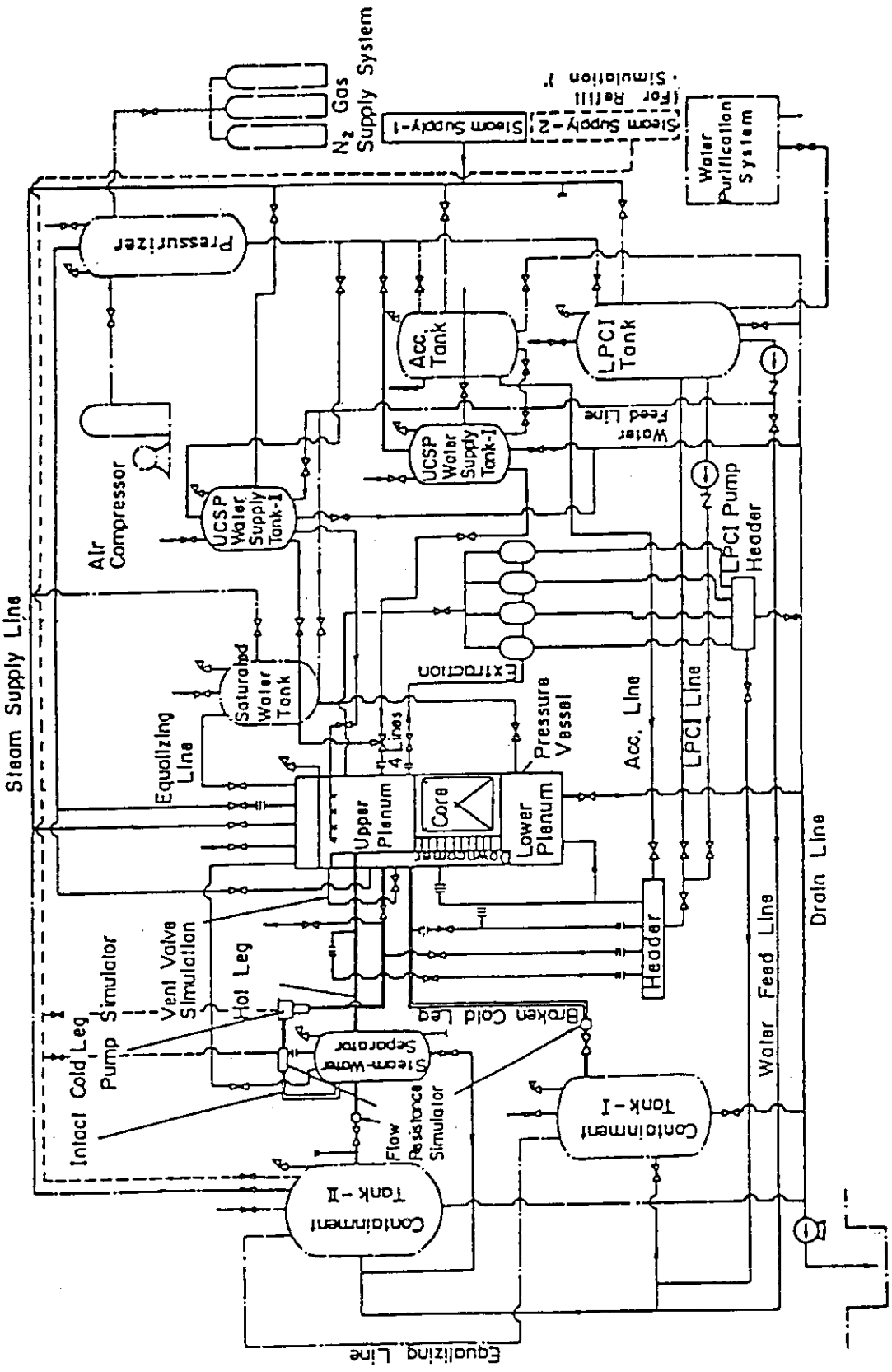

Fig. A-1 Schematic Diagram of Slab Core Test Facility

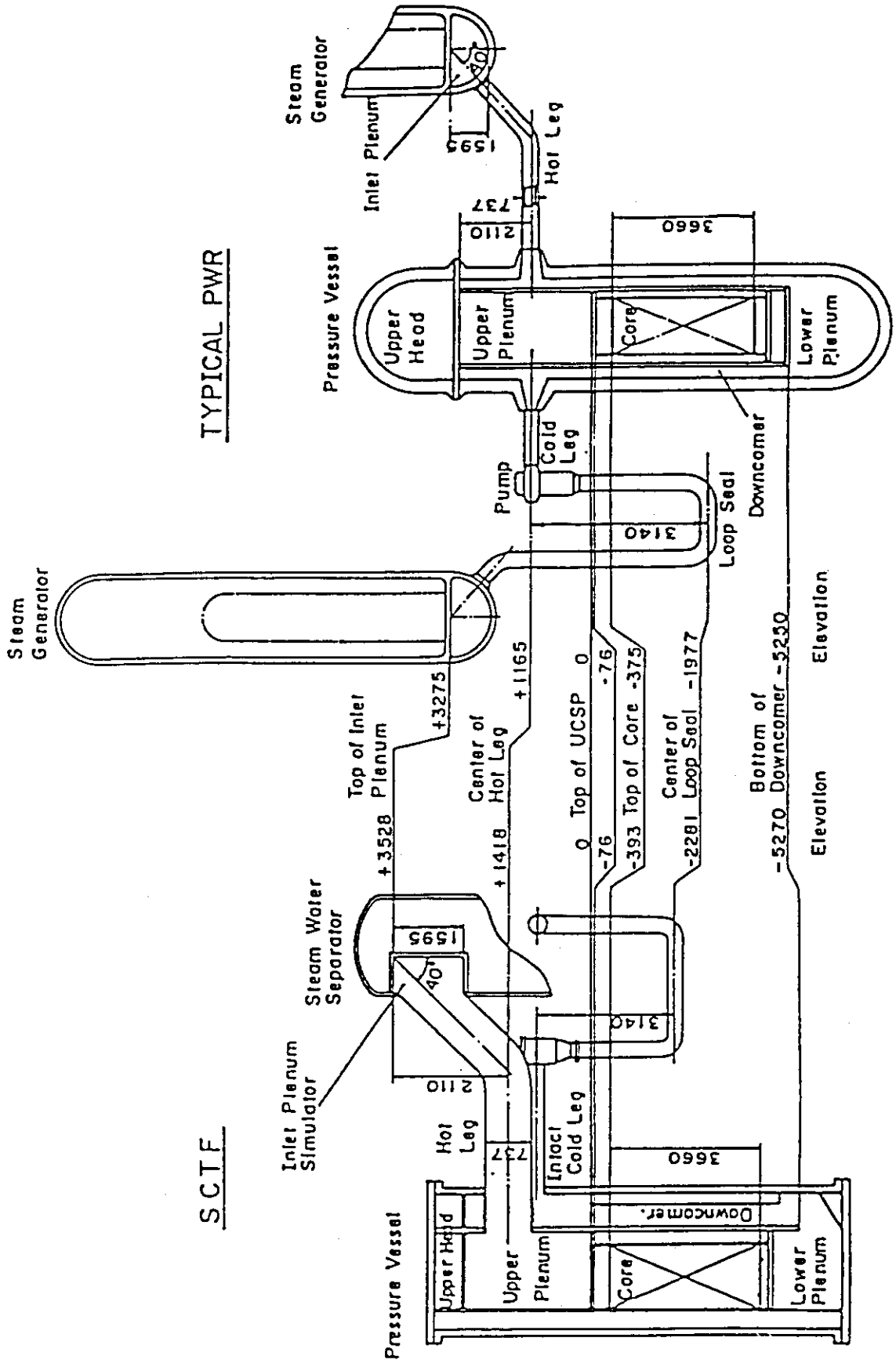

Fig. A-2 Comparison of Dimensions between SCTF and a Reference PWR

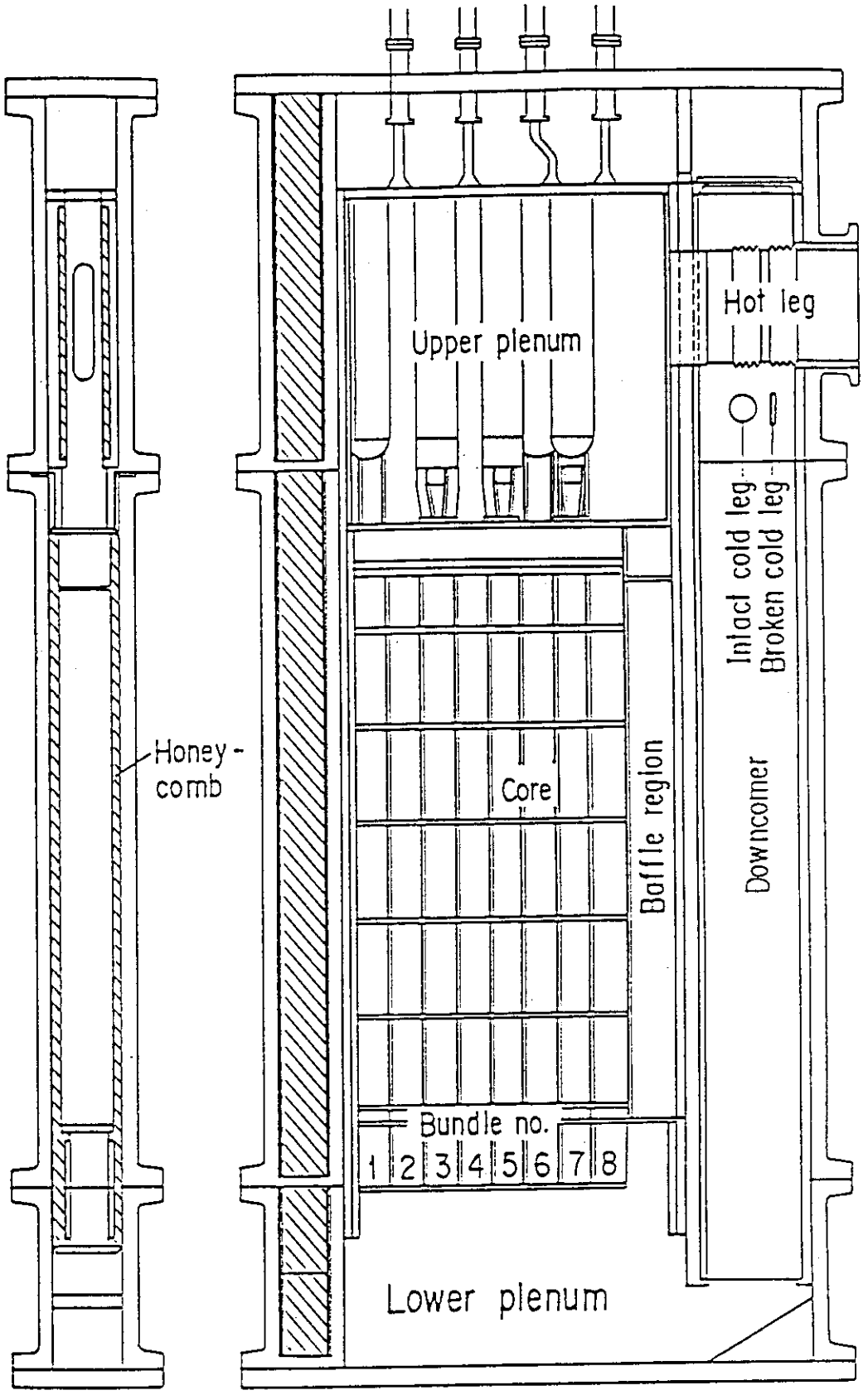

Fig. A-3 Vertical Cross Sections of Pressure Vessel

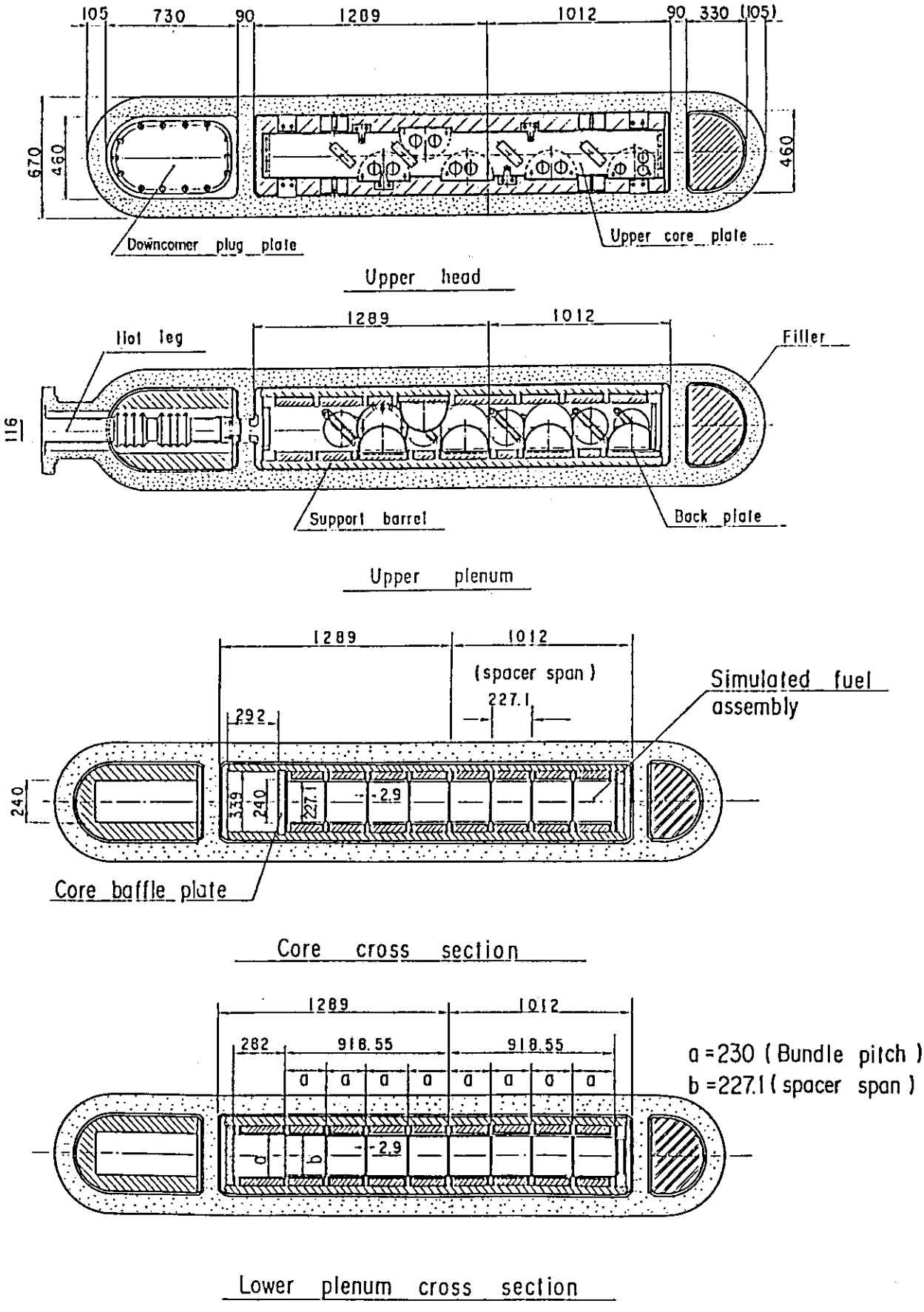

Fig. A-4 Horizontal Cross Sections of Pressure Vessel

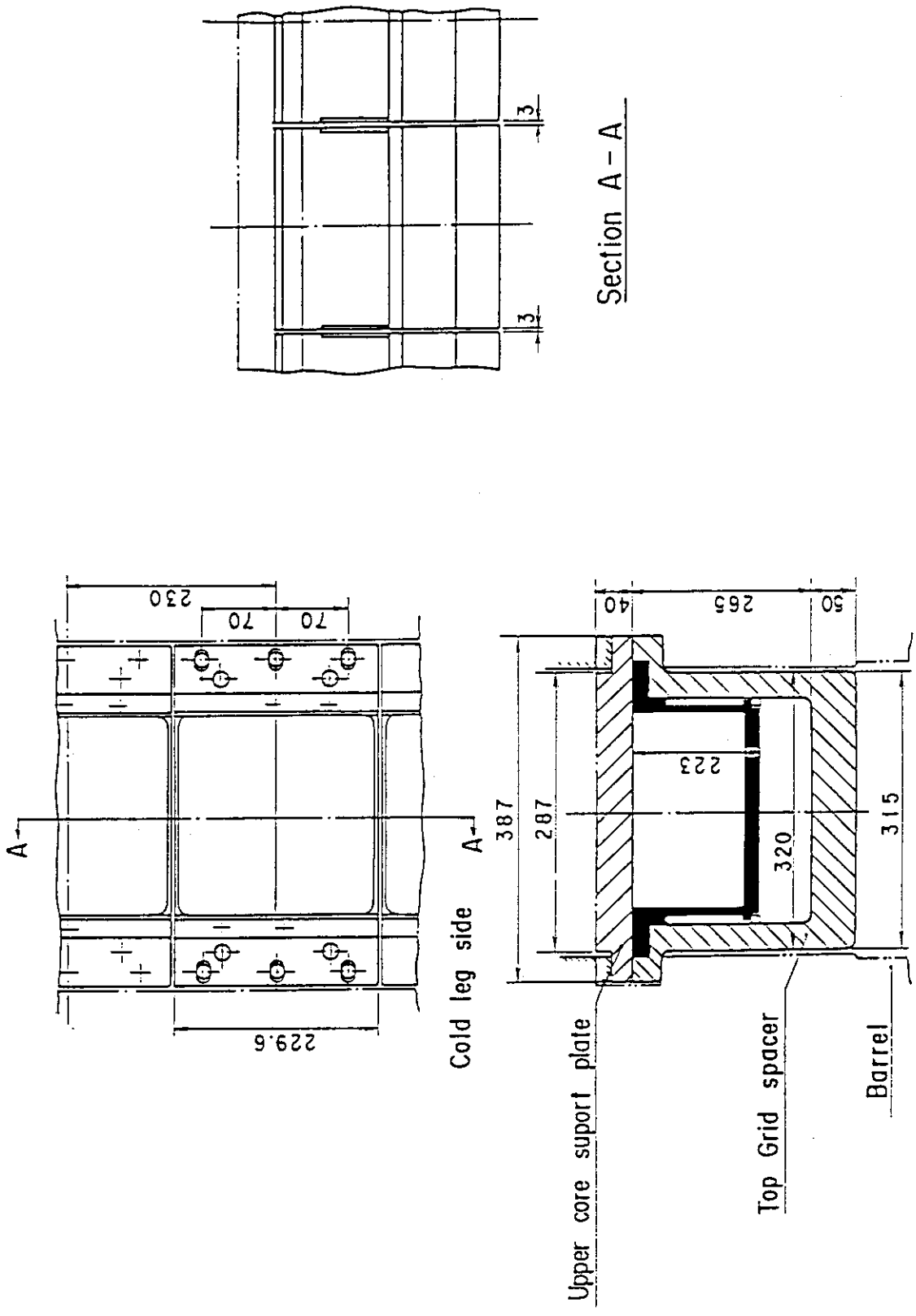

Fig. A-5 Arrangement and Principal Dimension of End Boxes and Top Grid Spacers

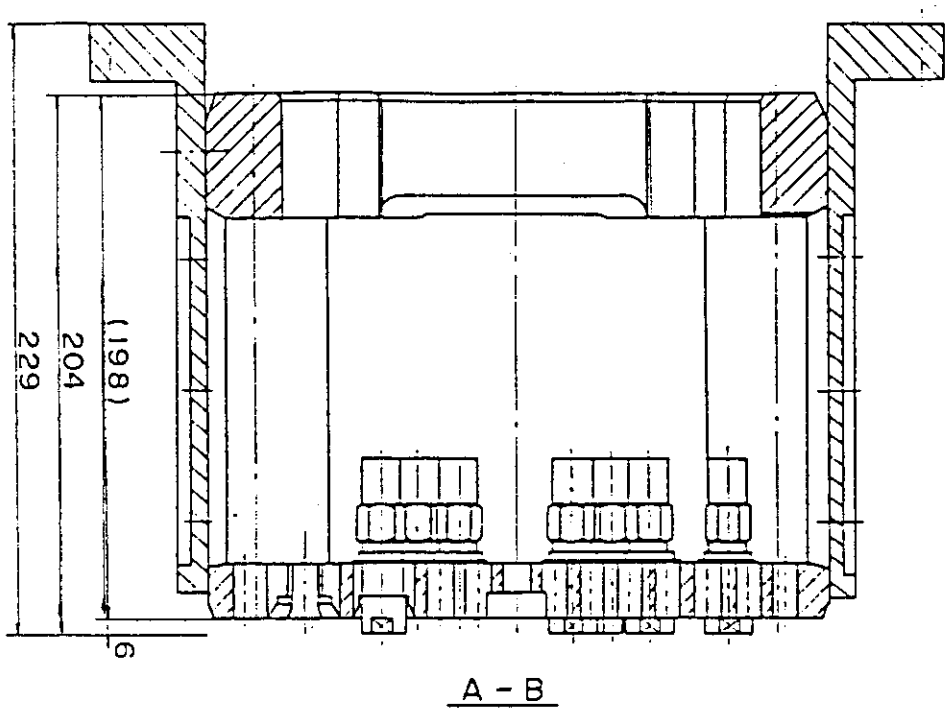

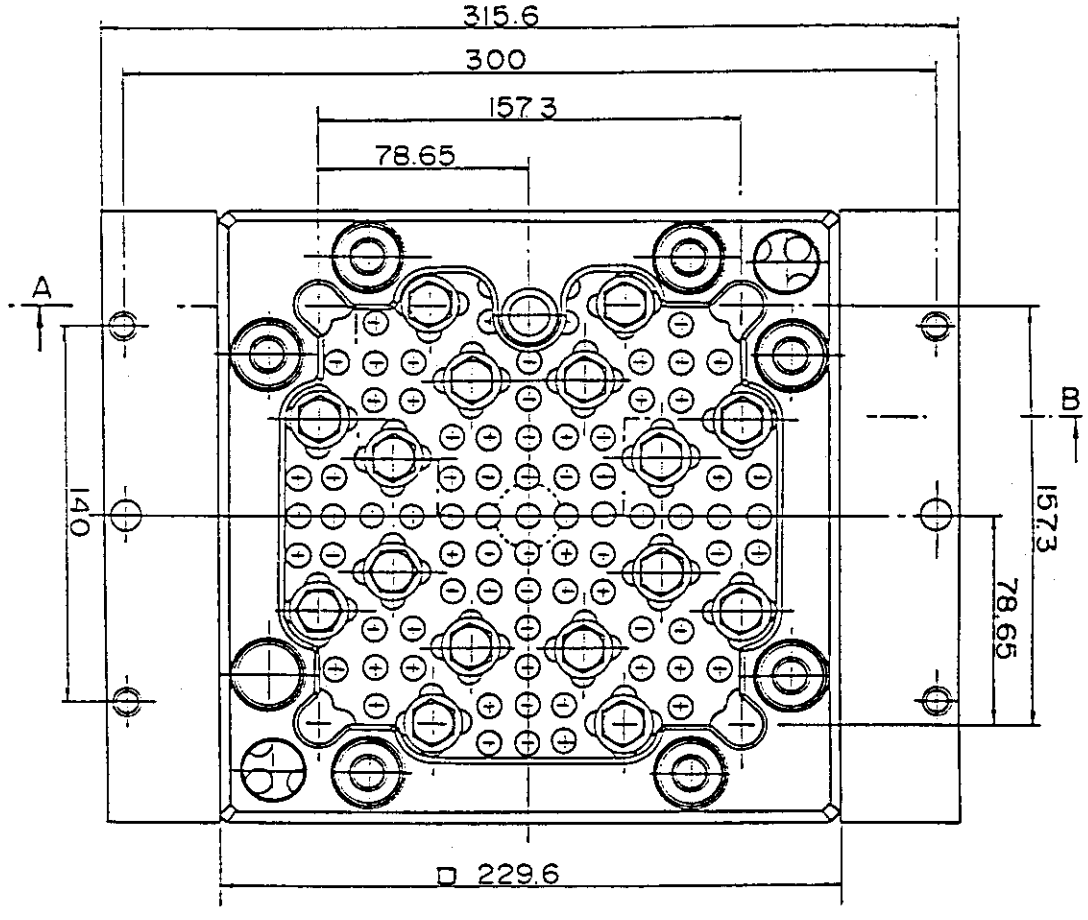

Fig. A-6 Configuration and Dimension of End Boxes

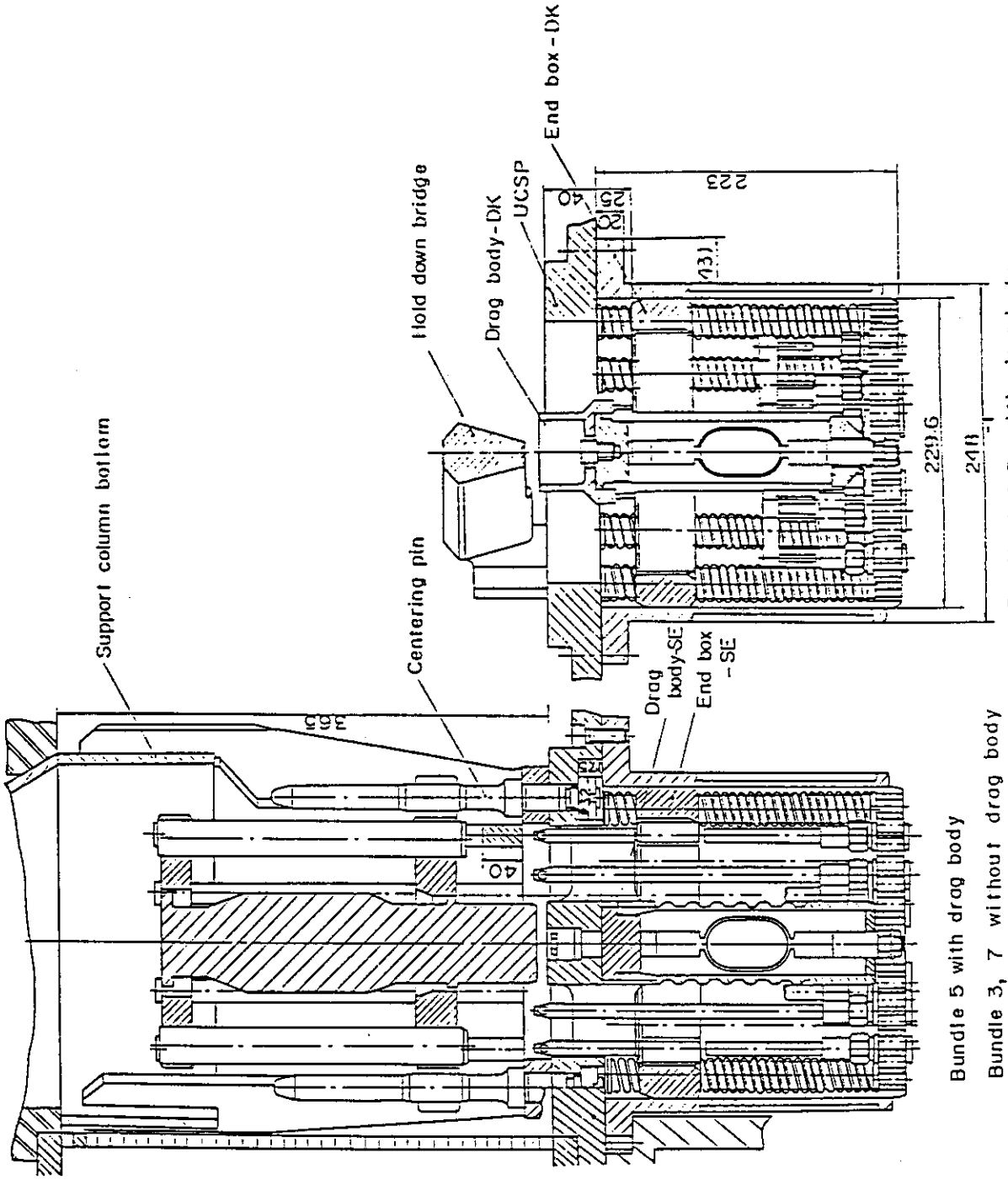

Fig. A-7 Detail of End Boxes with Drag Bodies

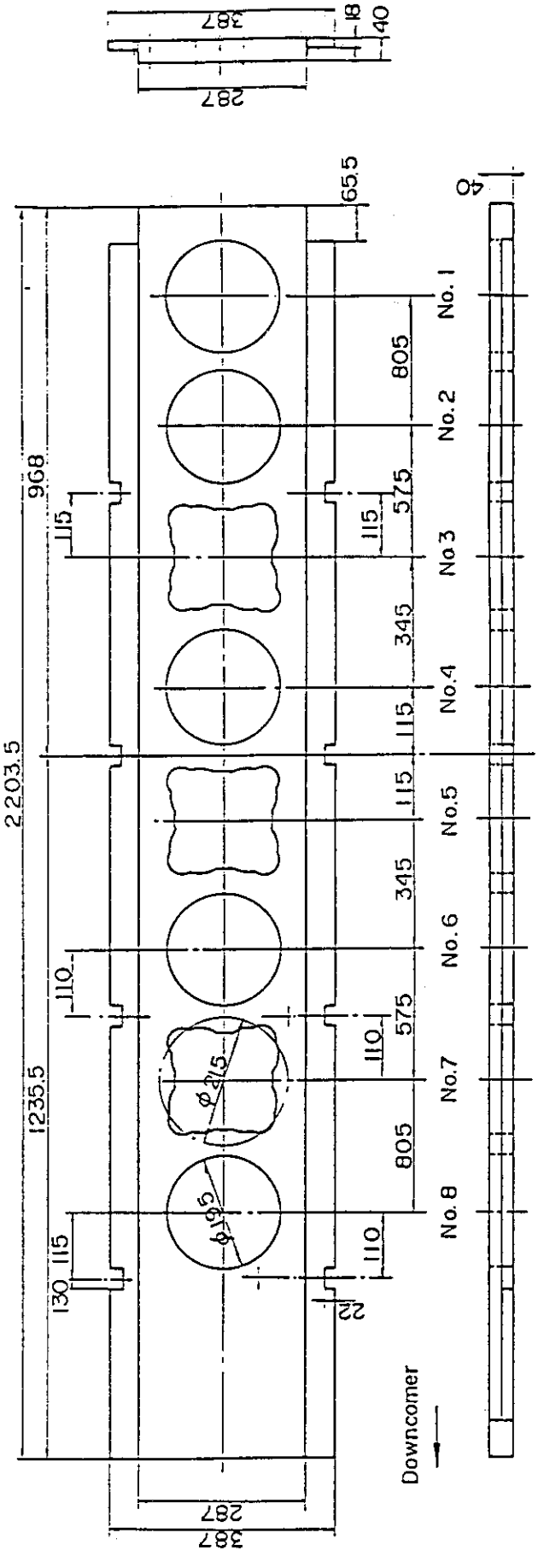

Fig. A-8 Dimension of Upper Core Support Plate

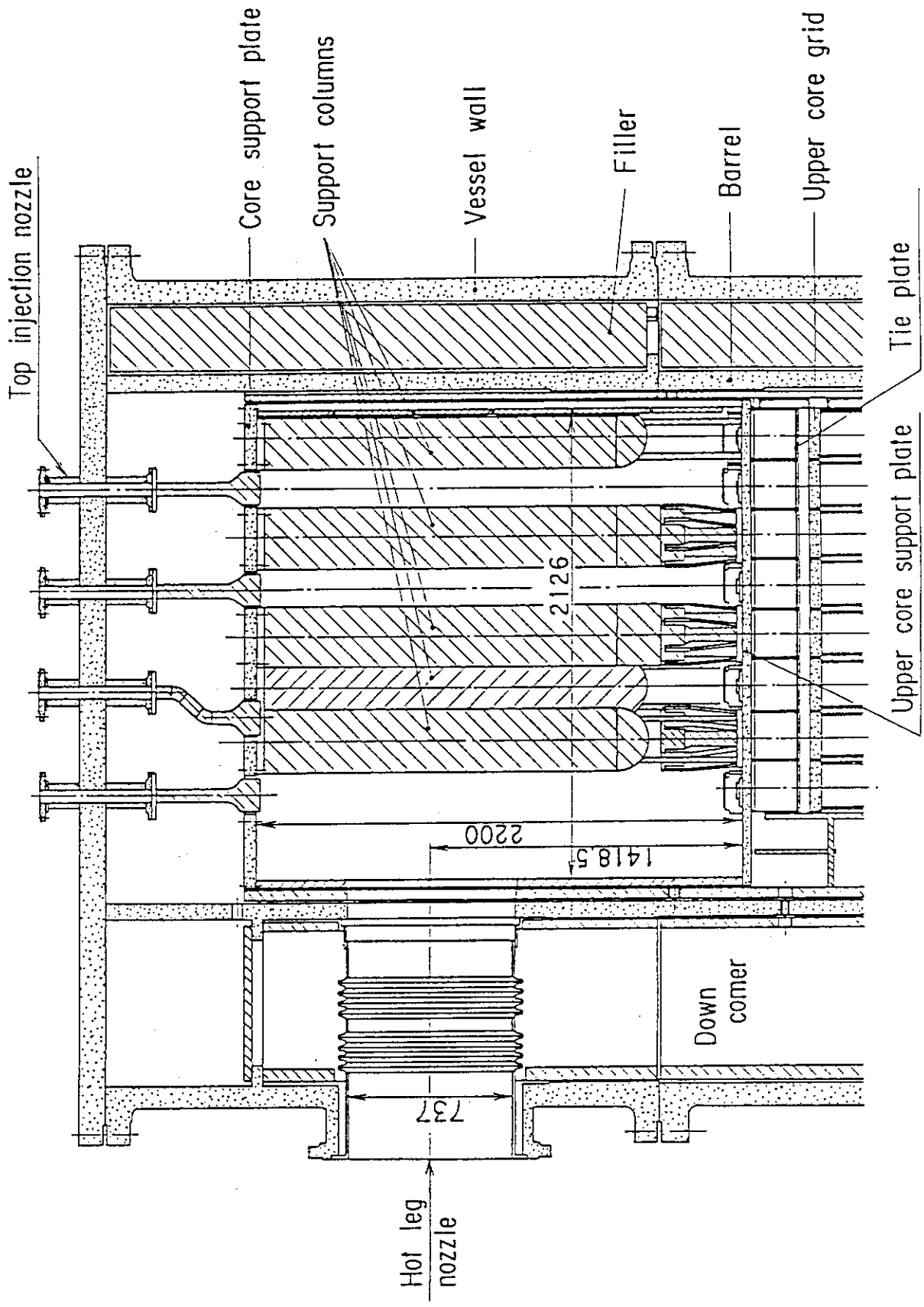

Fig. A-9 Vertical Cross Section of Upper Plenum Internals

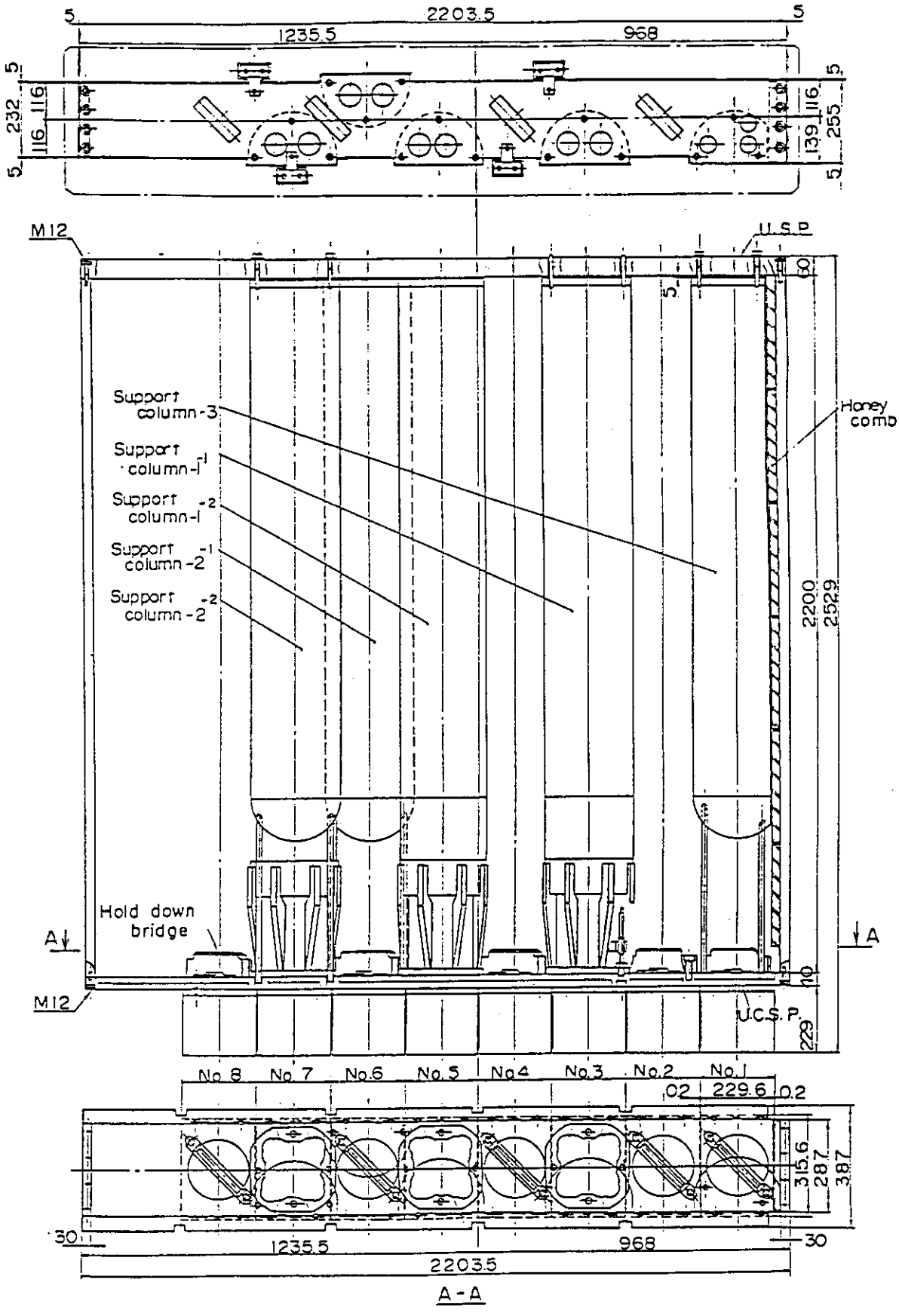

Fig. A-10 Three Kinds of CRGA Support Column

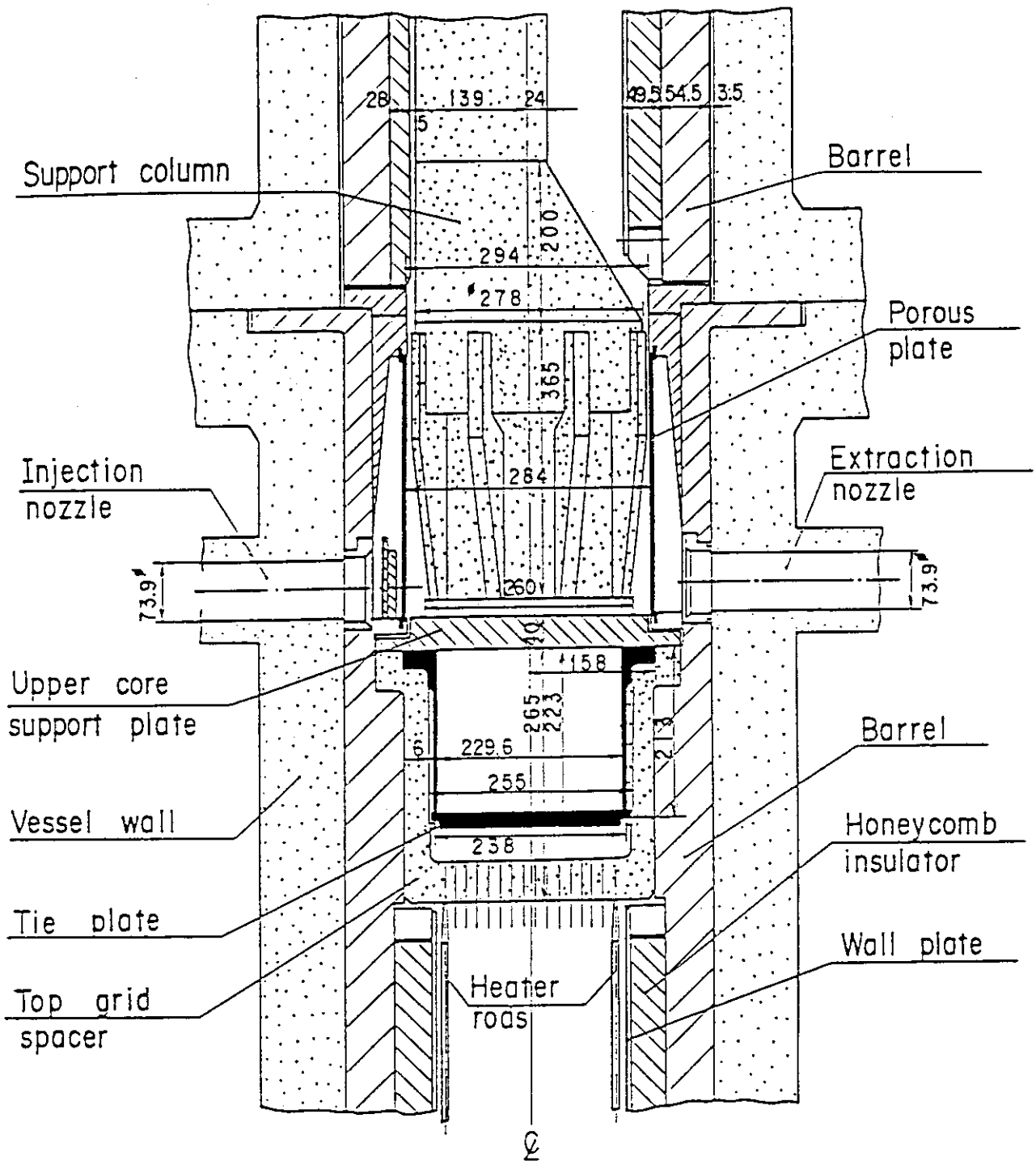

Fig. A-11 Vertical Cross Section of Interface between Core and Upper Plenum

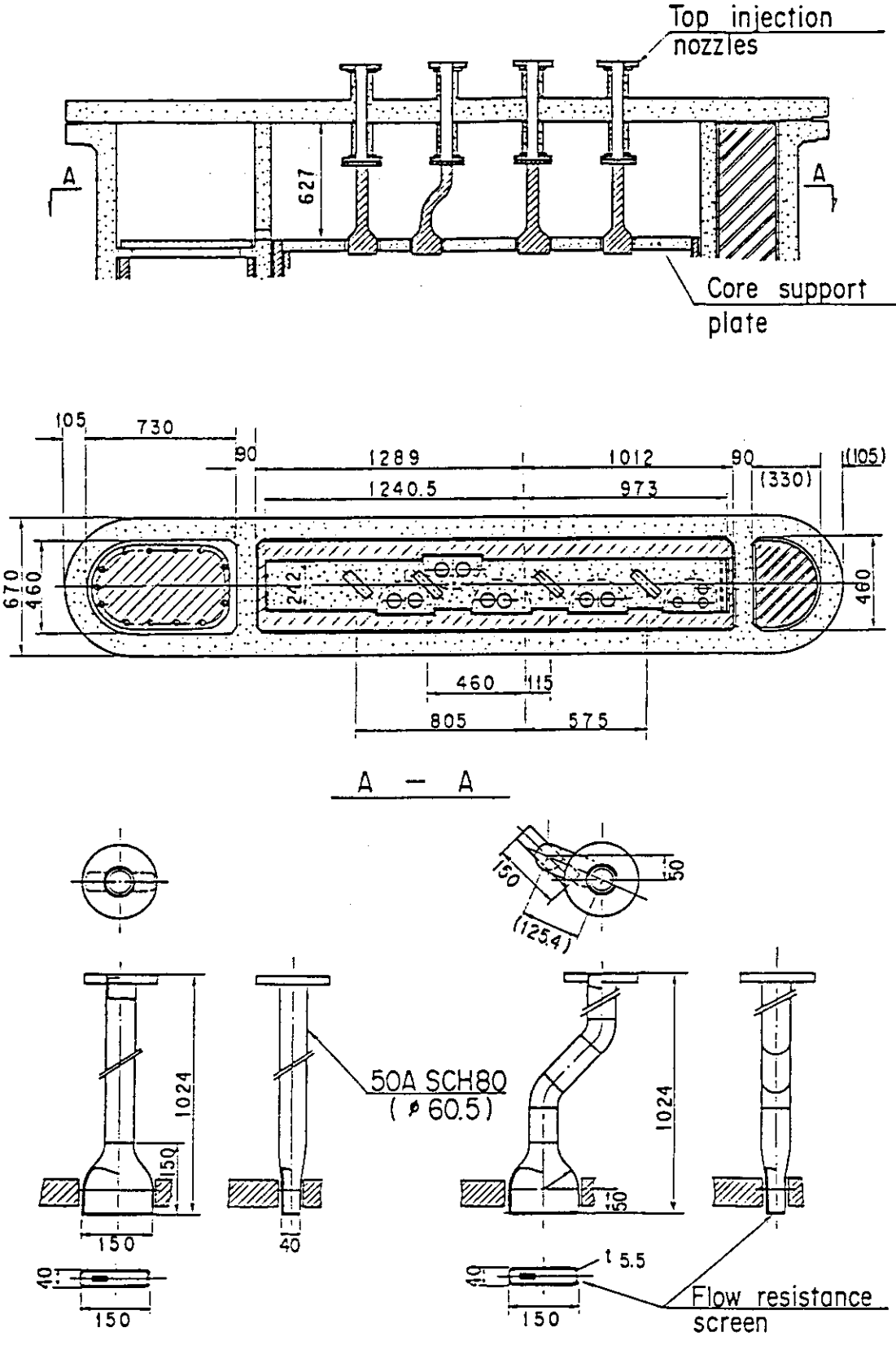

Fig. A-12 Schematic of Upper Head

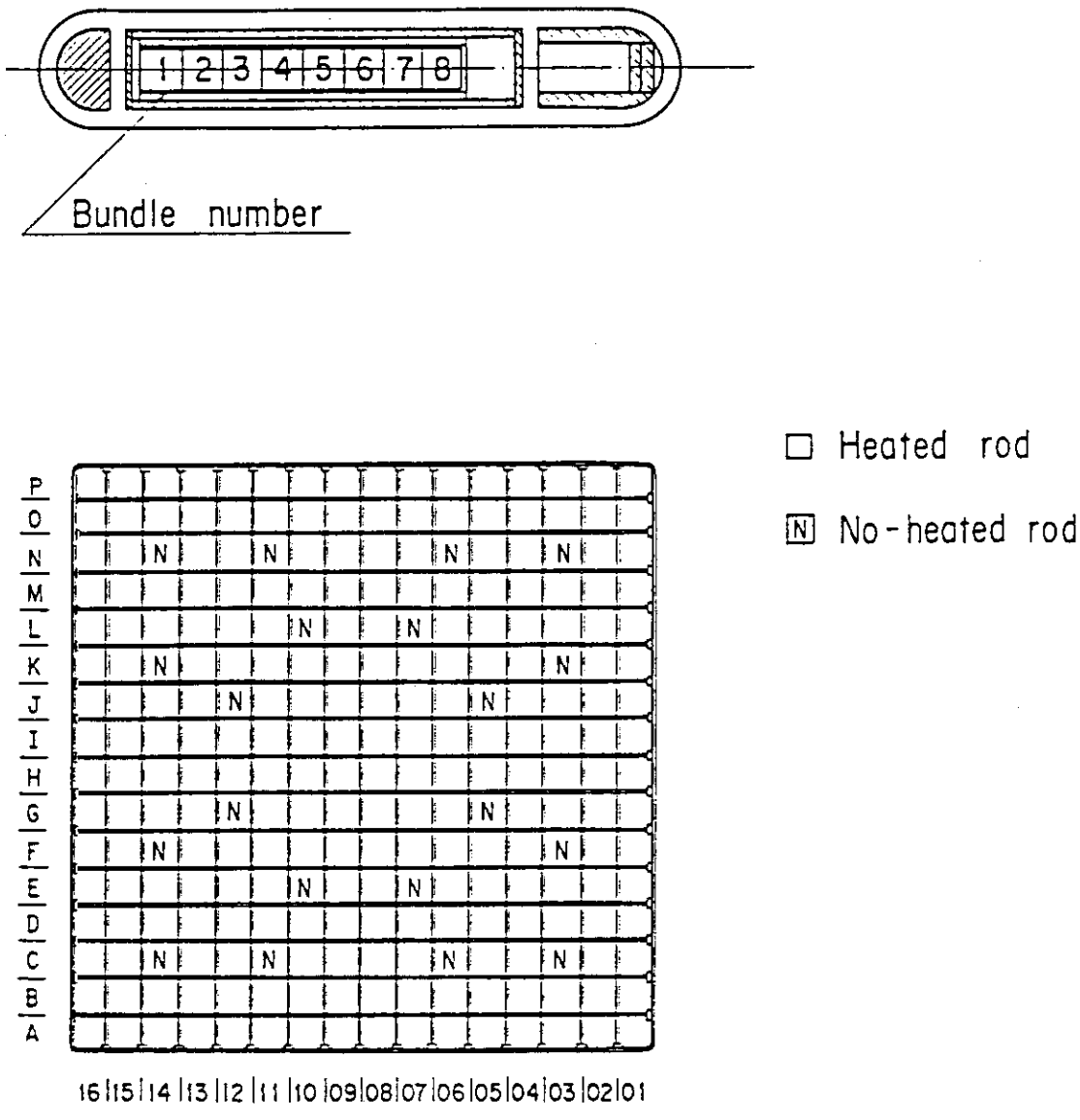

Fig. A-13 Arrangement of Heater Rod Bundles

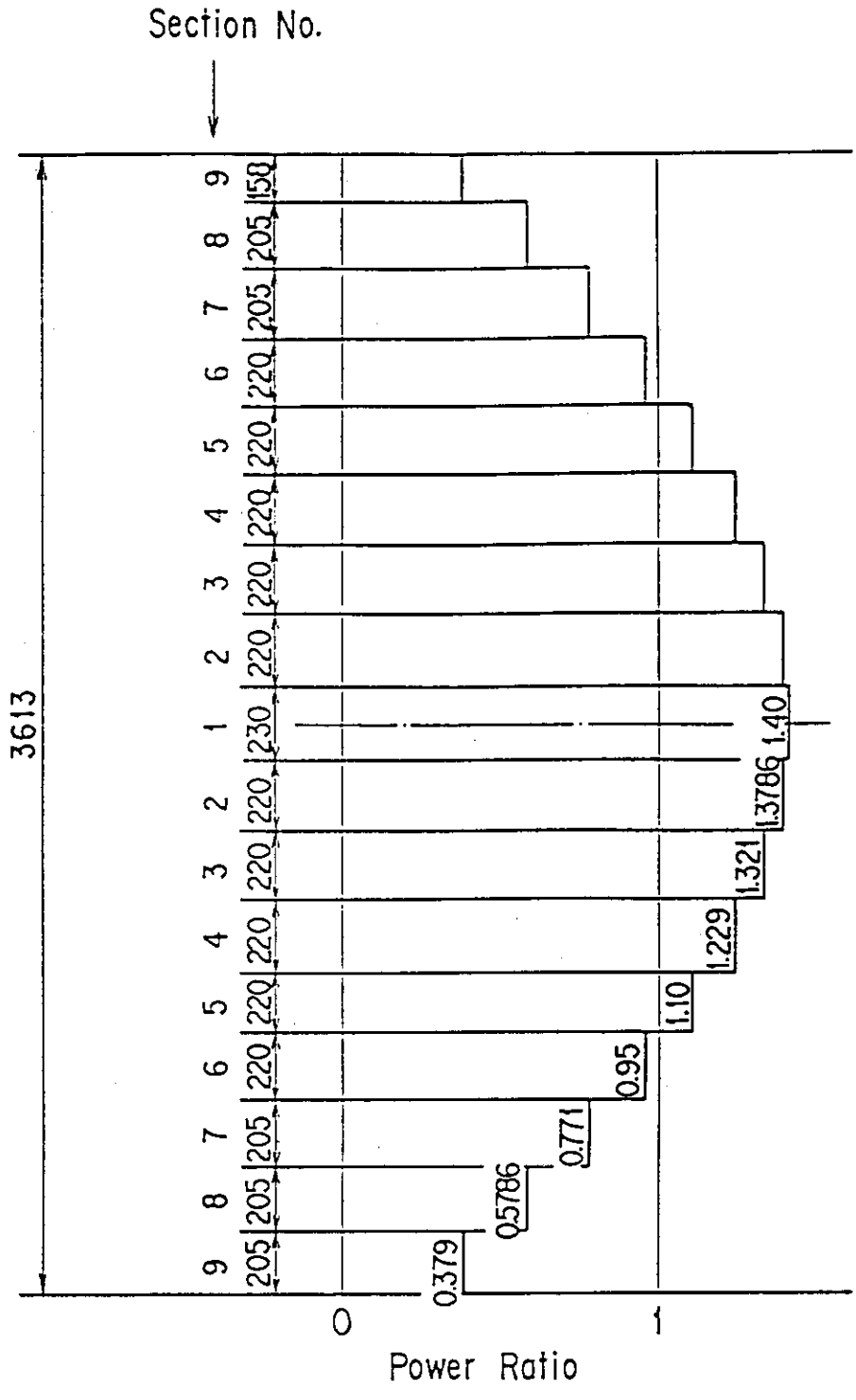

Fig. A-14 Axial Power Distribution of Heater Rods

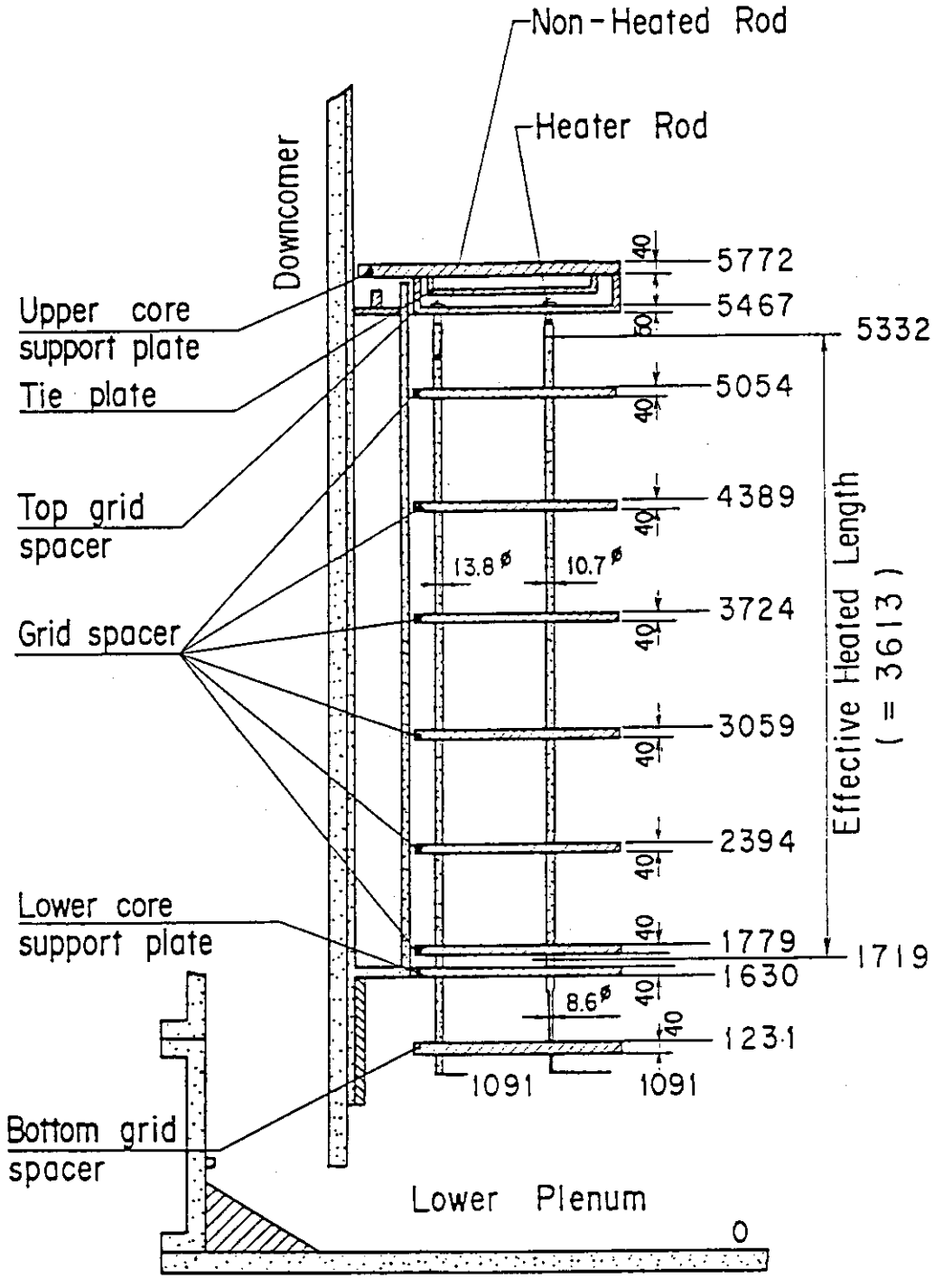

Fig. A-15 Relative Elevation and Dimension of Core

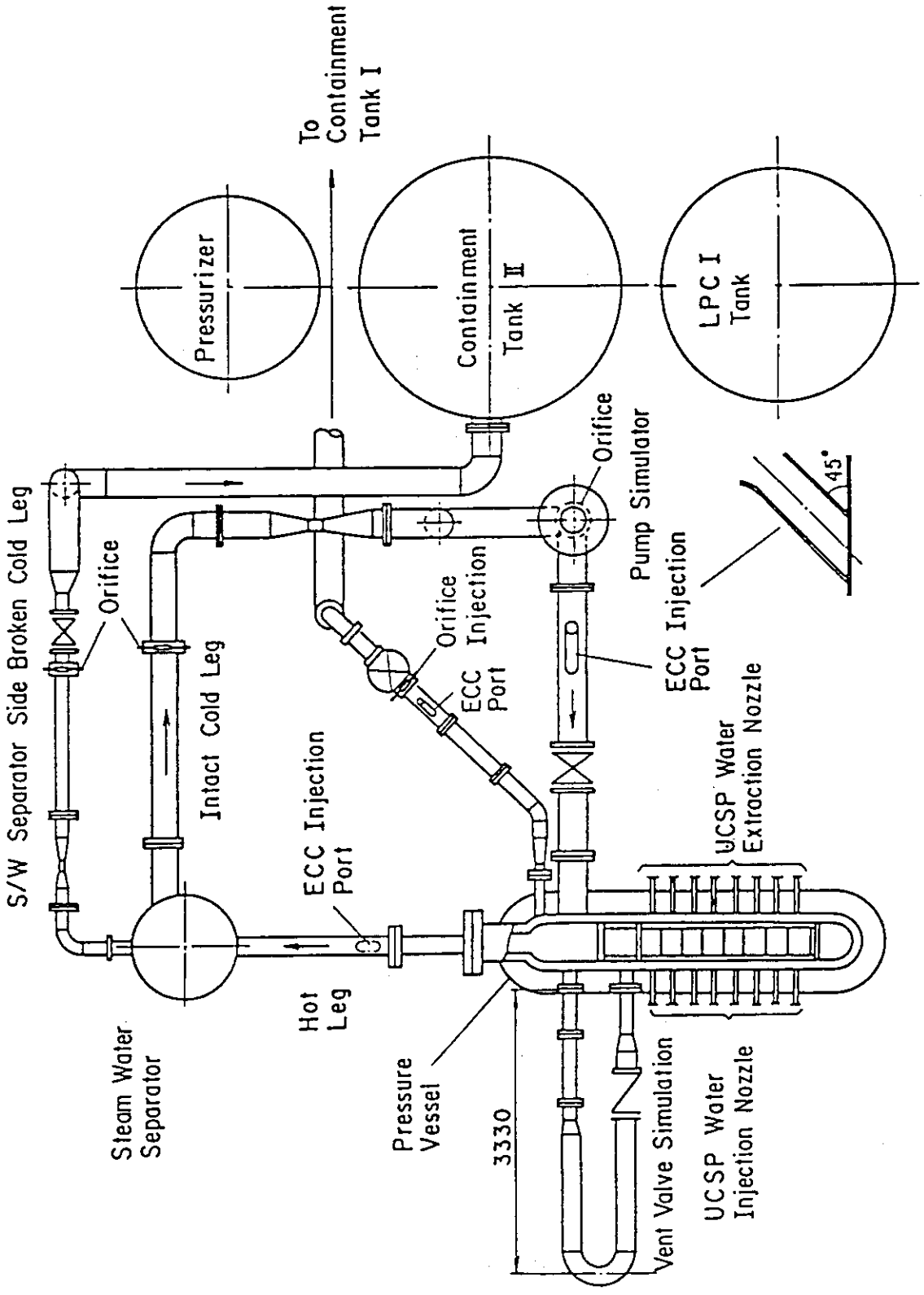

Fig. A-16 Overview of the Arrangements of SCTF

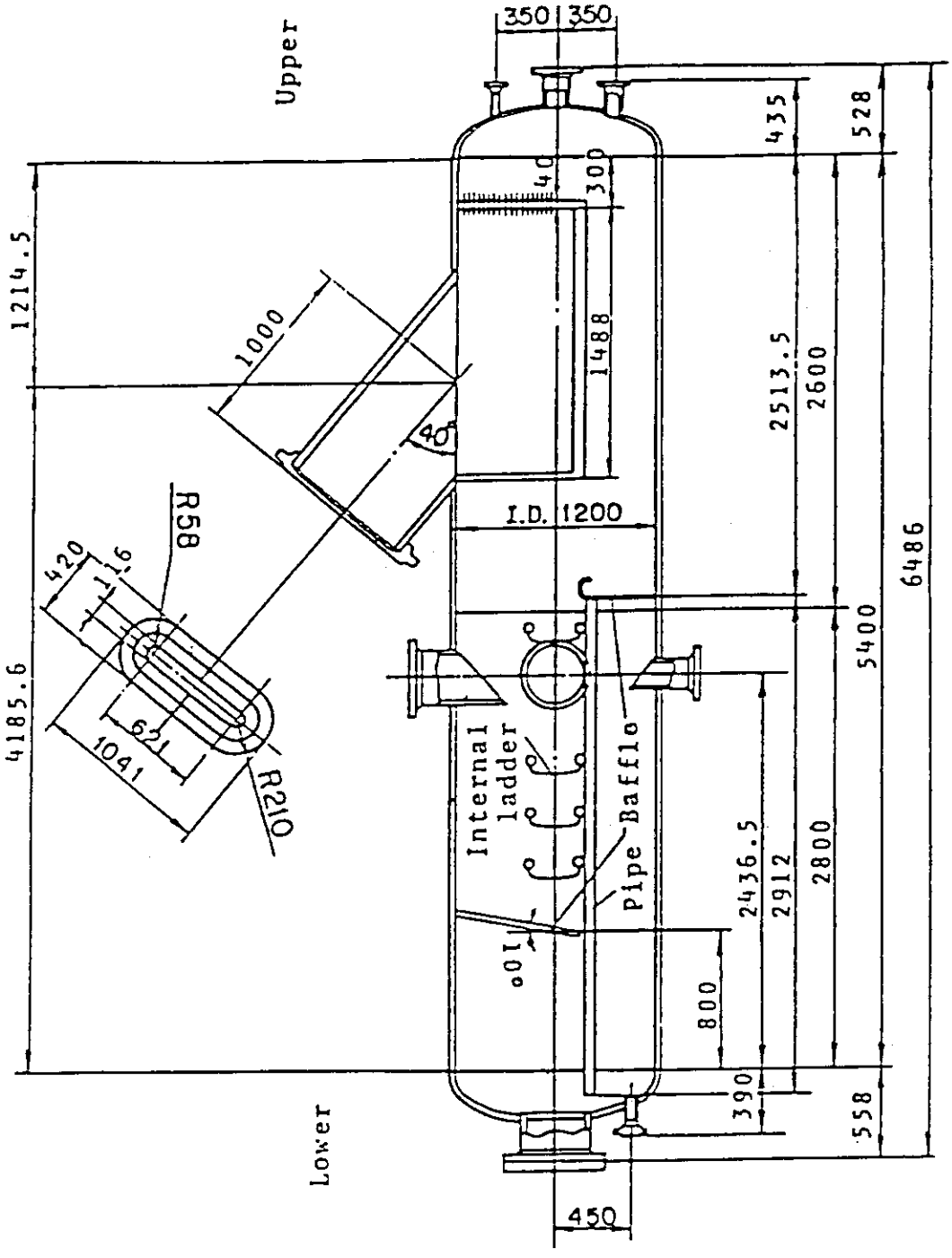

Fig. A-17 Steam/Water Separator

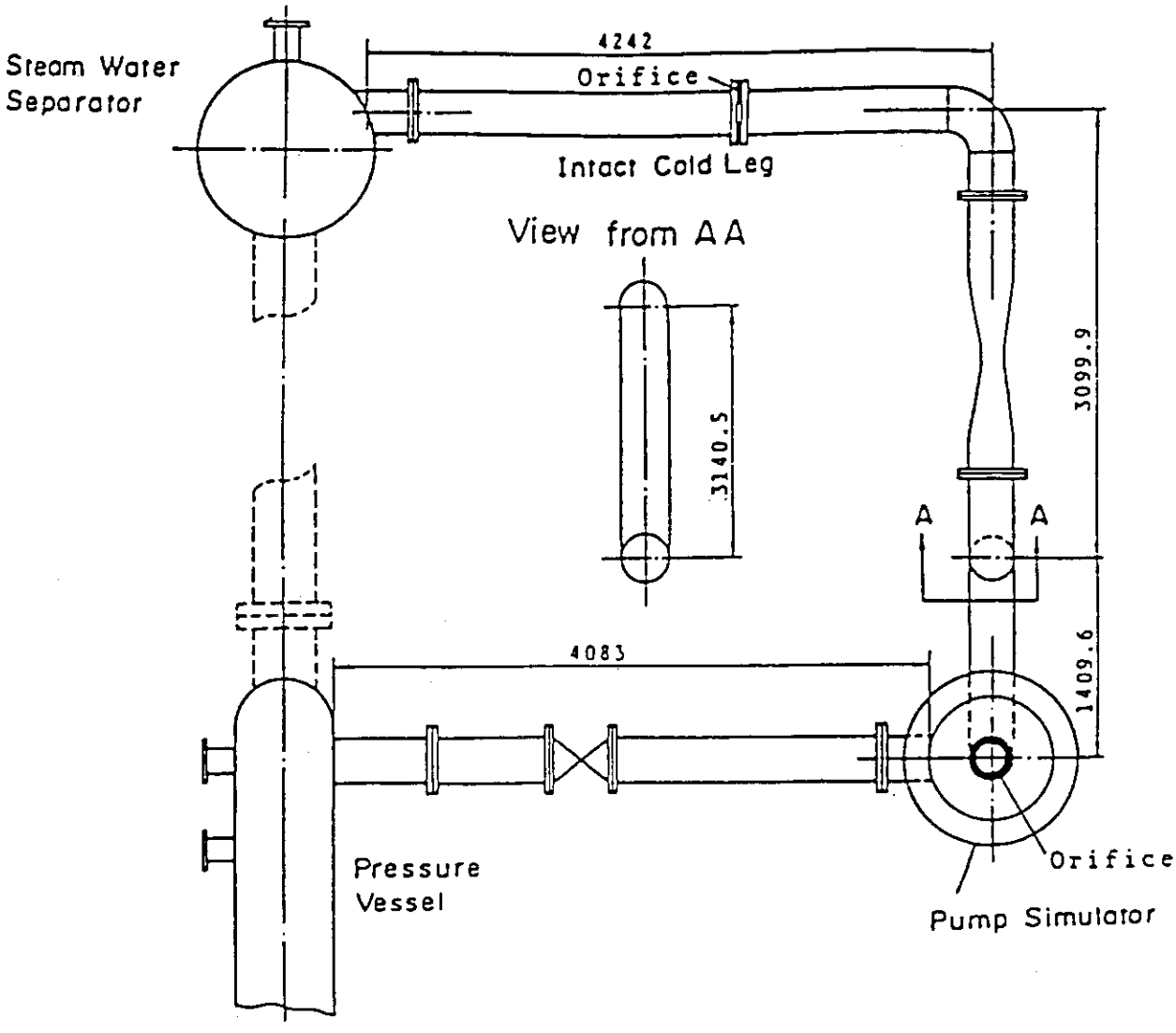

Fig. A-18 Arrangement of Intact Cold Leg

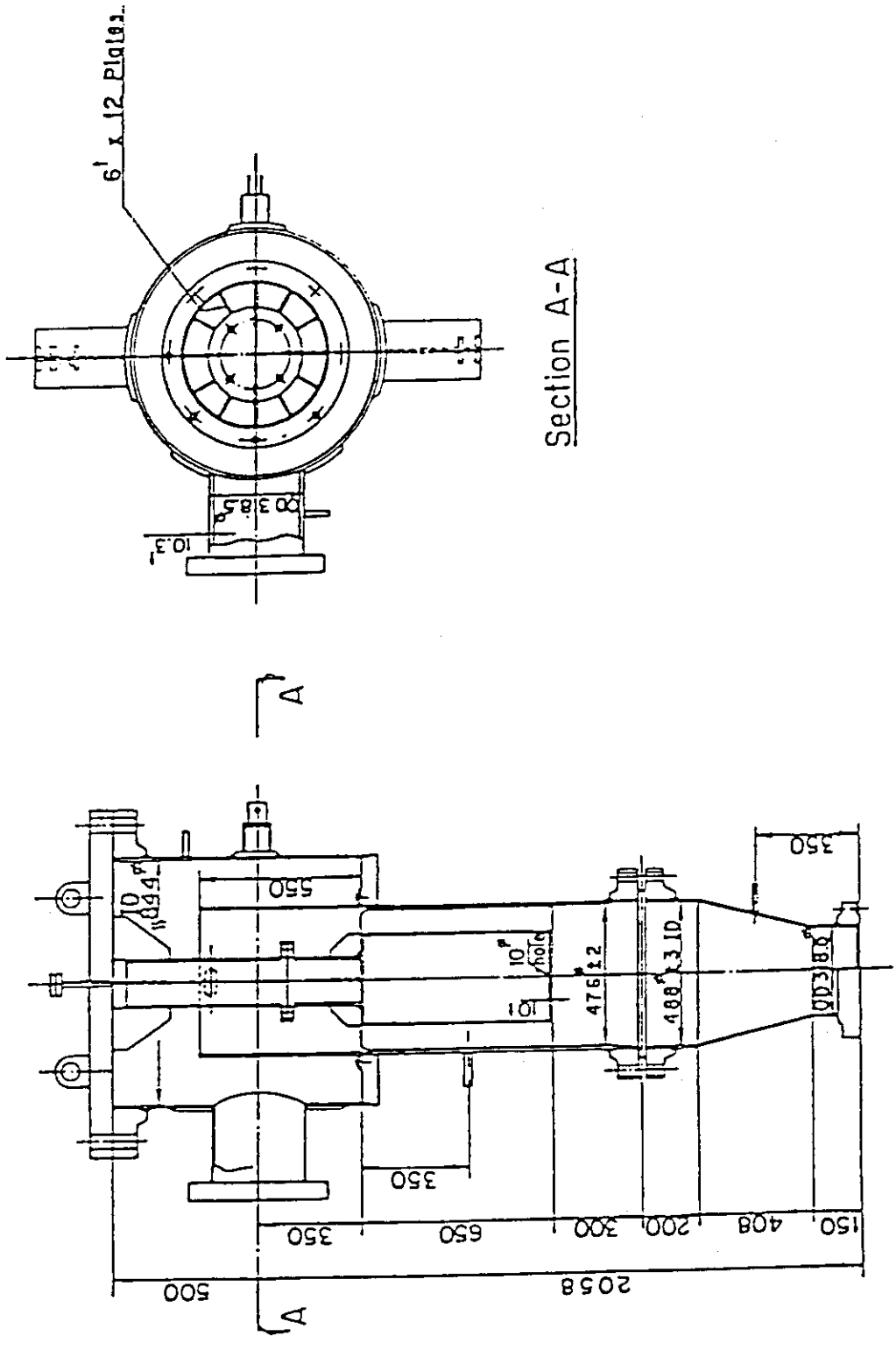

Fig. A-19 Configuration and Dimension of Pump Simulator

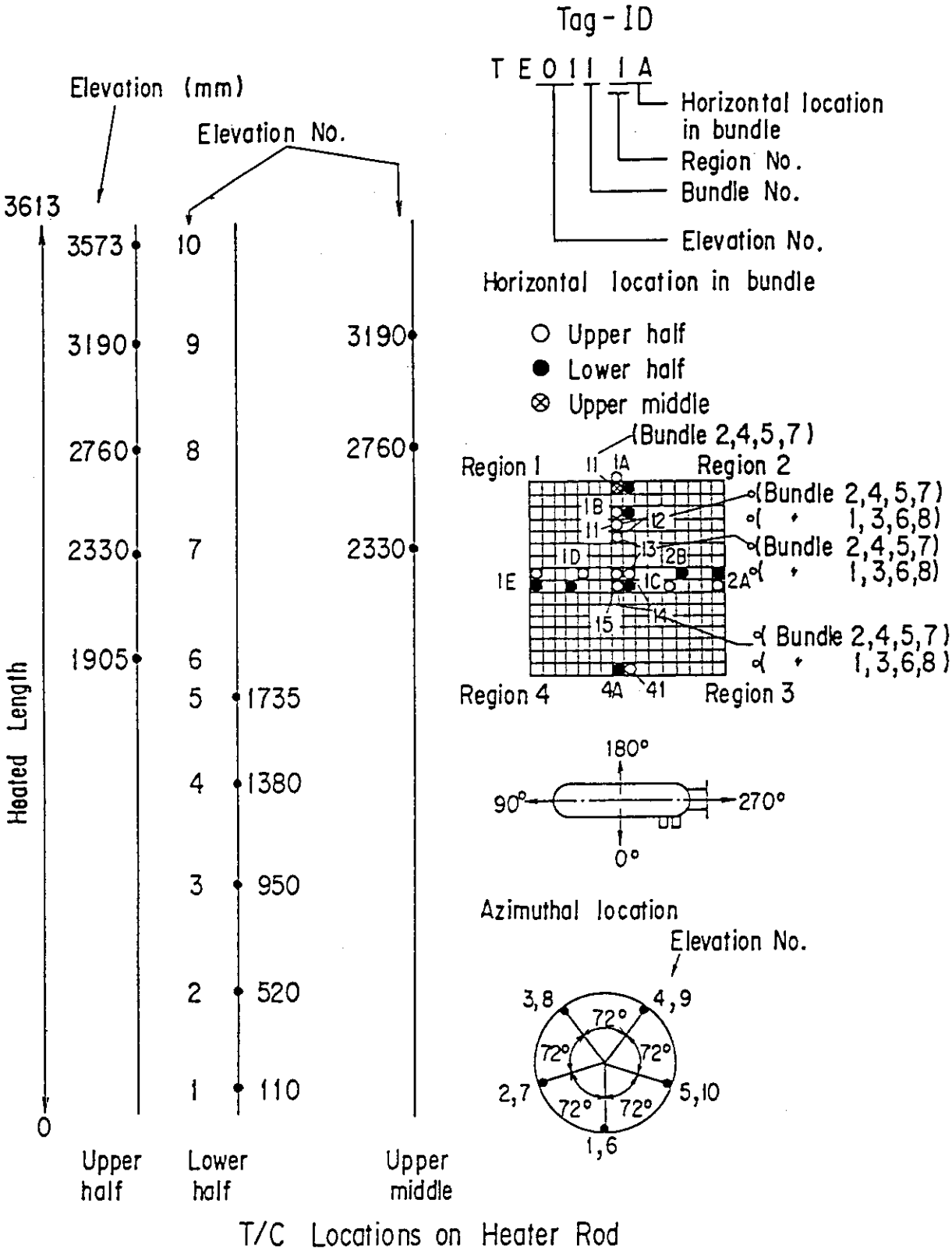

Fig. A-20 Thermocouple Locations of Heater Rod Surface Temperature Measurements

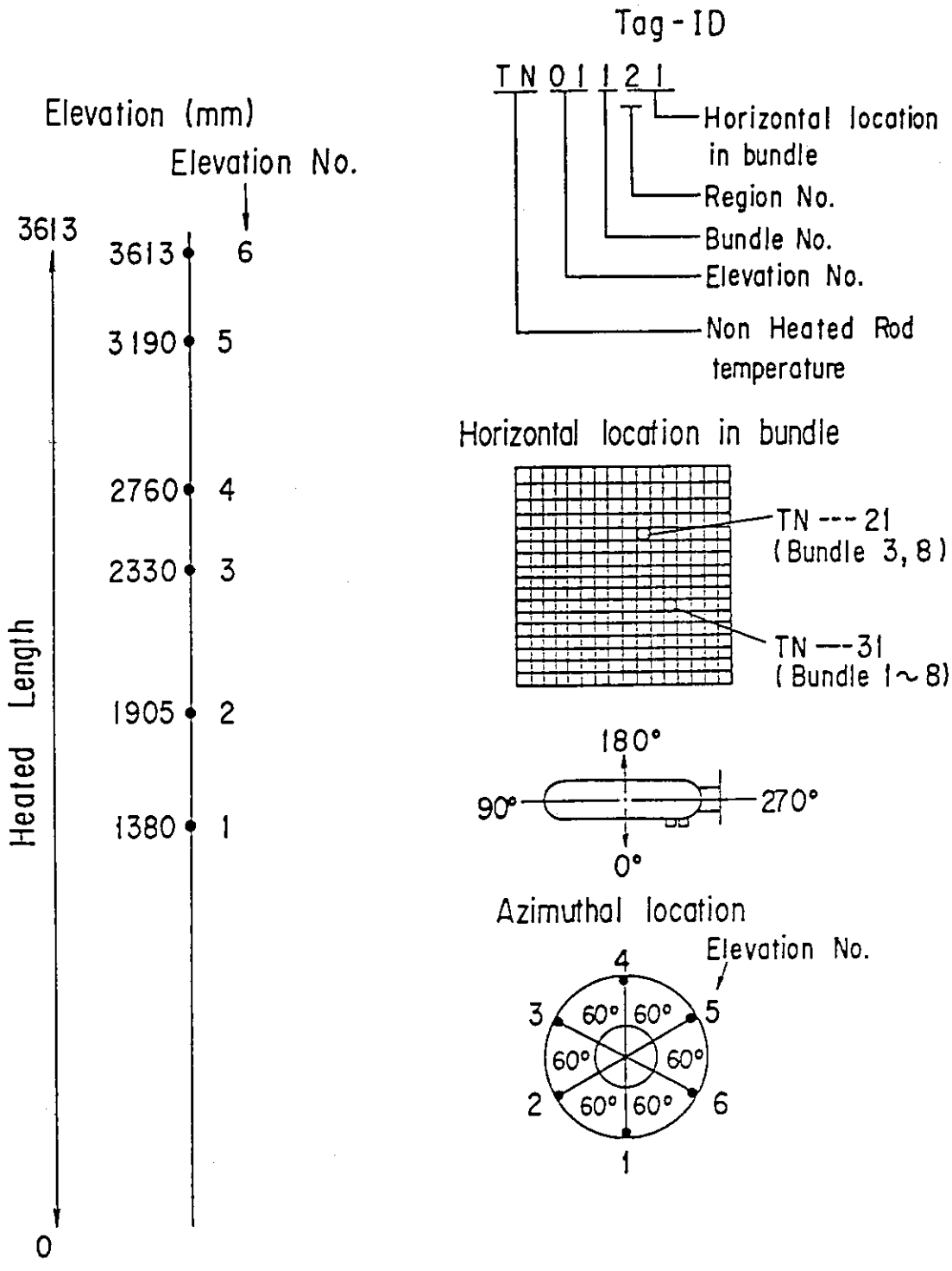

Fig. A-21 Thermocouple Locations of Non-Heated Rod Surface temperature Measurements

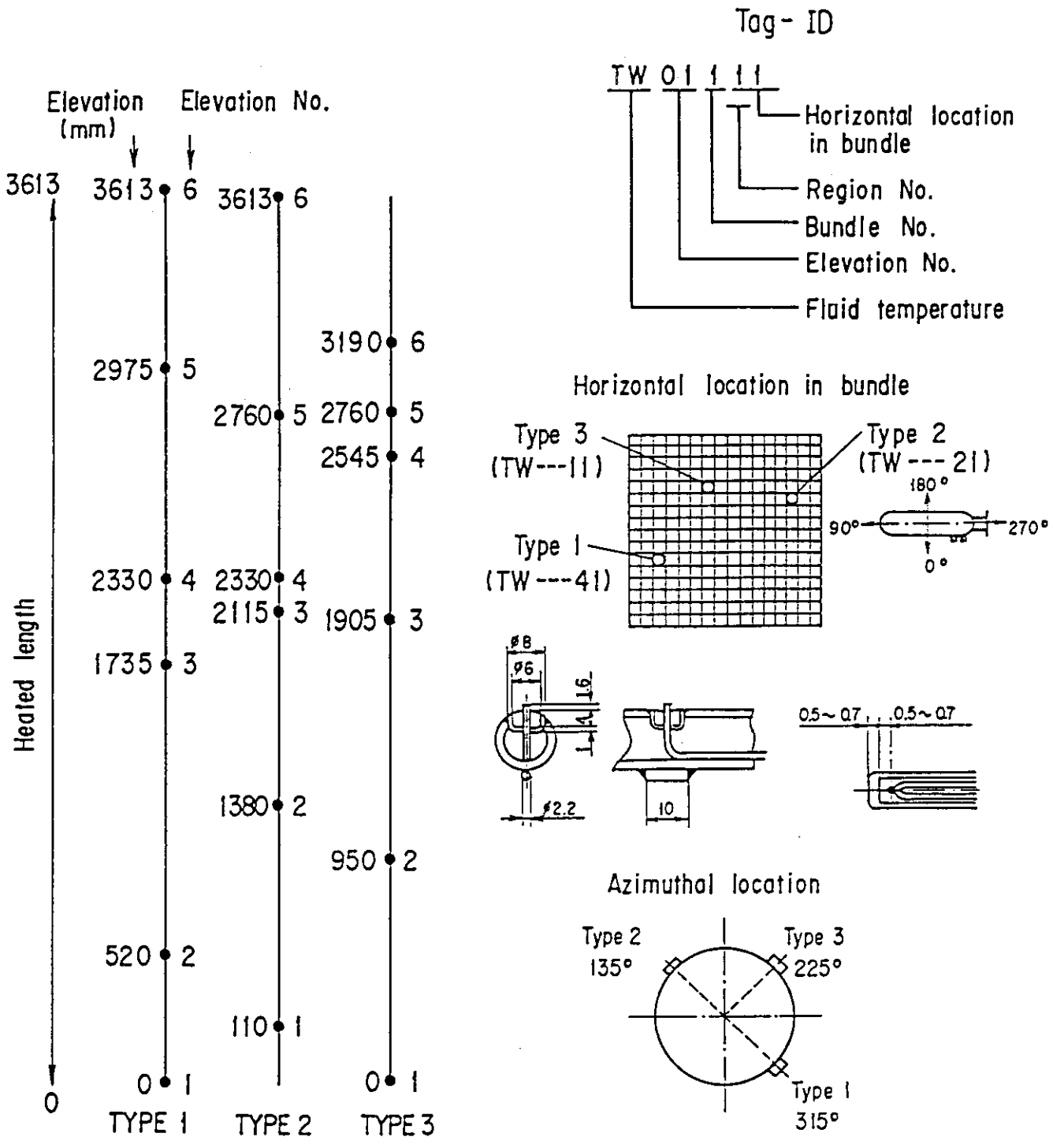

Fig. A-22 Thermocouple Locations of Fluid Temperature Measurements in Core

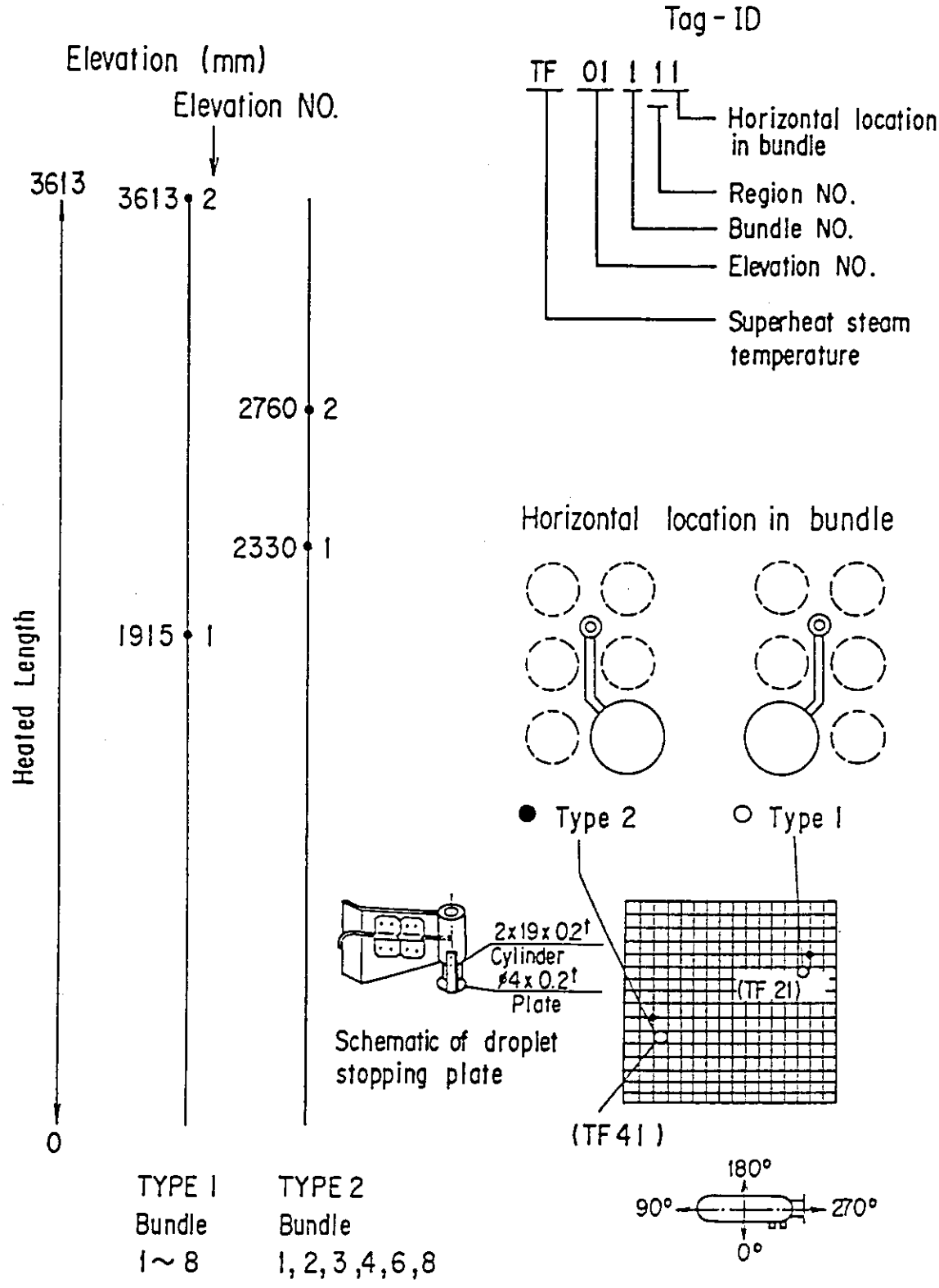

Fig. A-23 Thermocouple Locations of Steam Temperature Measurements in Core

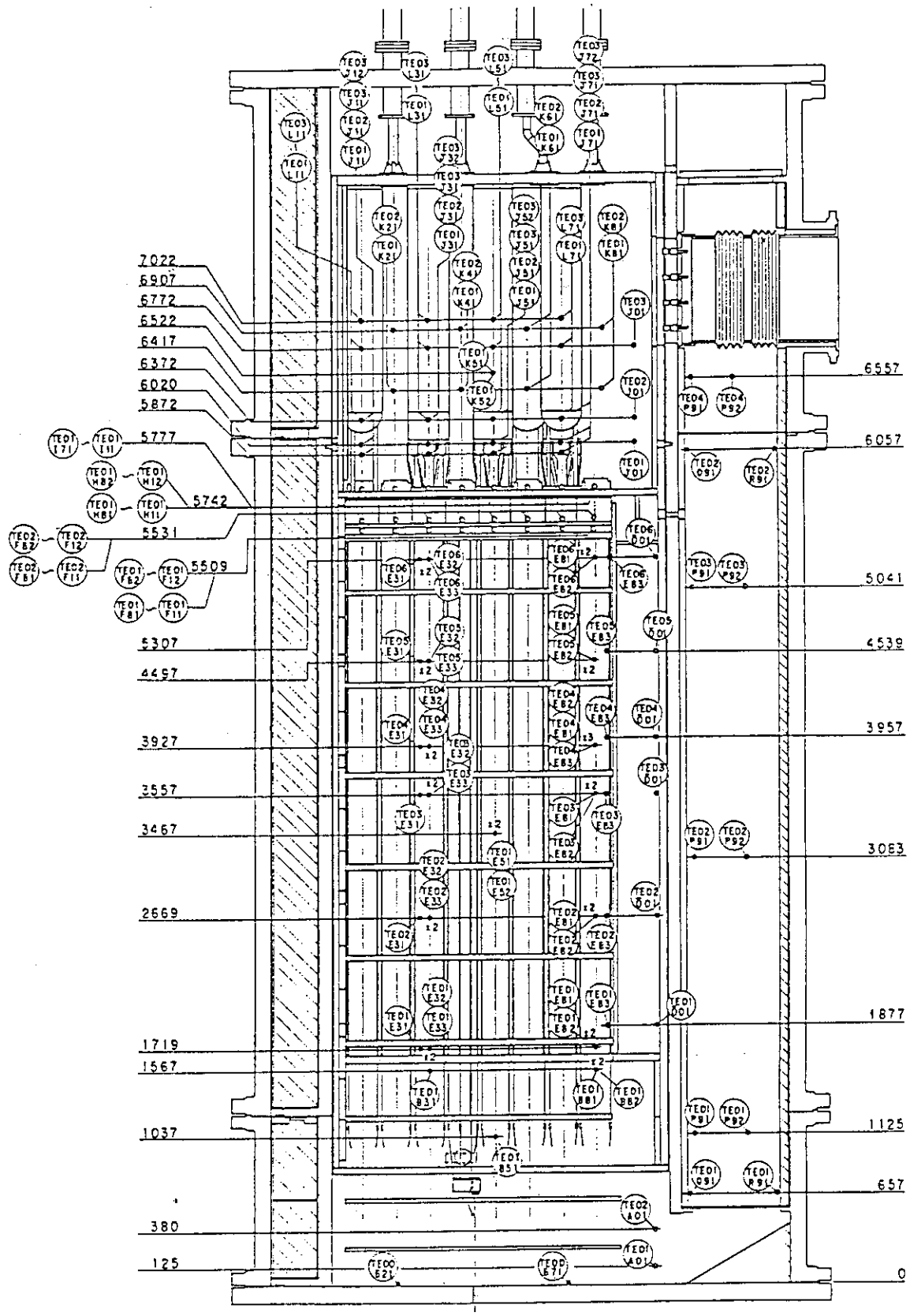

Fig. A-24 Thermocouple Locations of Temperature Measurements in Pressure Vessel except Core Region (Vertical View)

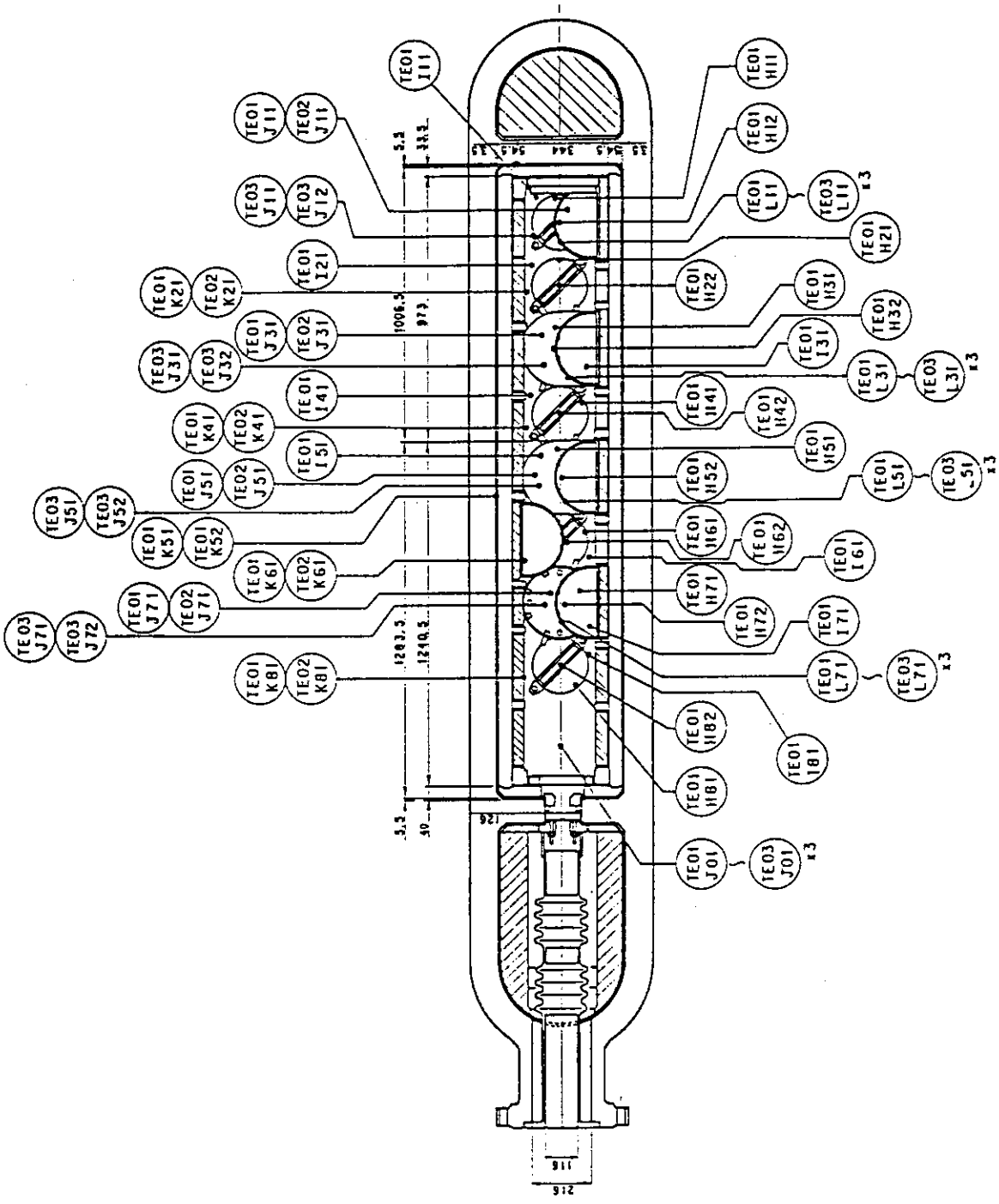

Fig. A-25 Thermocouple Locations of Temperature Measurements in Upper Plenum (Horizontal View)

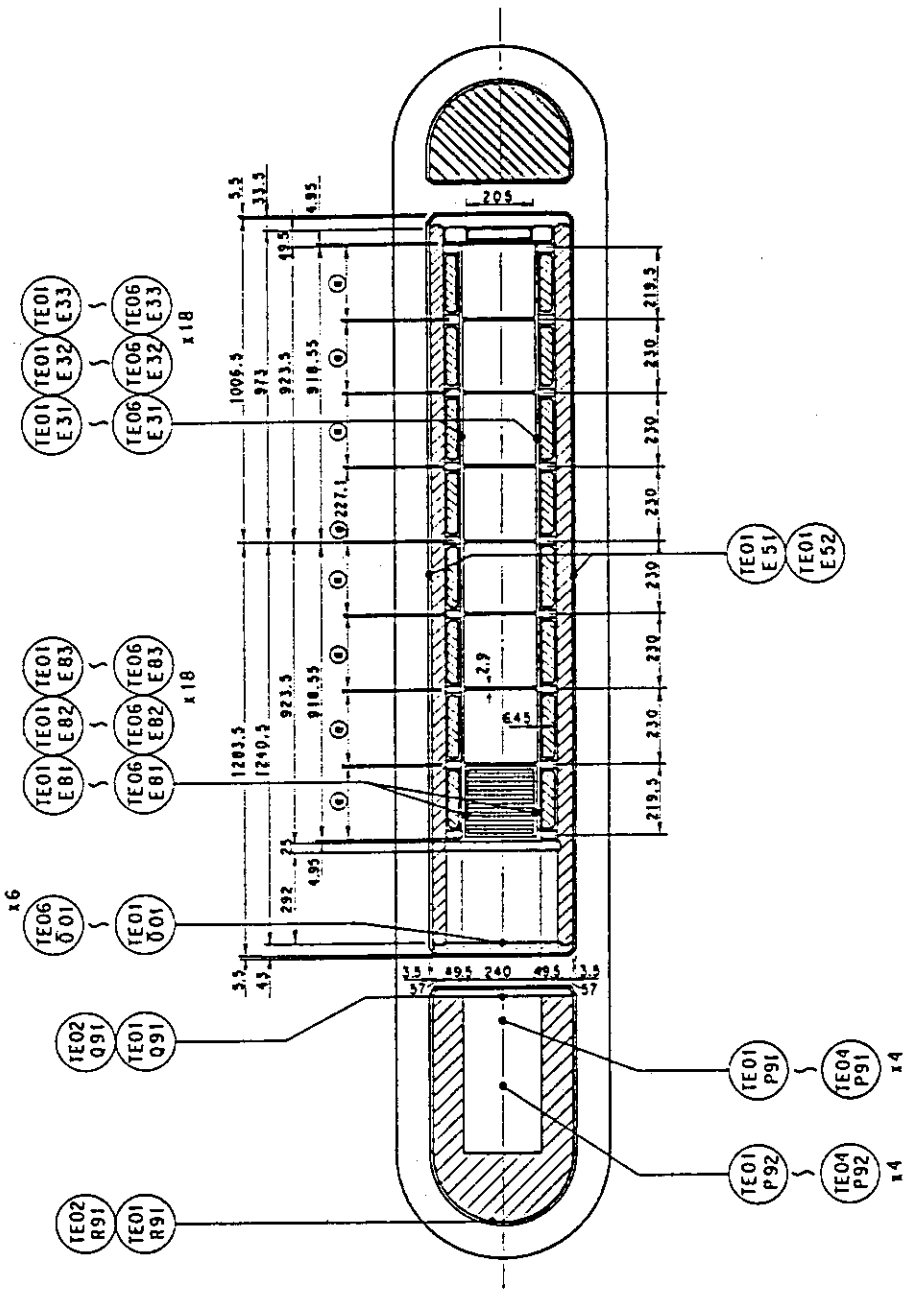

Fig. A-26 Thermocouple Locations of Temperature Measurements in Pressure Vessel except Upper Plenum (Horizontal View)

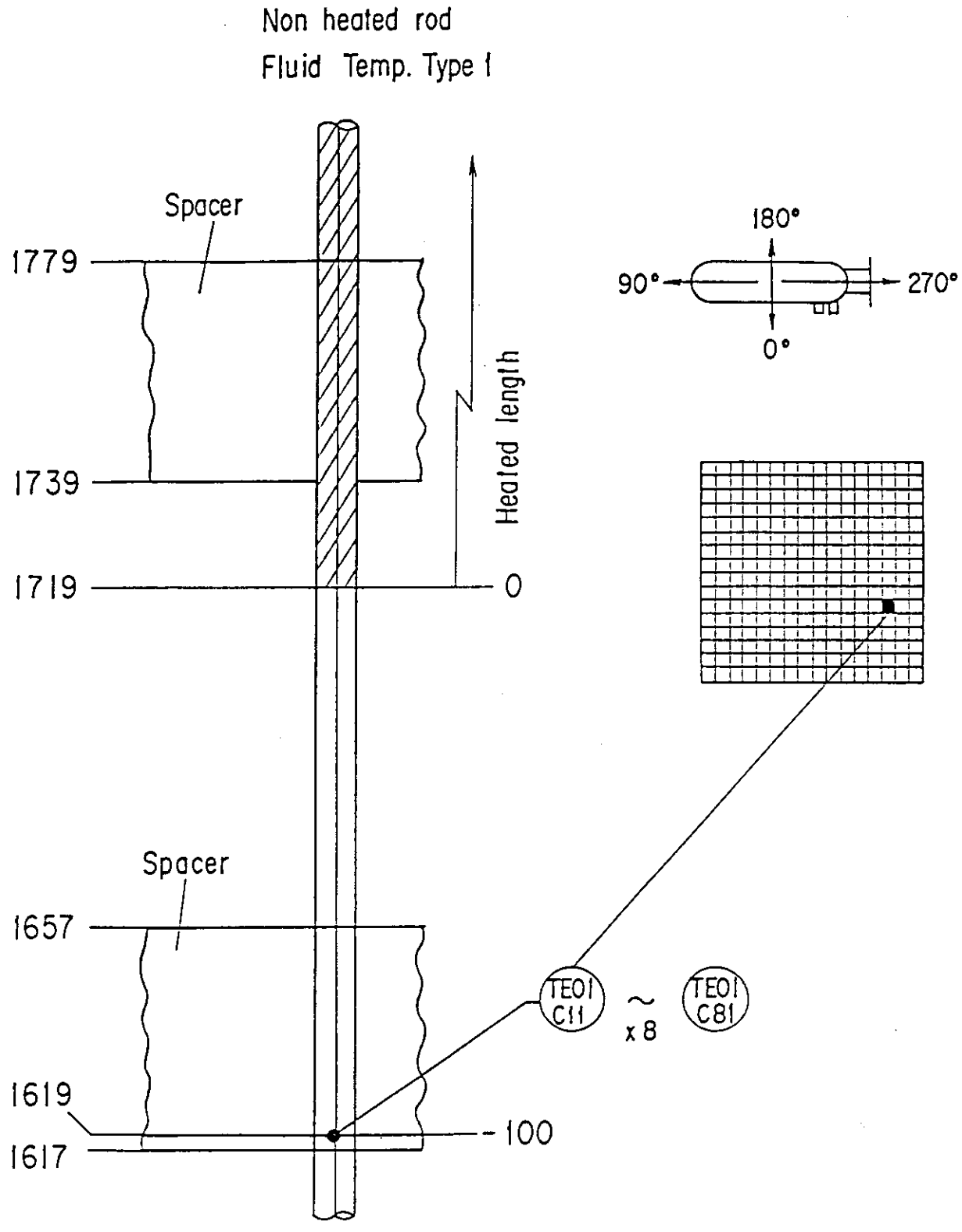

Fig. A-27 Thermocouple Locations of Fluid Temperature Measurements at Core Inlet

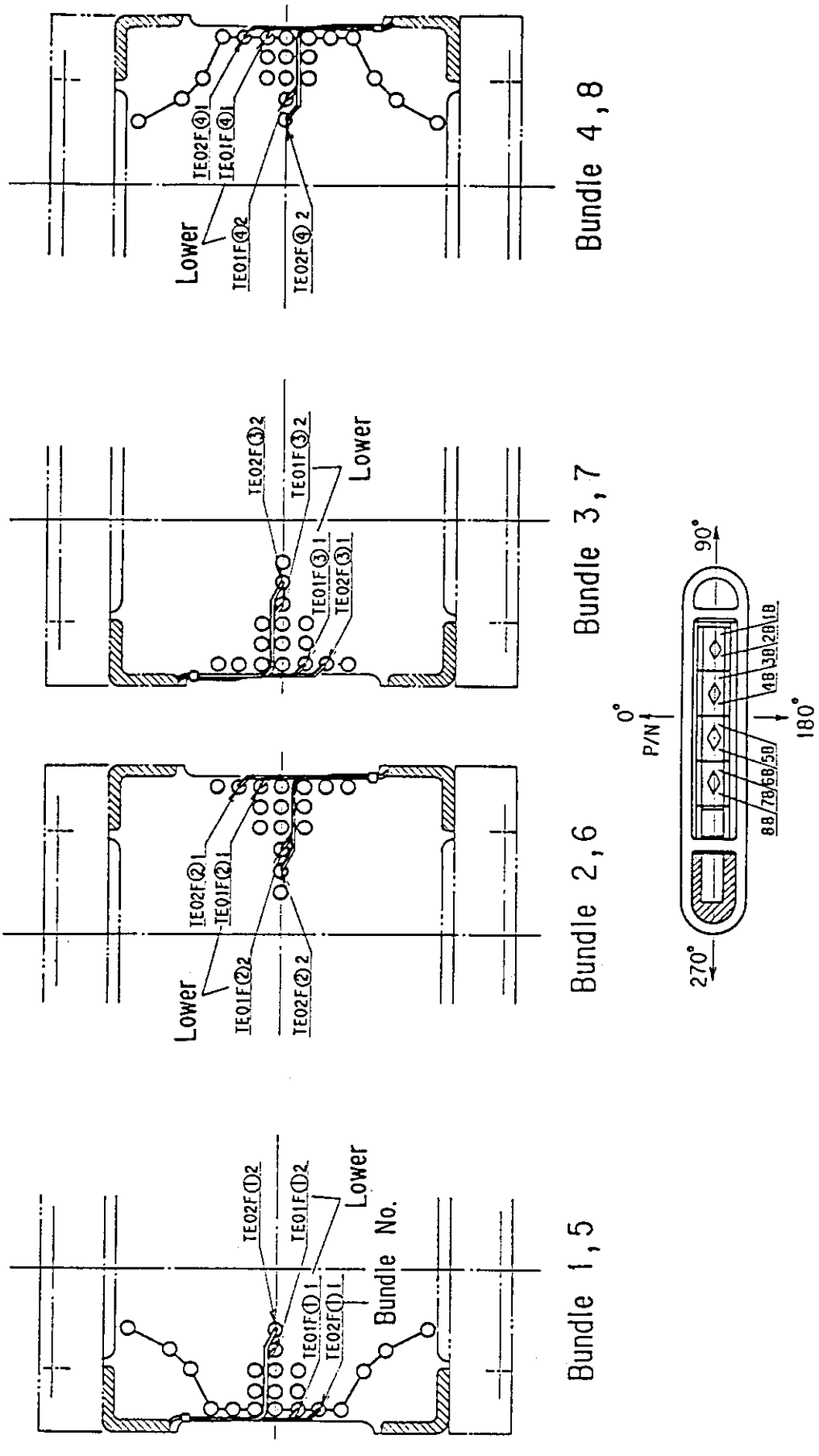

Fig. A-28 Thermocouple Locations of Fluid Temperature Measurements just above and below End Box Tie Plates

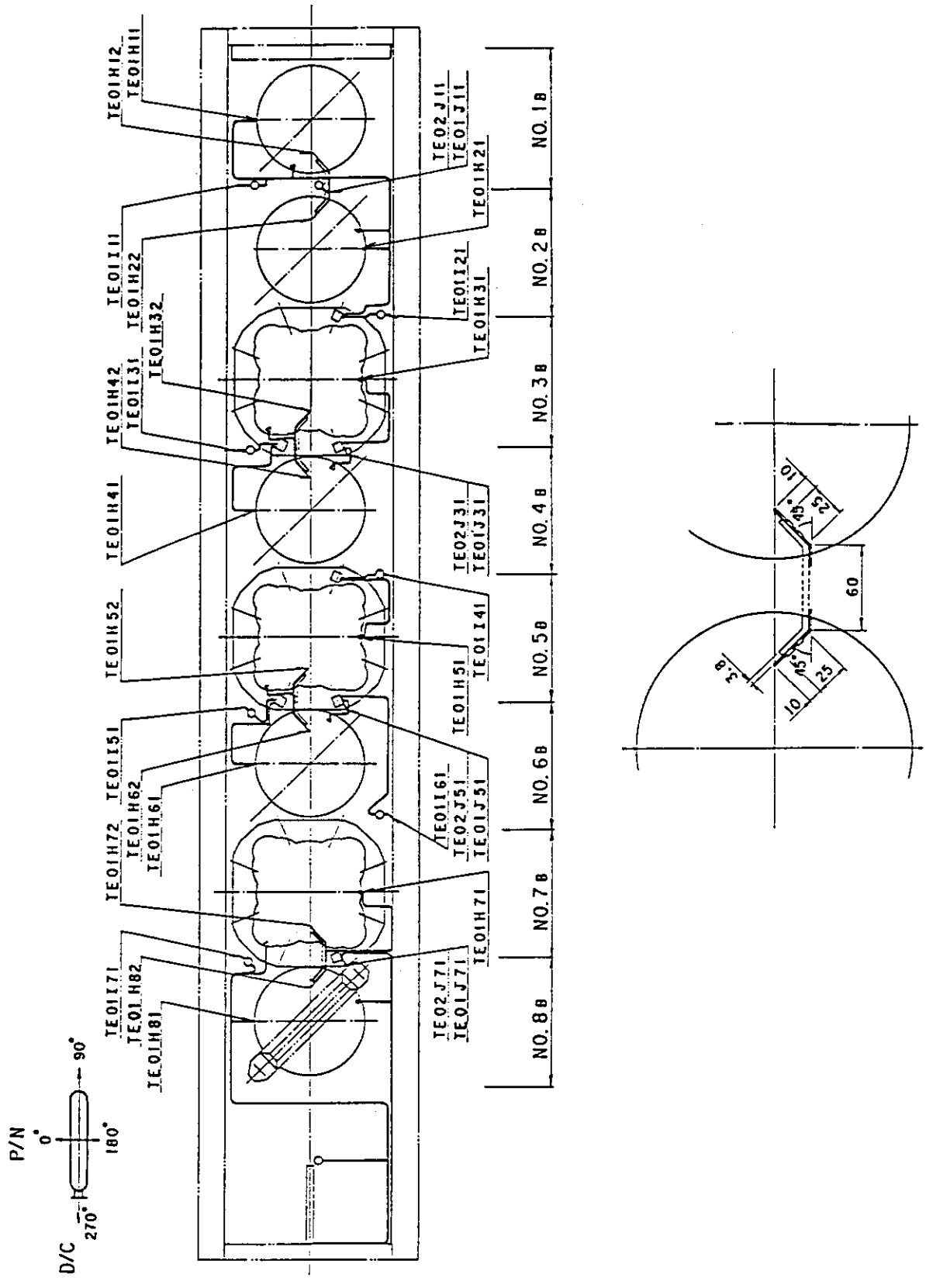

Fig. A-29 Thermocouple Locations of Fluid Temperature Measurements on UCSP and at Inside and Periphery of UCSP Holes

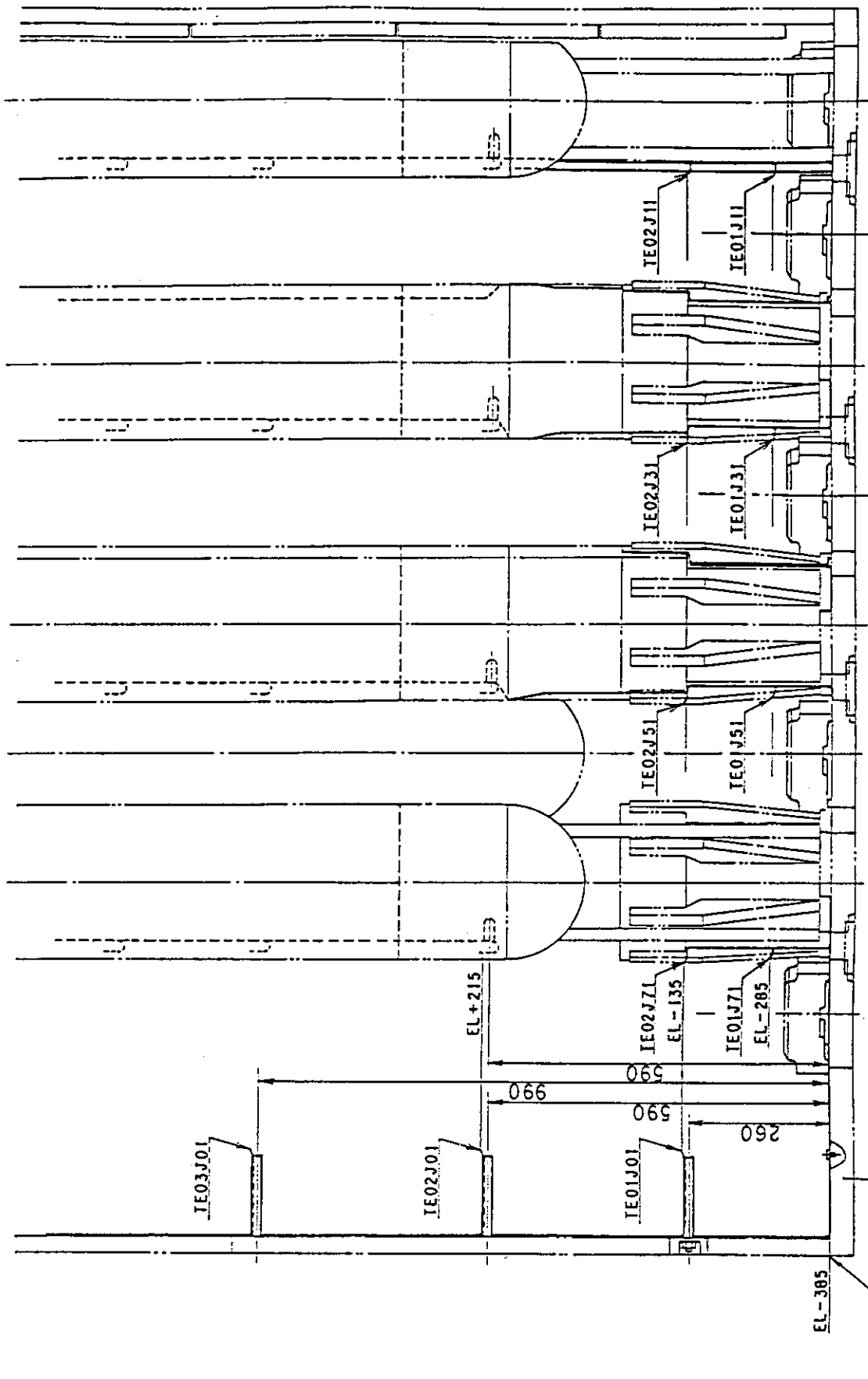

Fig. A-30 Thermocouple Locations of Fluid Temperature Measurements on and above UCSP

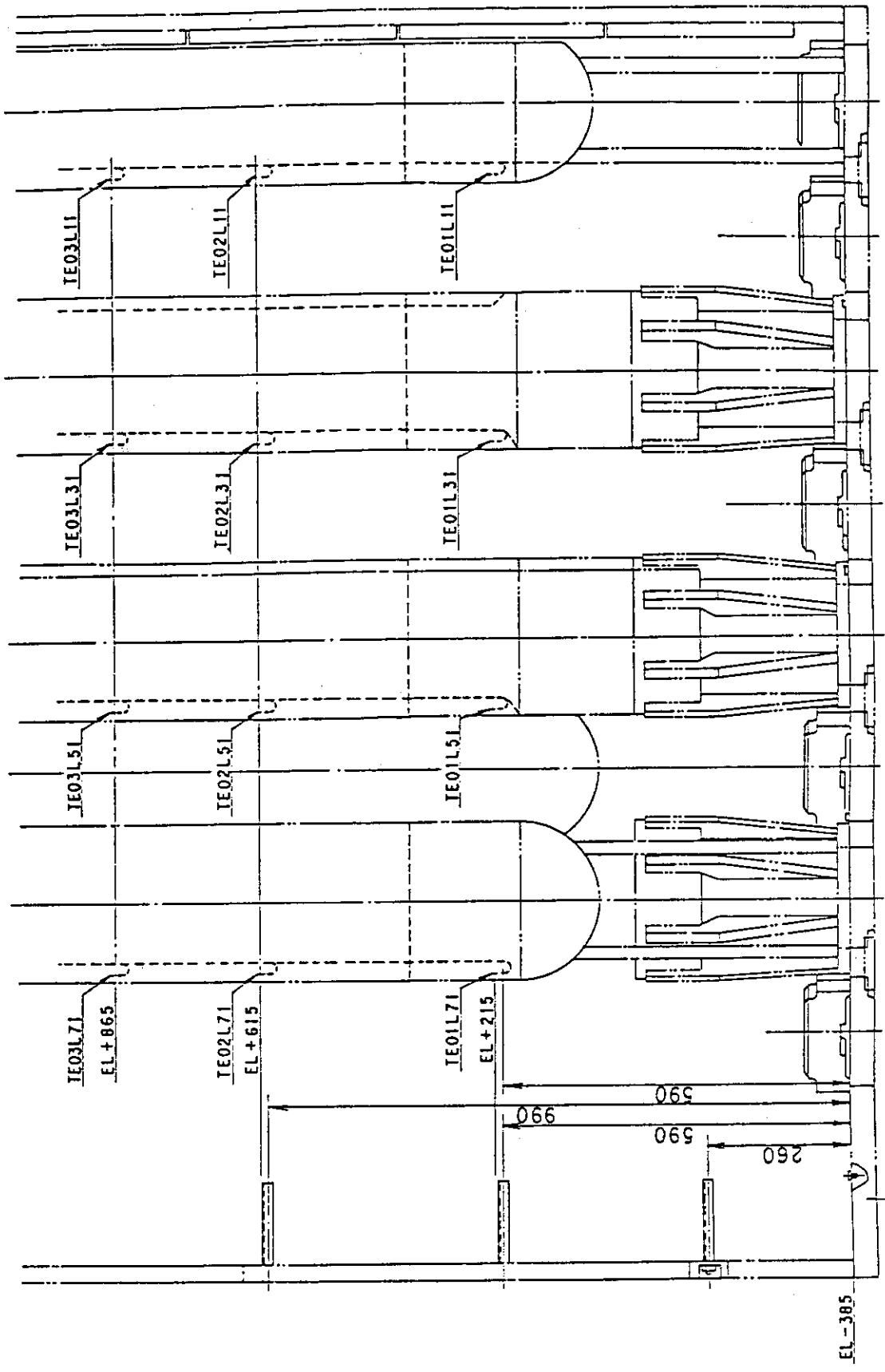

Fig. A-31 Thermocouple Locations of Surface Temperature Measurements of Upper Plenum Structures

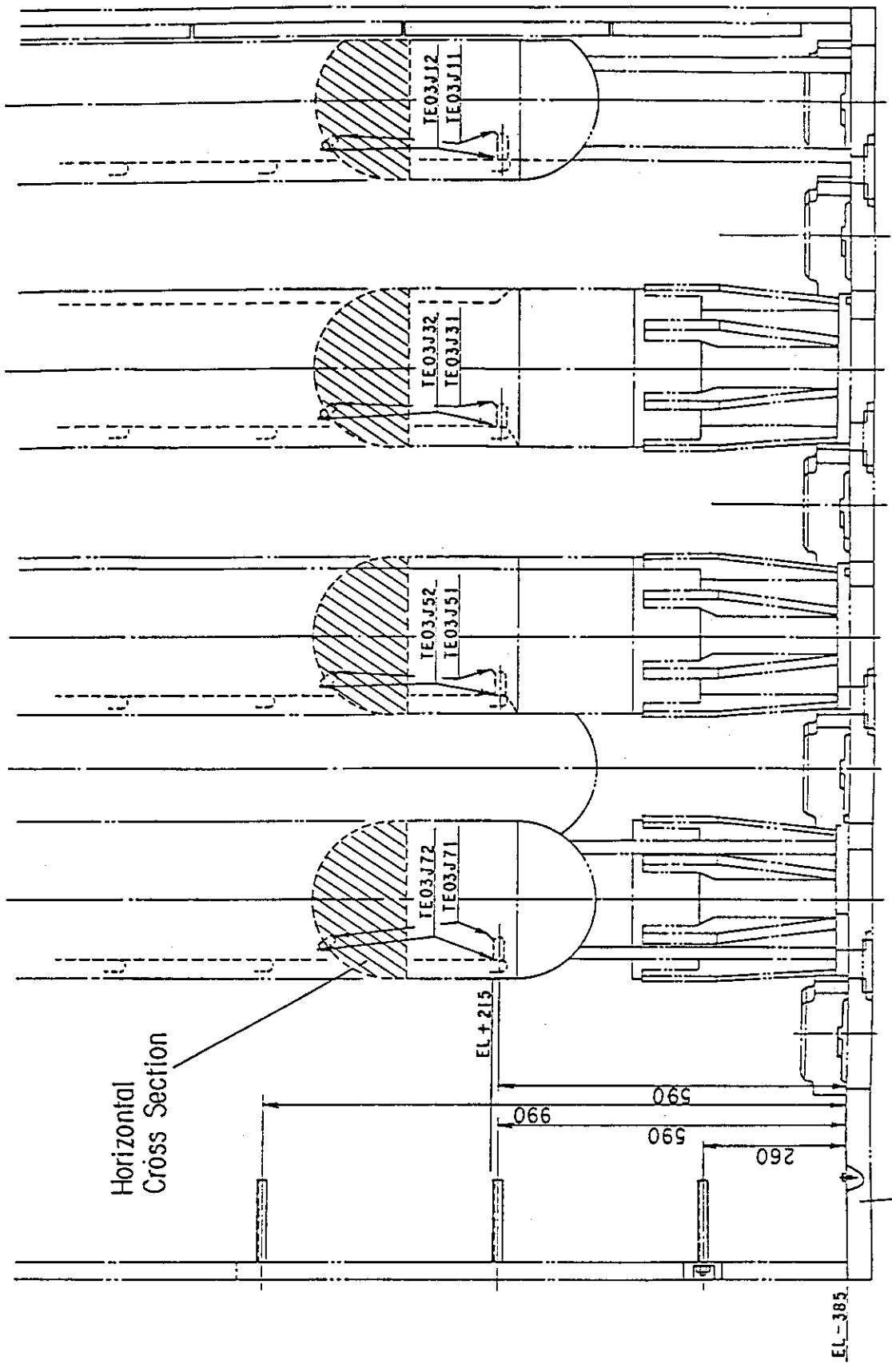

Fig. A-32 Thermocouple Locations of Steam Temperature Measurements above UCSP Holes

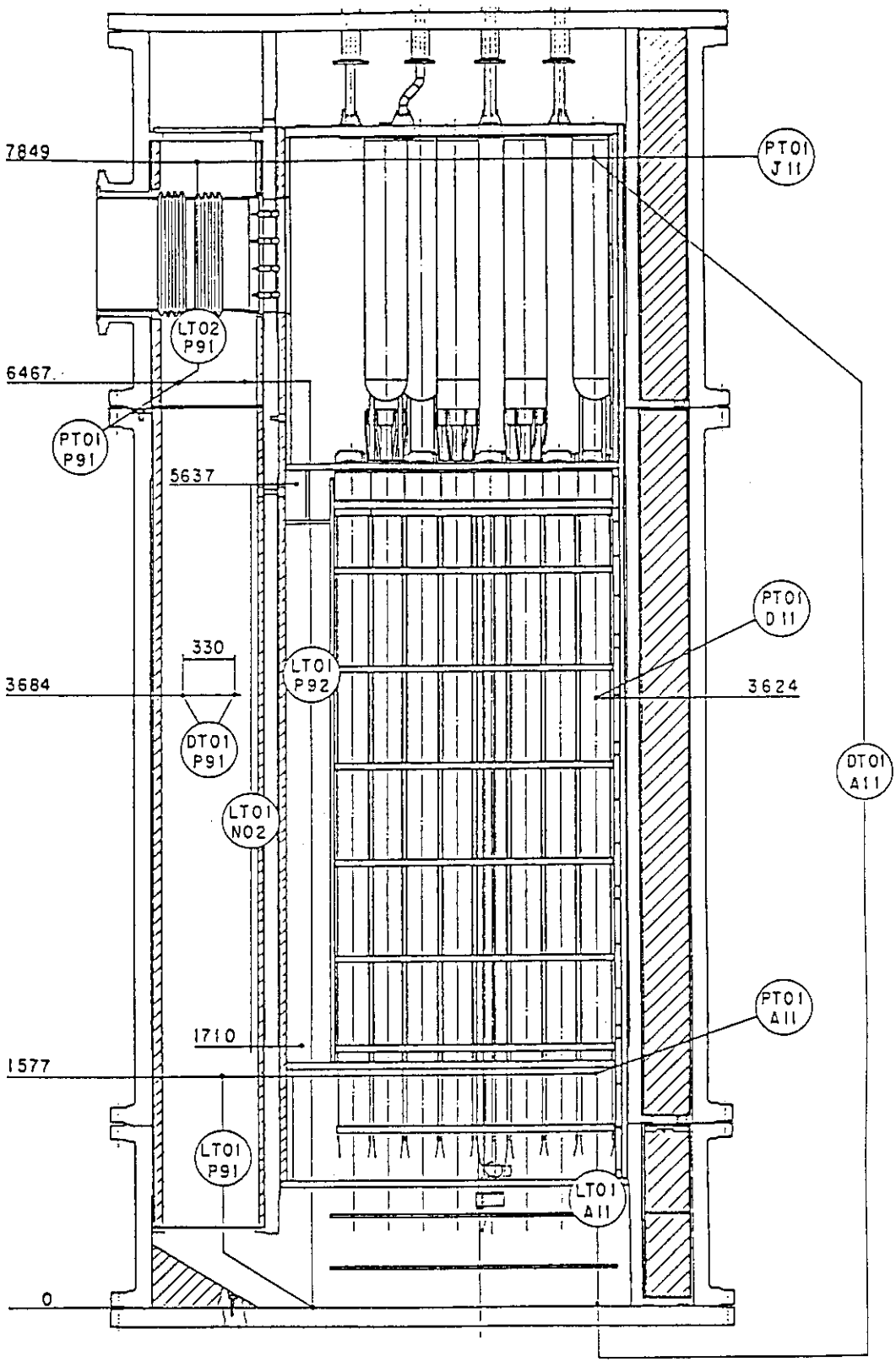

Fig. A-33 Locations of Pressure Measurements in Pressure Vessel, Differential Pressure Measurements between Upper and Lower Plenums and Liquid Level Measurements in Downcomer and Lower Plenum

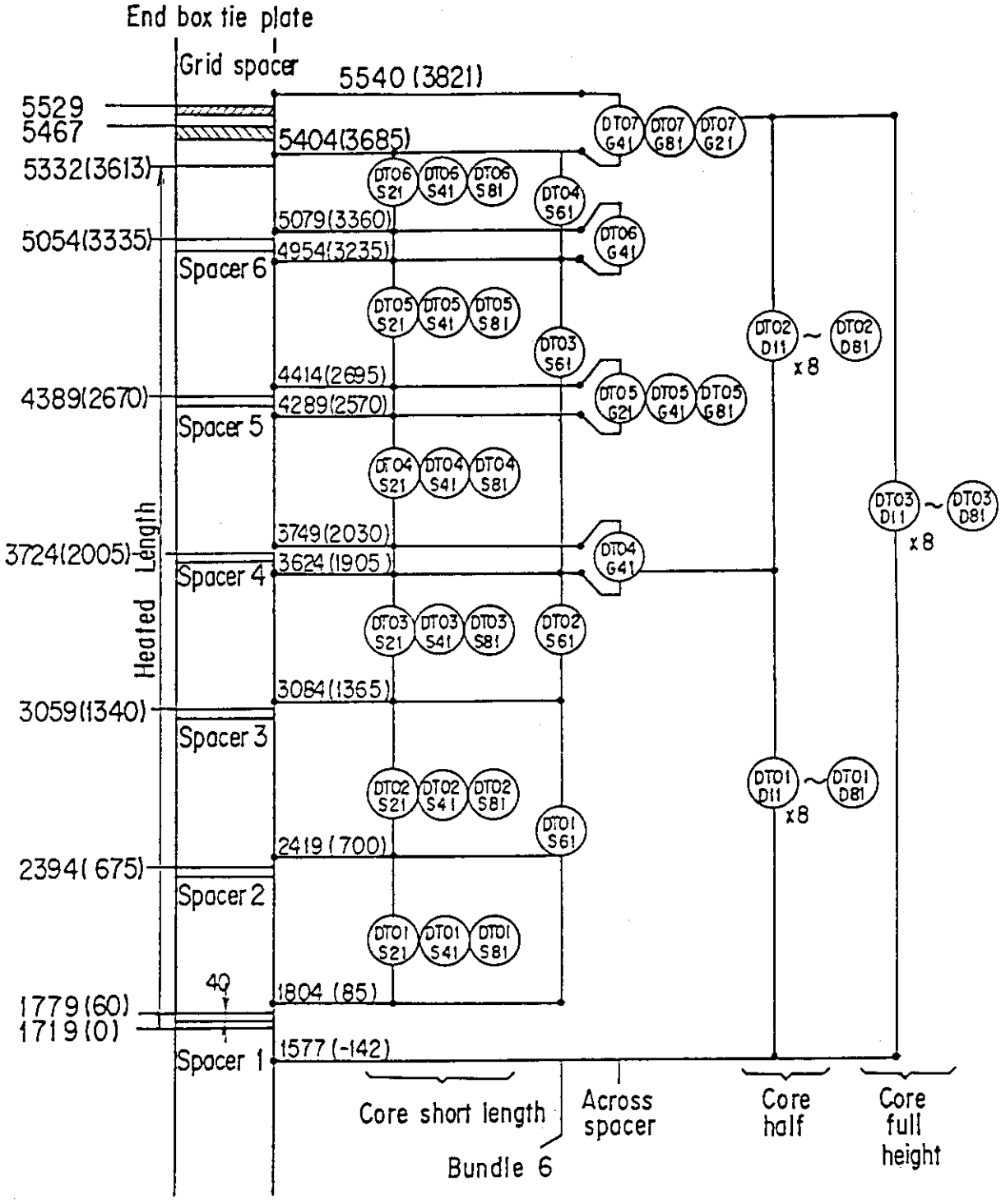

Fig. A-34 Locations of Vertical Differential Pressure Measurements in Core

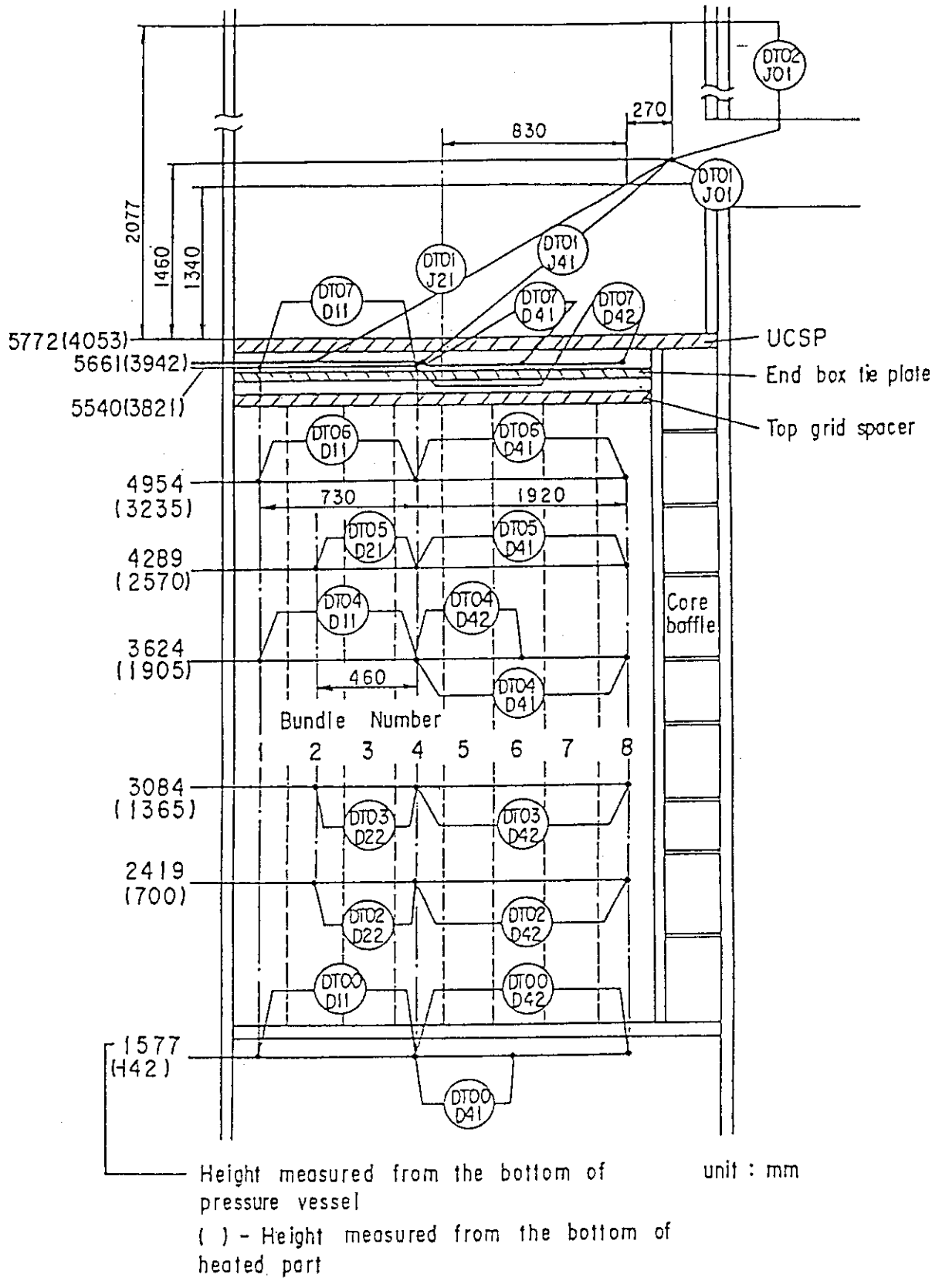

Fig. A-35 Locations of Horizontal Differential Pressure Measurements in Core and Differential Pressure Measurements between End Boxes and Inlet of Hot Leg

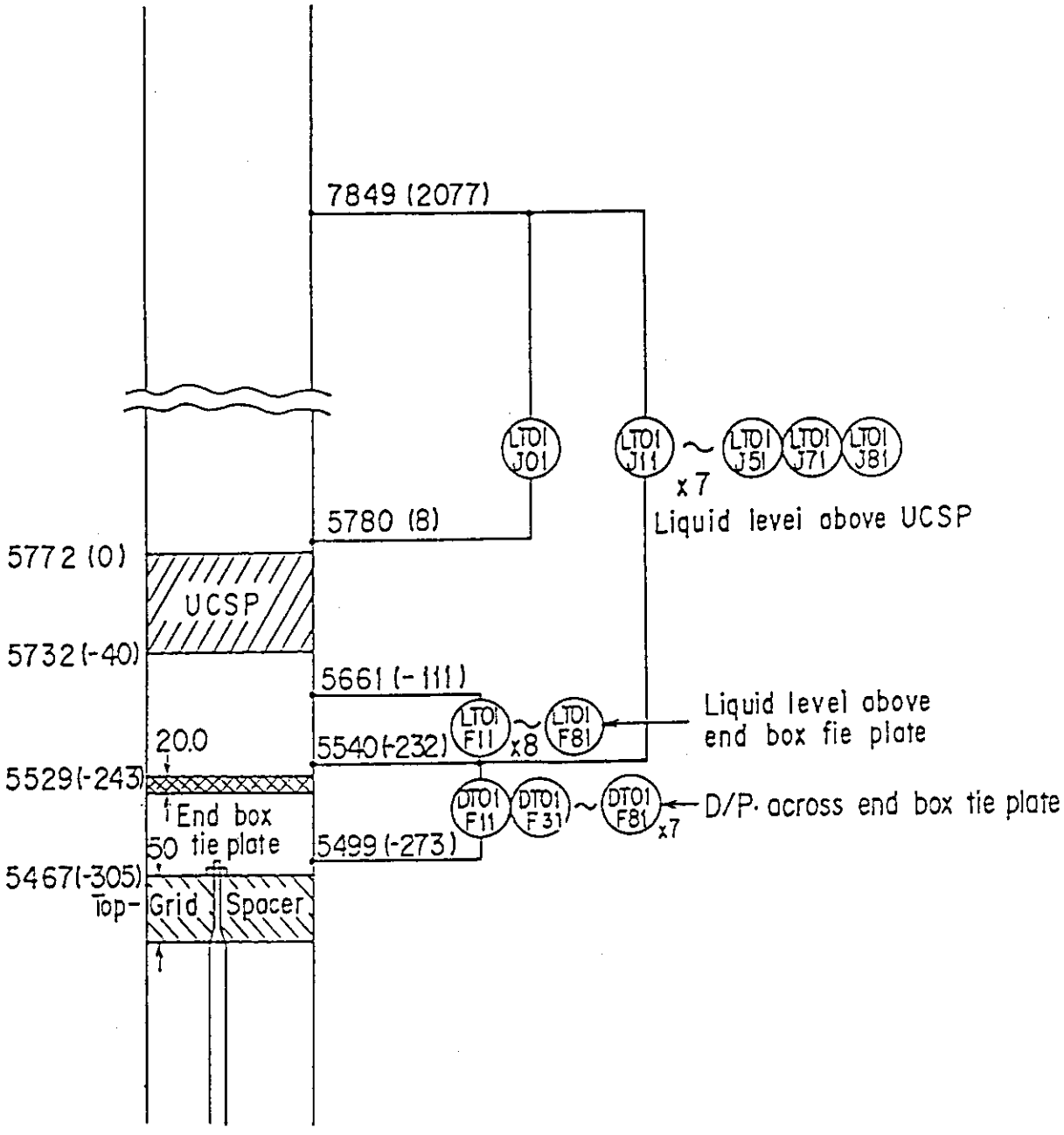

Fig. A-35 Locations of Differential Pressure Measurements across End Box Tie Plate

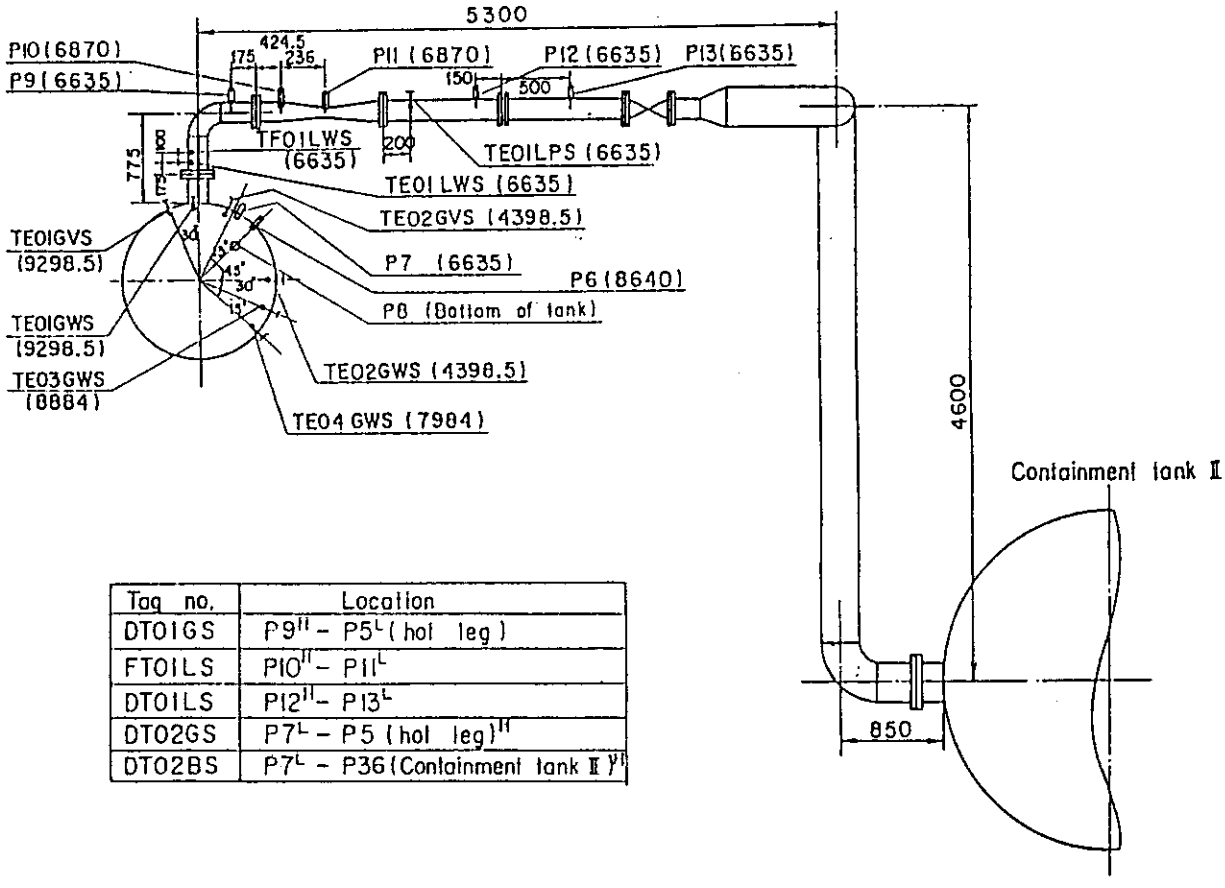

Tag no.	Location
DT01GS	$P9^{H}$ – $P5^{L}$ (hot leg)
FT01LS	$P10^{H}$ – $P11^{L}$
DT01LS	$P12^{H}$ – $P13^{L}$
DT02GS	$P7^{L}$ – P5 (hot leg)^{H}
DT02BS	$P7^{L}$ – P36(Containment tank II)^{H}

Fig. A-37 Locations of Broken Cold Leg Instruments
(Steam-Water Separator Side)

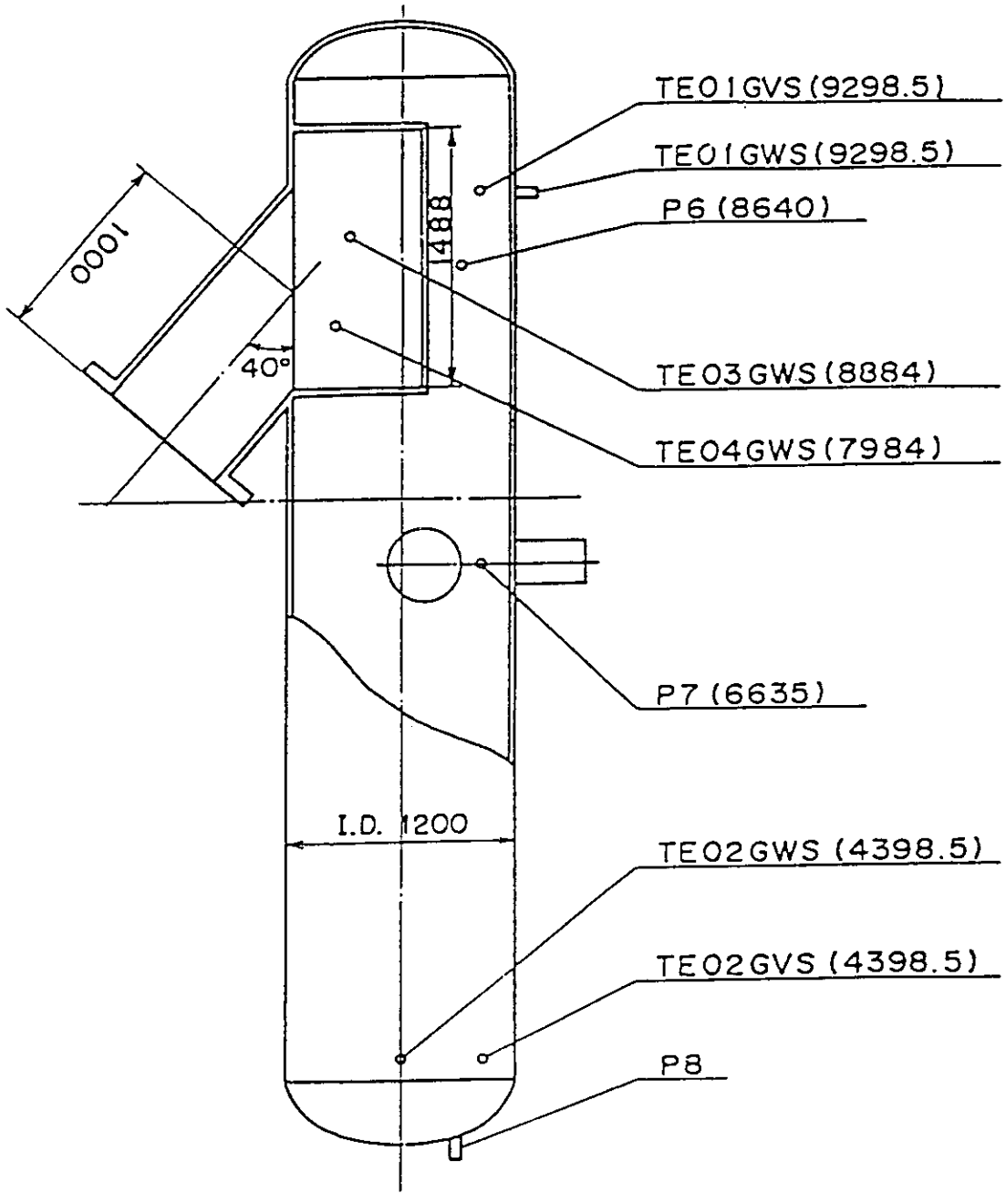

Fig. A-38 Locations of Steam-Water Separator Instruments

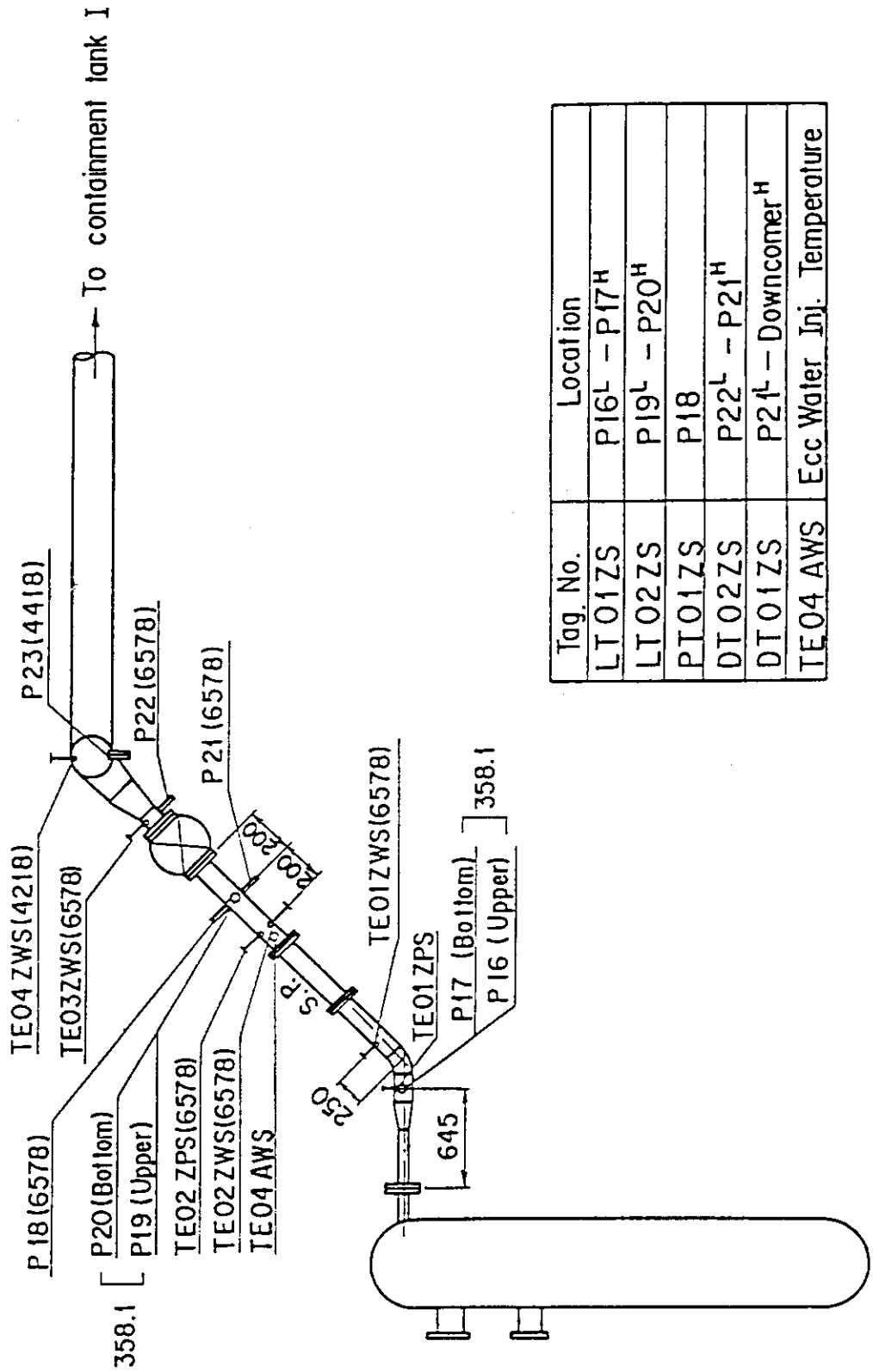

Fig. A-39 Locations of Broken Cold Leg Instruments
(Pressure Vessel Side)

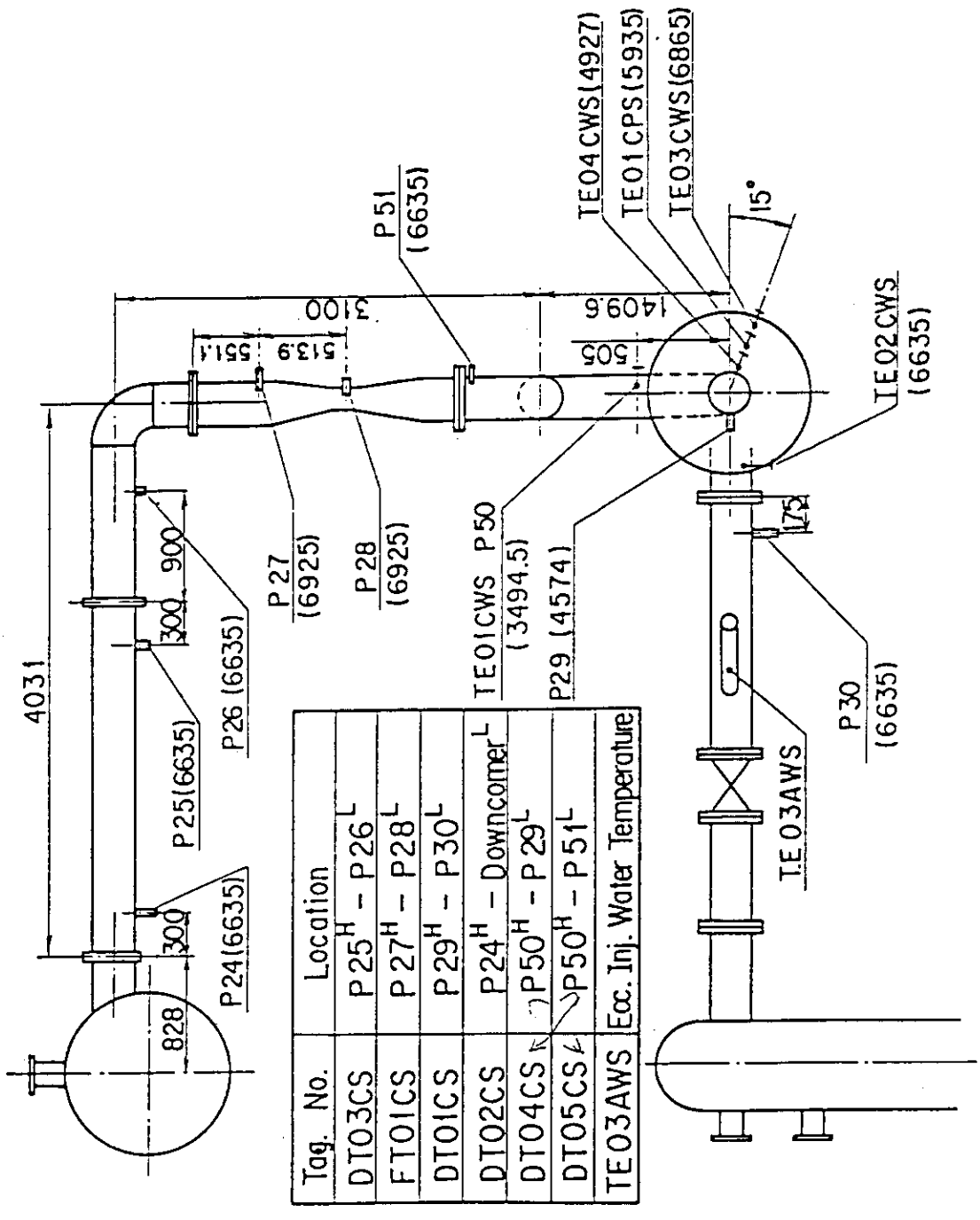

Fig. A-40 Locations of Intact Cold Leg Instruments

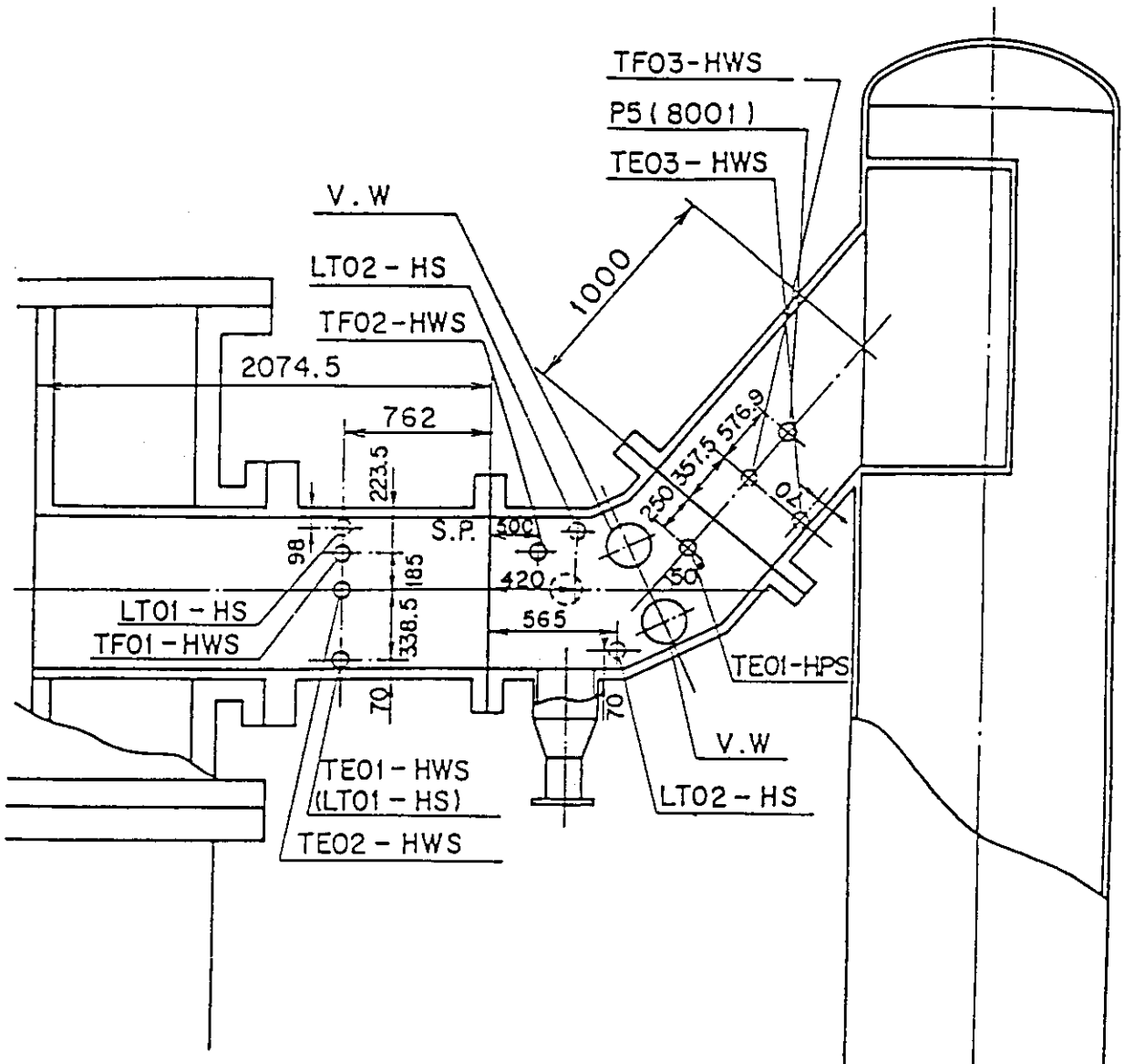

Tag no.	Location
DT01HS	$P5^{L}$ – Inlet of hot leg^{H}
DT01GS	$P5^{L}$ – Broken cold leg (S-W separator side)^{H}
DT02GS	$P5^{H}$ – S-W separator $tank^{L}$

Fig. A-41 Locations of Hot Leg Instruments

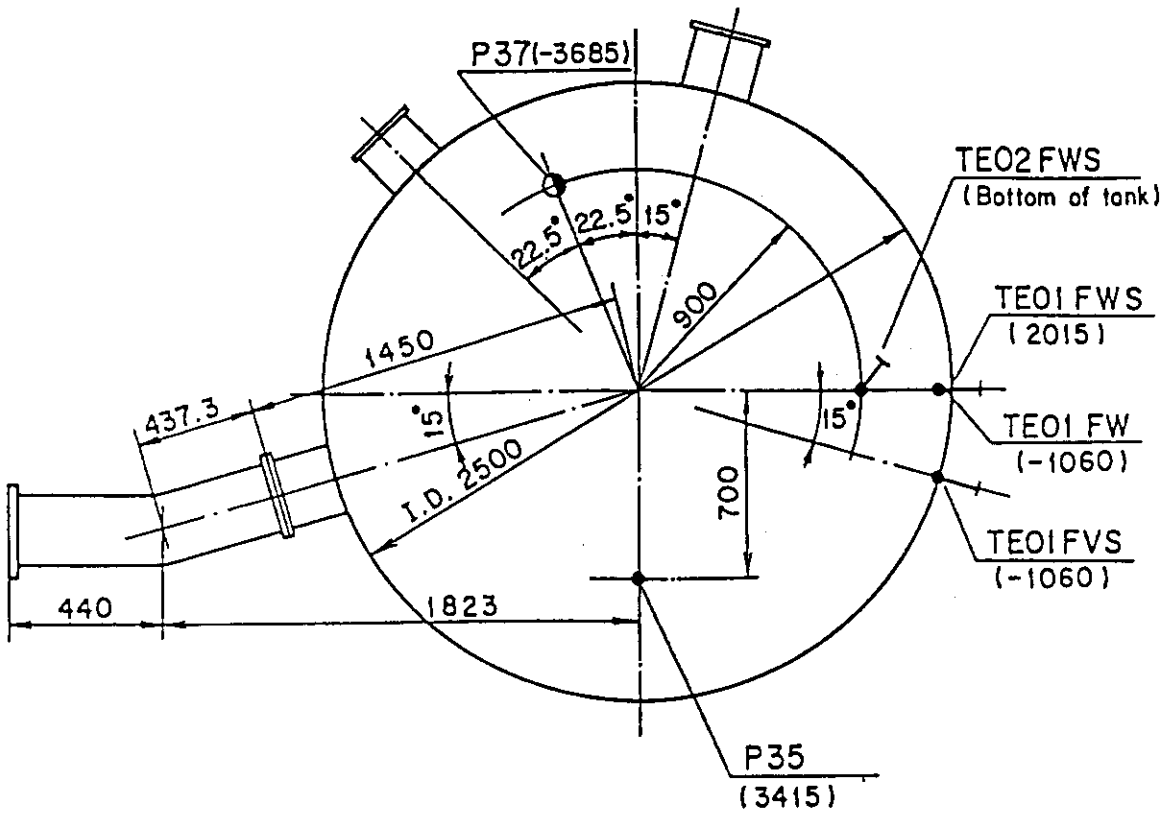

Tag. no.	Location
LT01 FS	$P35^{L}$ – $P37^{H}$
DT01 FS	$P35^{H}$ – $Downcomer^{L}$
DT01 E	$P35^{L}$ – P36(C.T. II)^{H}
PT01 F	P35

Fig. A-42 Locations of Containment Tank-I Instruments

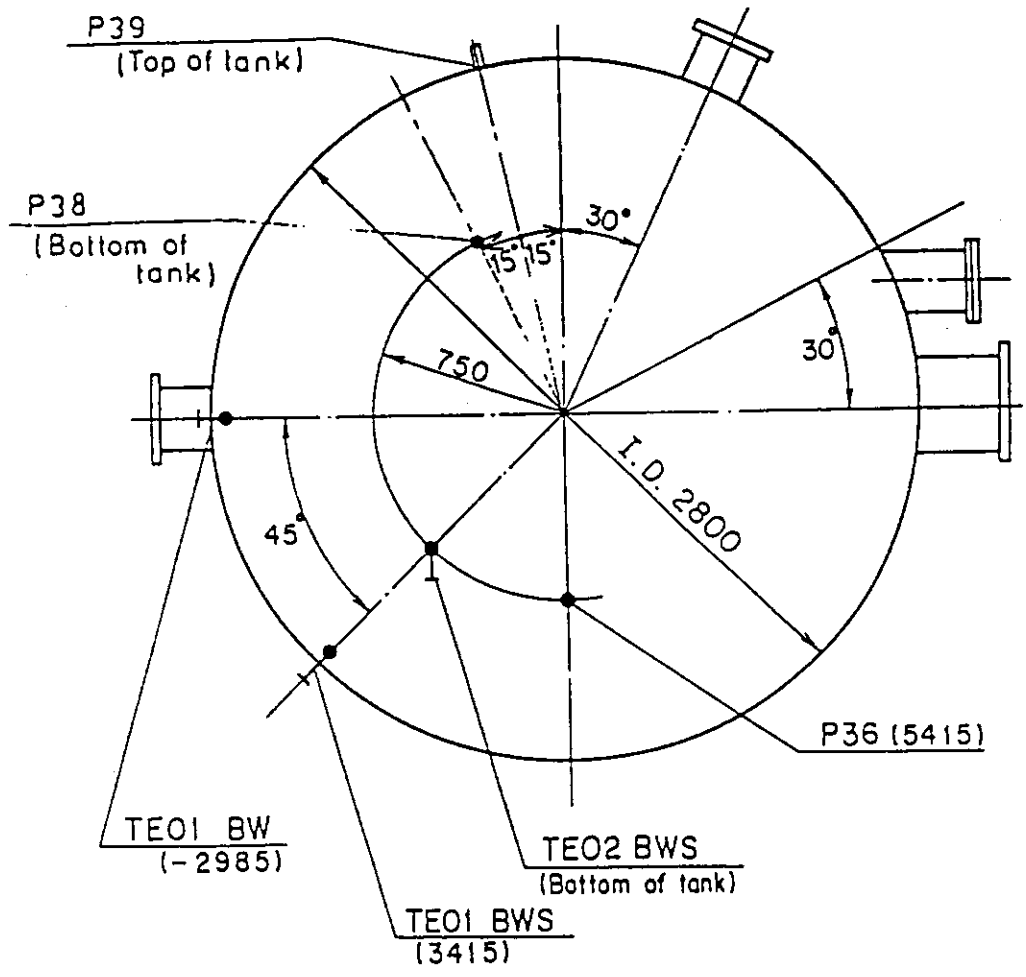

Tag no.	Location
DT01 BS	$P36^{H}$－ Upper plenum^{L}
DT02 BS	$P36^{H}$－ S-W Separator^{L}
DT01 E	$P36^{H}$－ P35 (C.T.I)^{L}
PT01 B	P36
LT01 1B	$P38^{H}$－ $P39^{L}$

Fig. A-43 Locations of Containment Tank-II Instruments

Appendix B

Selected Data from Test S3-9

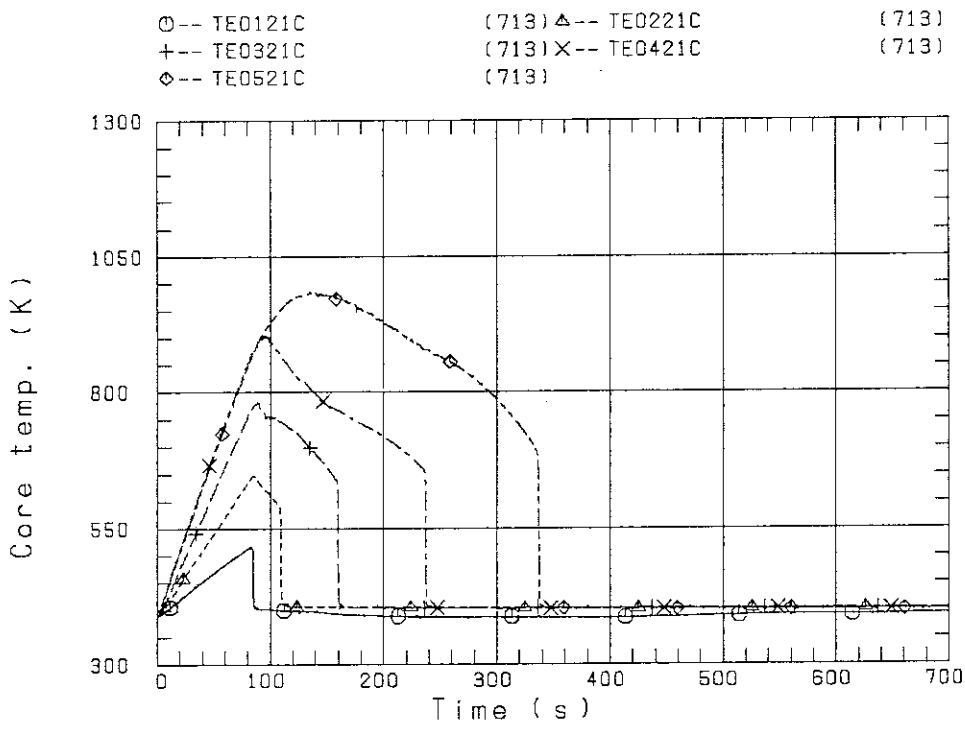

FIG. B-1 HEATER ROD TEMPERATURE
(BUNDLE 2-1C, LOWER HALF)

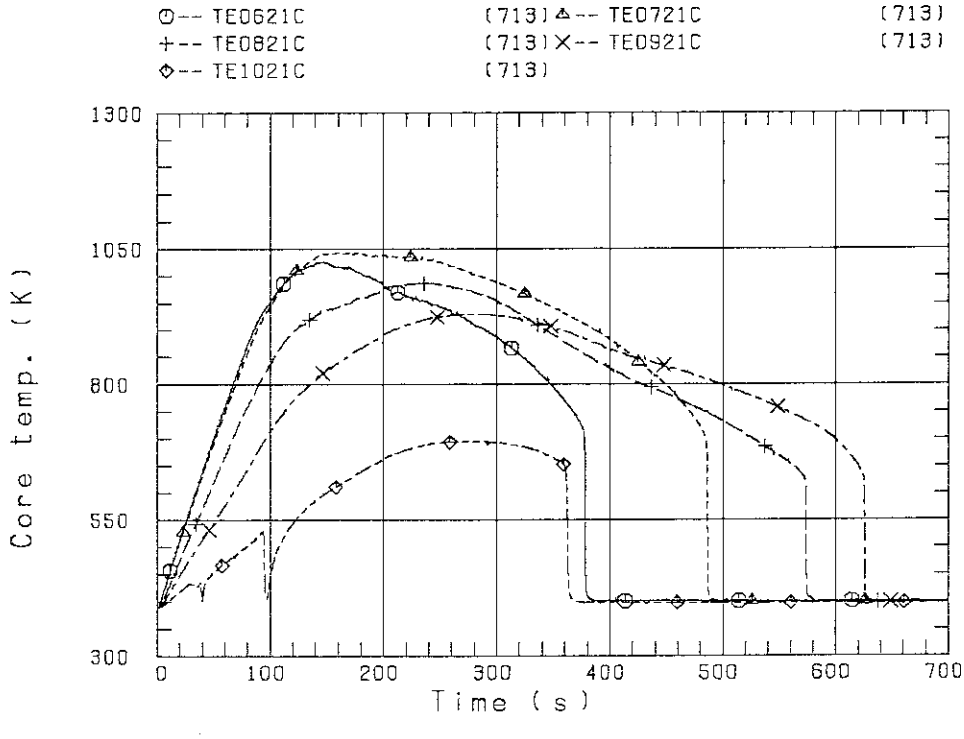

FIG. B-2 HEATER ROD TEMPERATURE
(BUNDLE 2-1C, UPPER HALF)

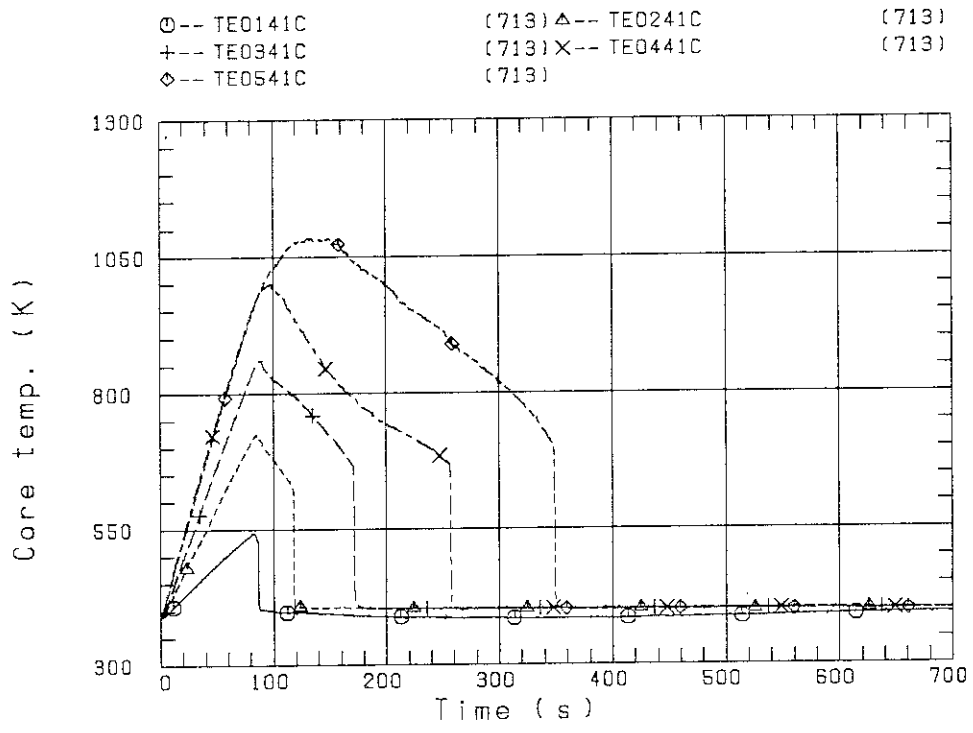

FIG. B-3 HEATER ROD TEMPERATURE
(BUNDLE 4-1C, LOWER HALF)

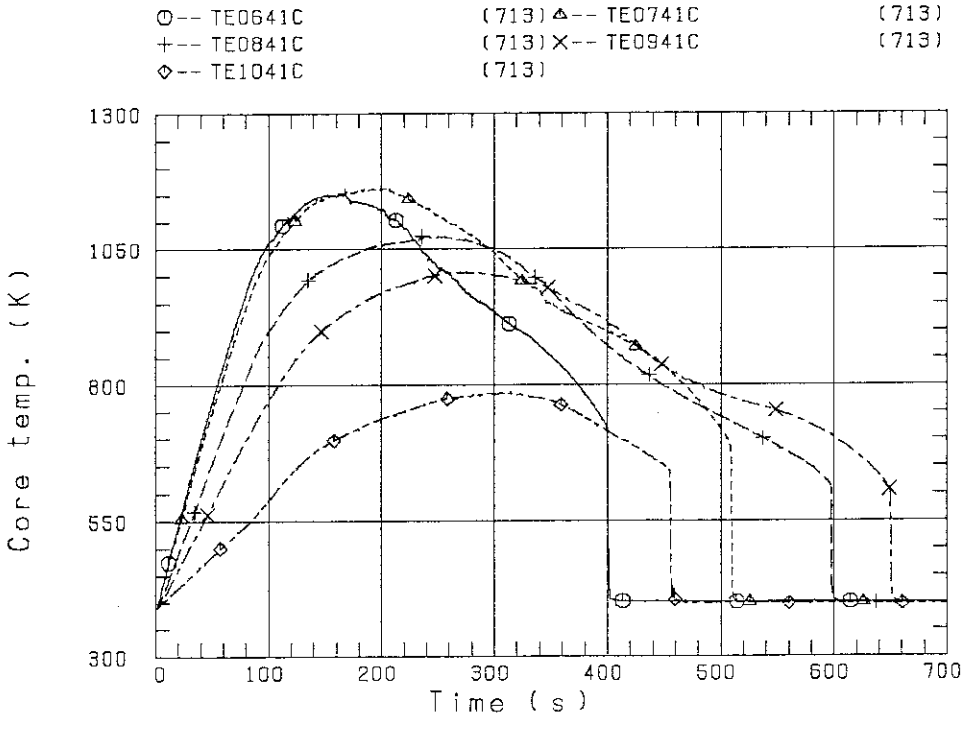

FIG. B-4 HEATER ROD TEMPERATURE
(BUNDLE 4-1C, UPPER HALF)

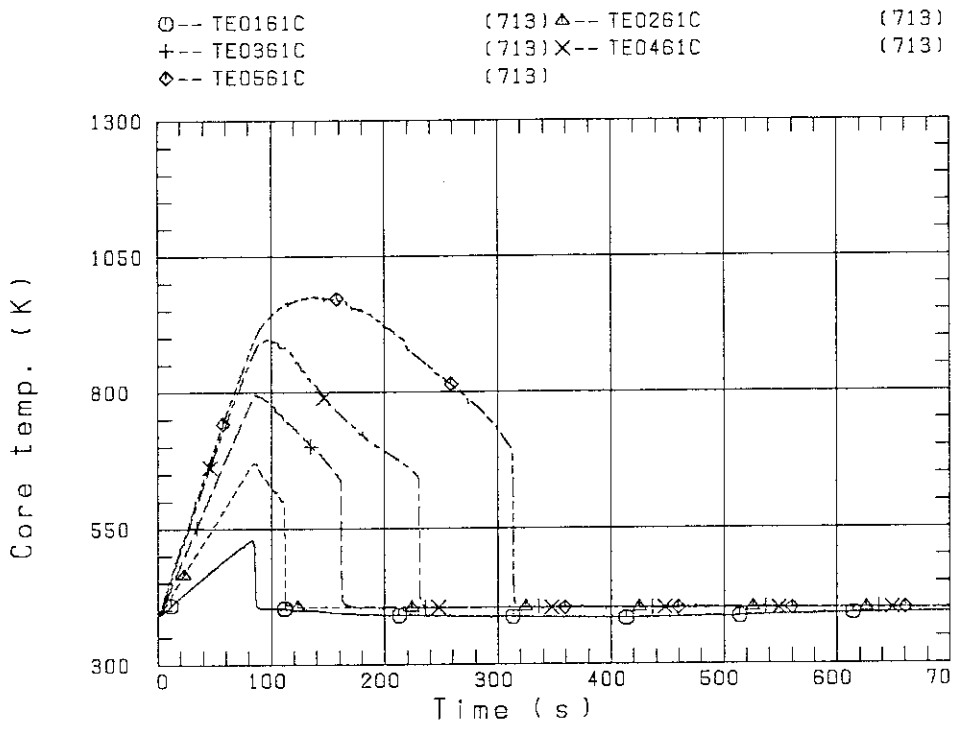

FIG. B-5 HEATER ROD TEMPERATURE
(BUNDLE 6-1C, LOWER HALF)

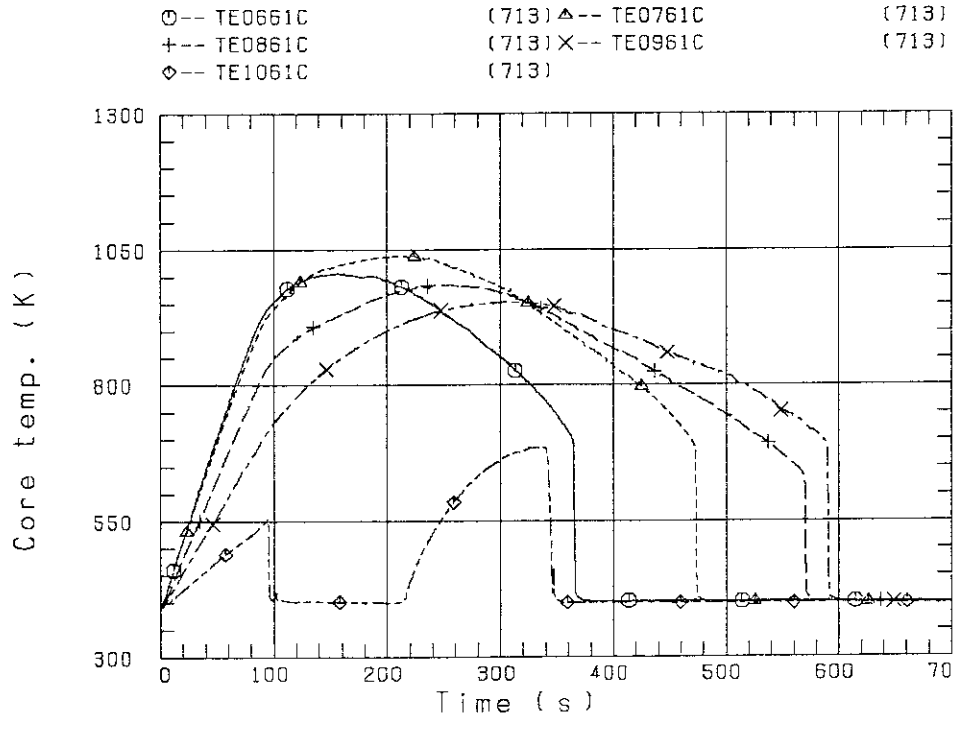

FIG. B-6 HEATER ROD TEMPERATURE
(BUNDLE 6-1C, UPPER HALF)

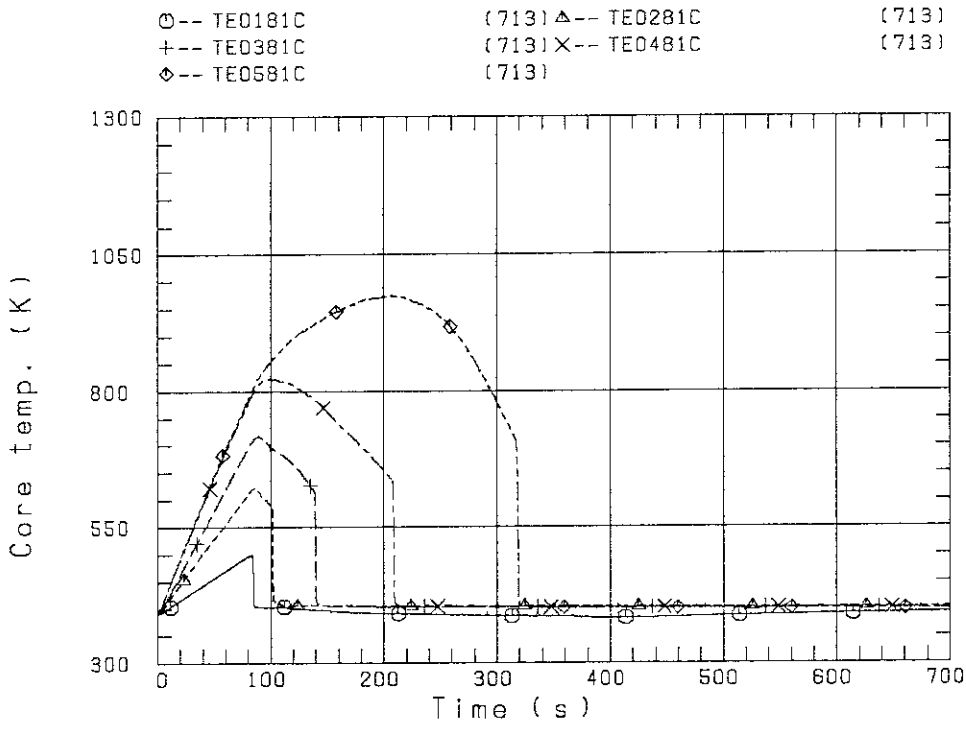

FIG. B-7 HEATER ROD TEMPERATURE
(BUNDLE 8-1C, LOWER HALF)

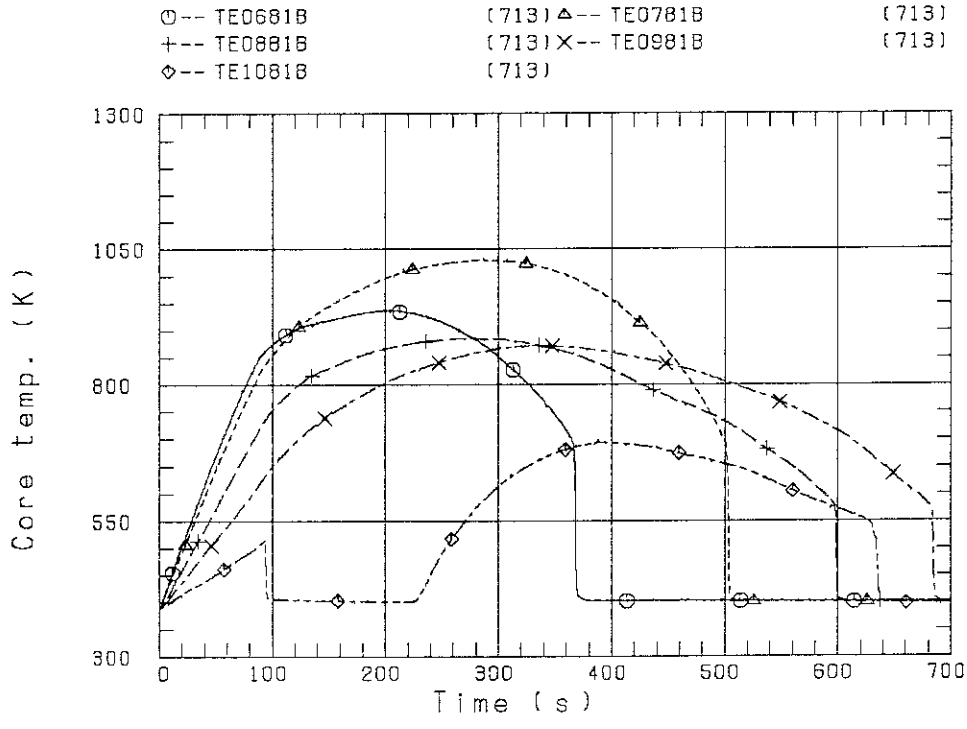

FIG. B-8 HEATER ROD TEMPERATURE
(BUNDLE 8-1B, UPPER HALF)

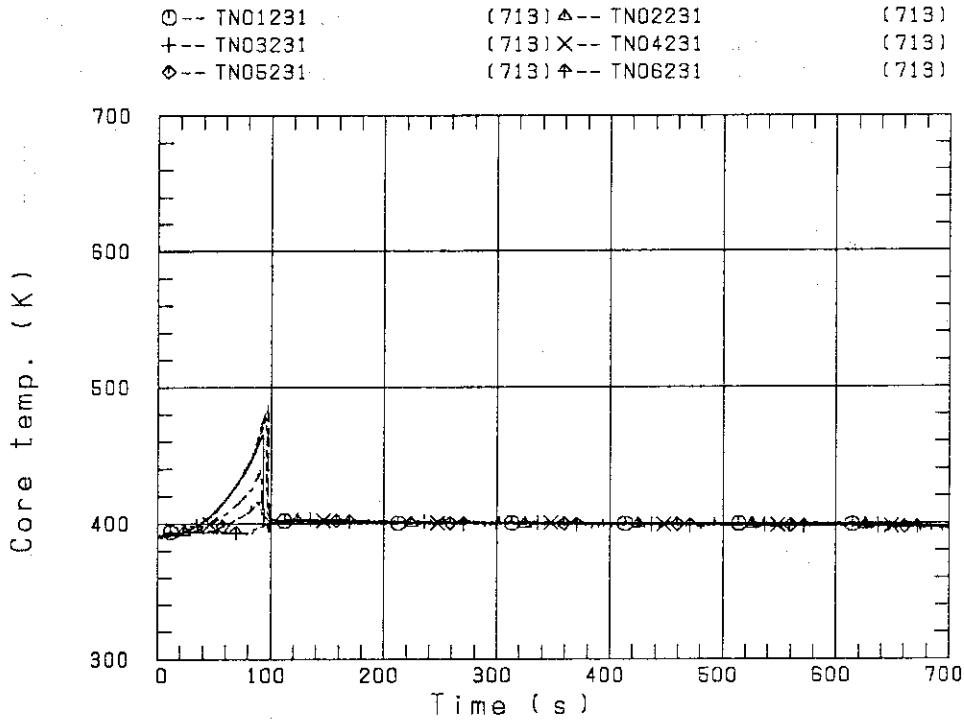

FIG. B-9 NON-HEATED ROD TEMPERATURE
(BUNDLE 2-31)

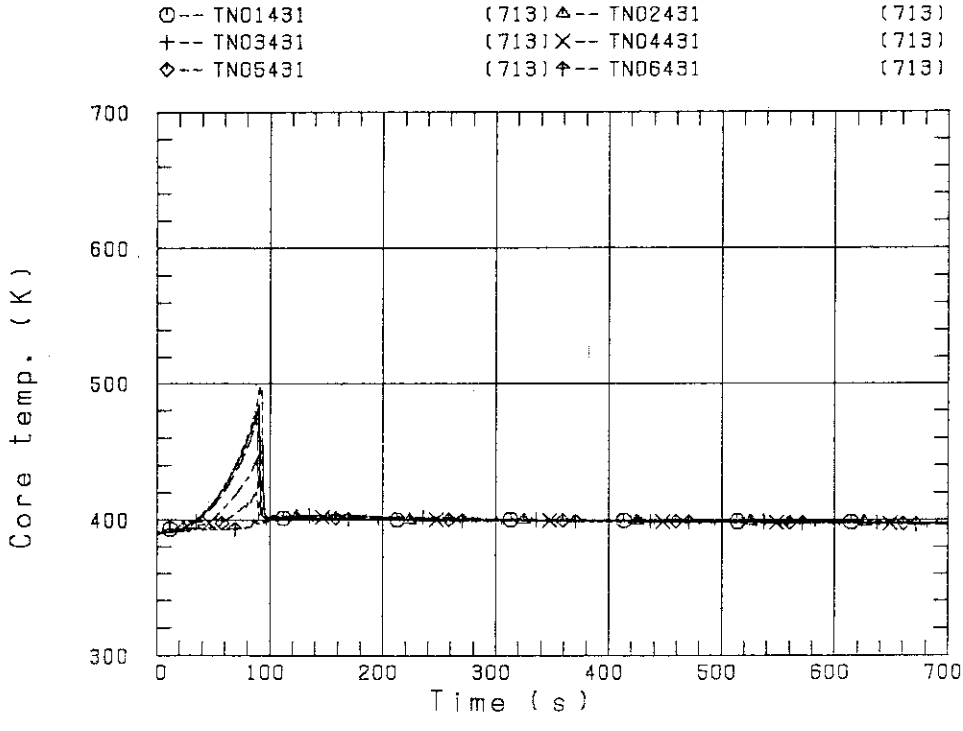

FIG. B-10 NON-HEATED ROD TEMPERATURE
(BUNDLE 4-31)

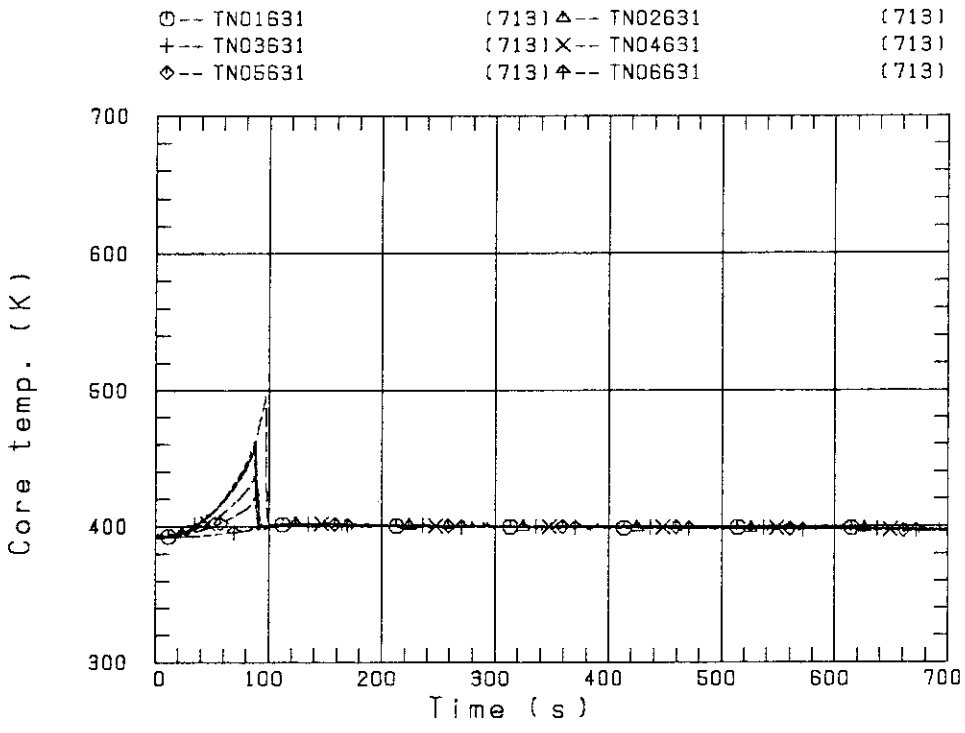

FIG. B-11 NON-HEATED ROD TEMPERATURE
(BUNDLE 6-31)

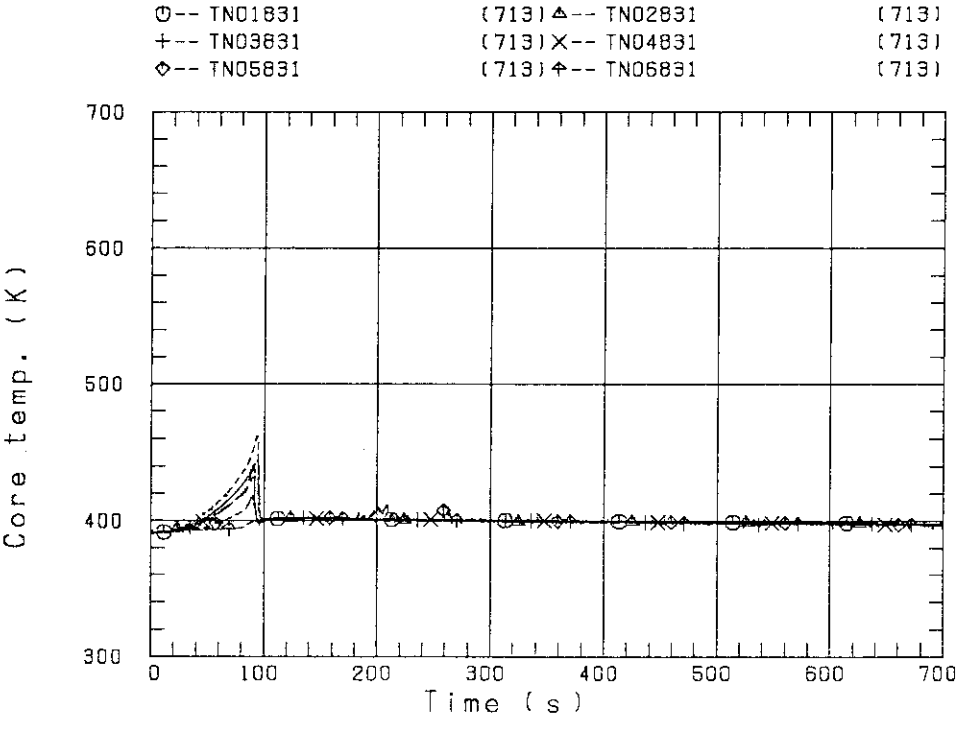

FIG. B-12 NON-HEATED ROD TEMPERATURE
(BUNDLE 6-31)

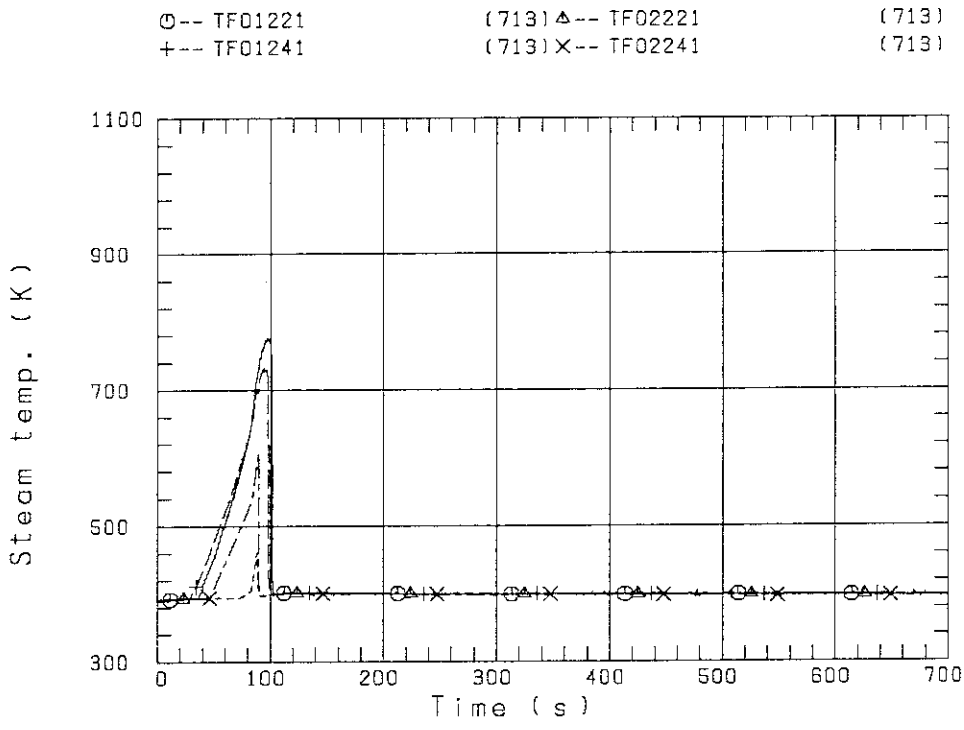

FIG. B-13 STEAM TEMPERATURE IN CORE, BUNDLE 2

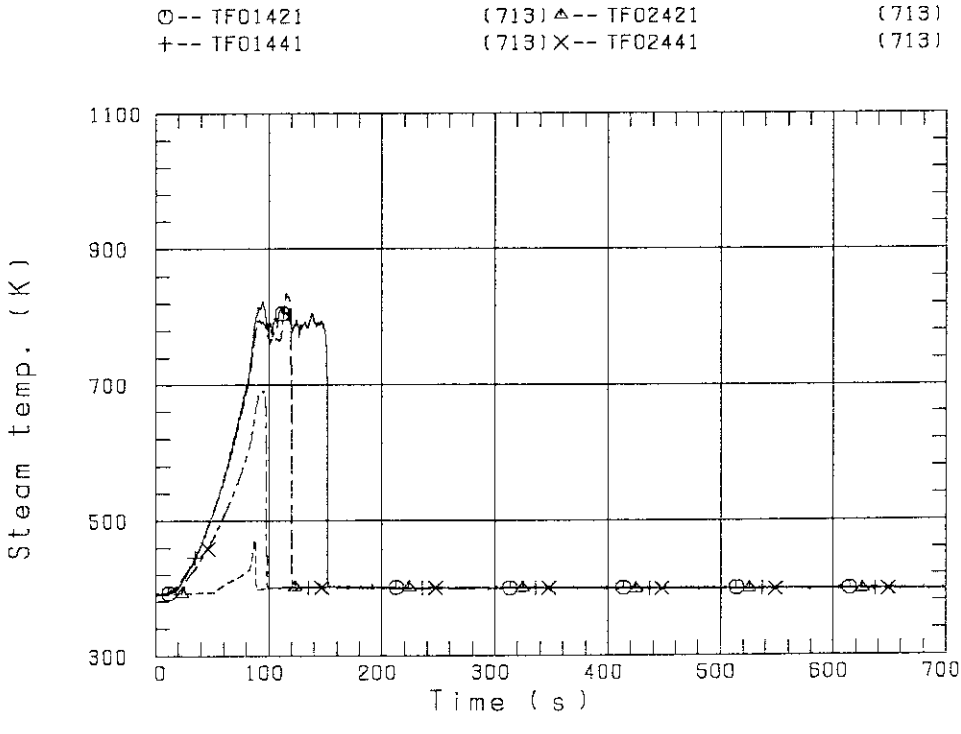

FIG. B-14 STEAM TEMPERATURE IN CORE, BUNDLE 4

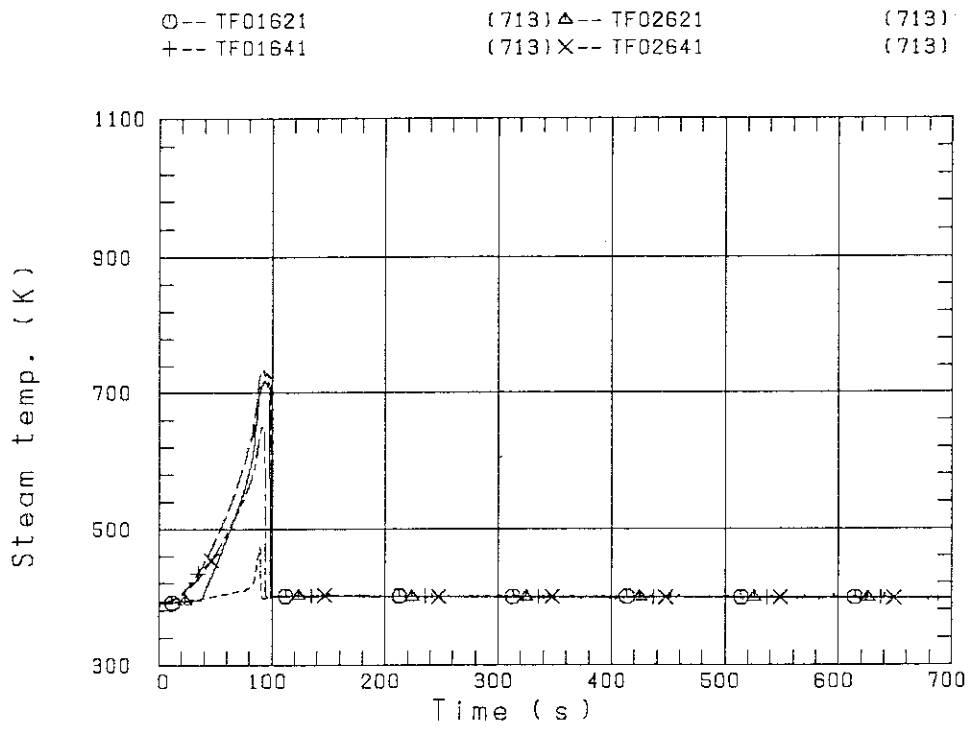

FIG. B-15 STEAM TEMPERATURE IN CORE, BUNDLE 6

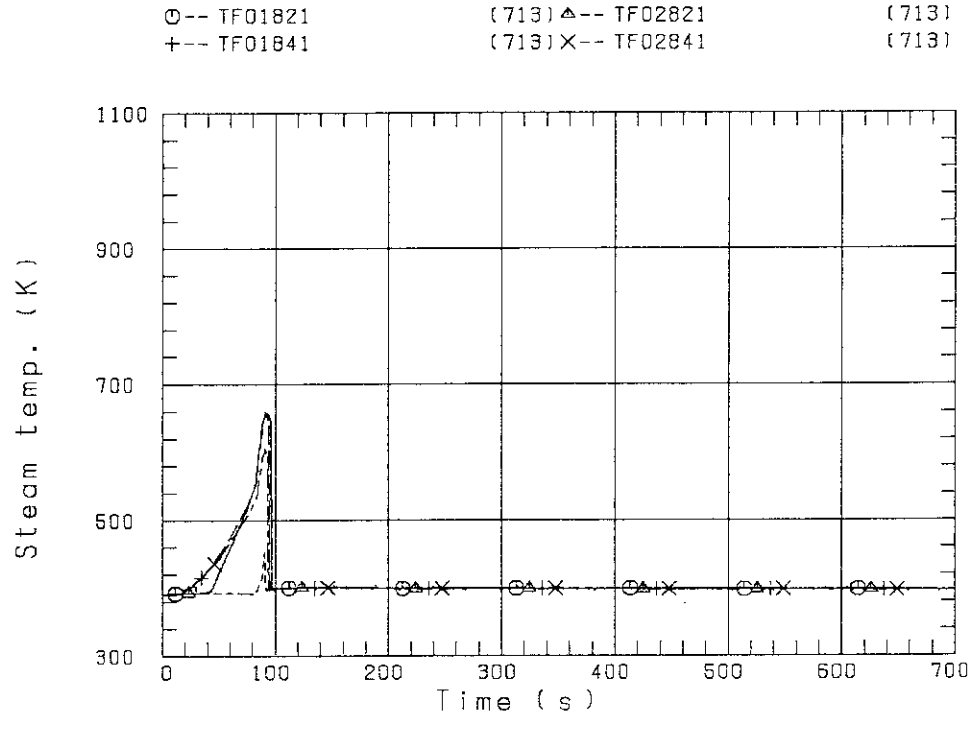

FIG. B-16 STEAM TEMPERATURE IN CORE, BUNDLE 8

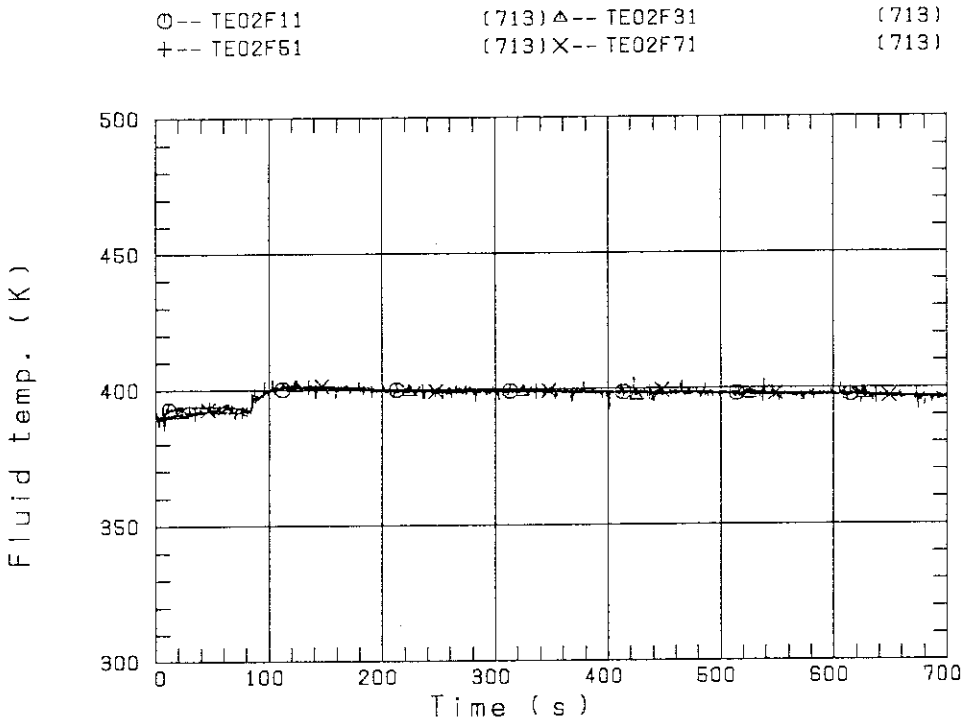

FIG. B-17 FLUID TEMPERATURE JUST ABOVE END BOX TIE PLATE
(BUNDLE 1,3,5,7 OPPOSITE SIDE OF COLD LEG, OUTER)

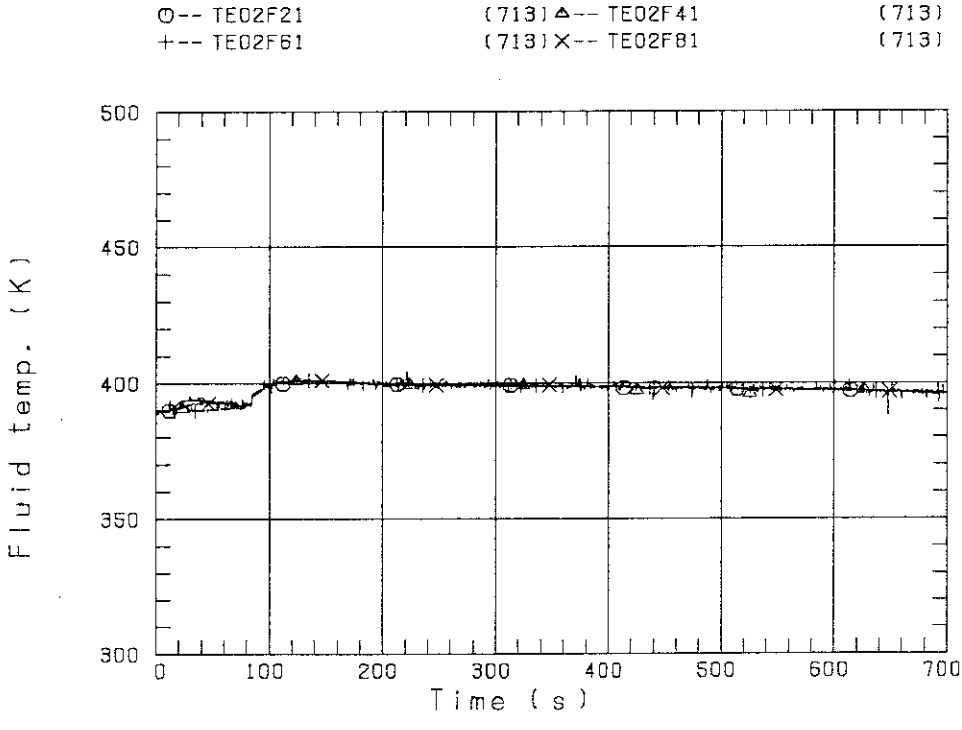

FIG. B-18 FLUID TEMPERATURE JUST ABOVE END BOX TIE PLATE
(BUNDLE 2,4,6,8 OPPOSITE SIDE OF COLD LEG, OUTER)

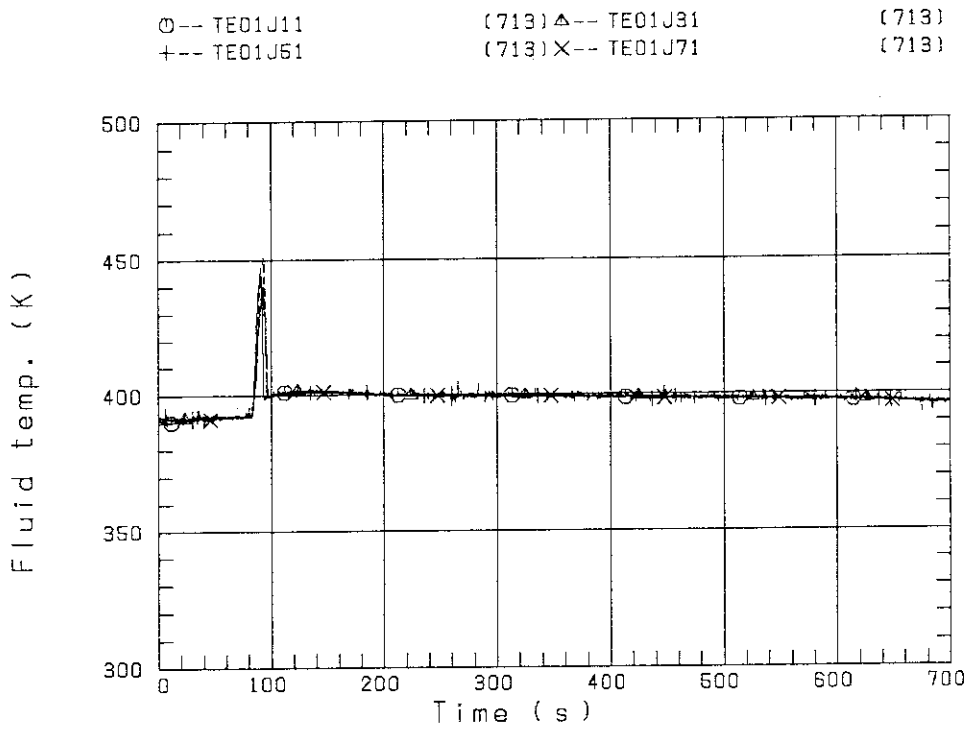

FIG. B-19 FLUID TEMPERATURE ABOVE UCSP
(BUNDLE 1,3,5,7 100MM ABOVE UCSP)

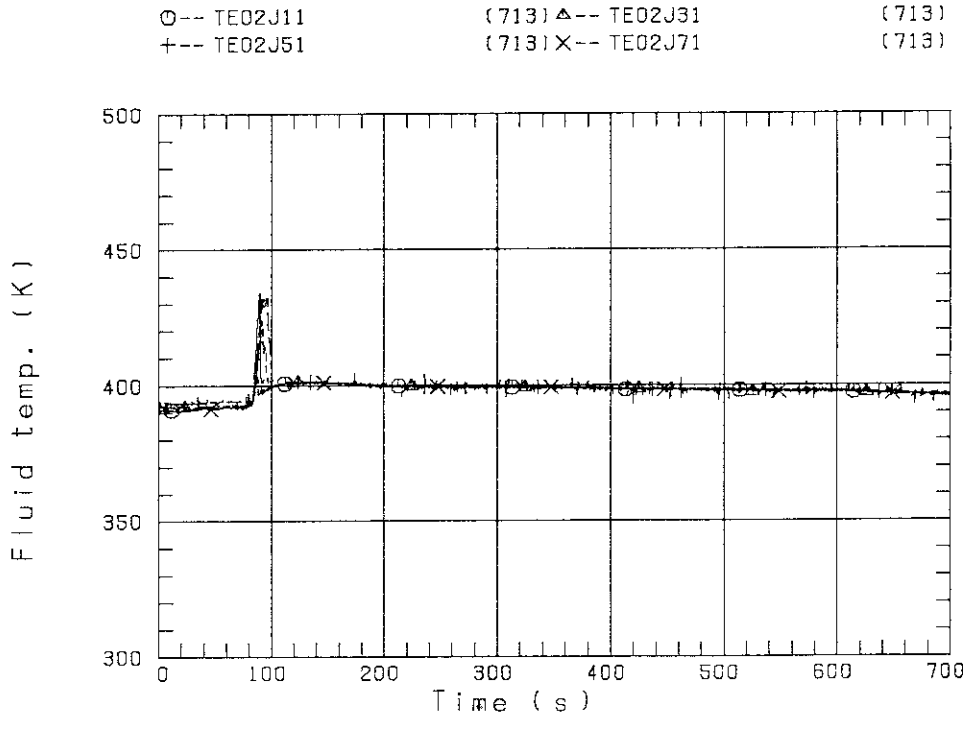

FIG. B-20 FLUID TEMPERATURE ABOVE UCSP
(BUNDLE 1,3,5,7 250MM ABOVE UCSP)

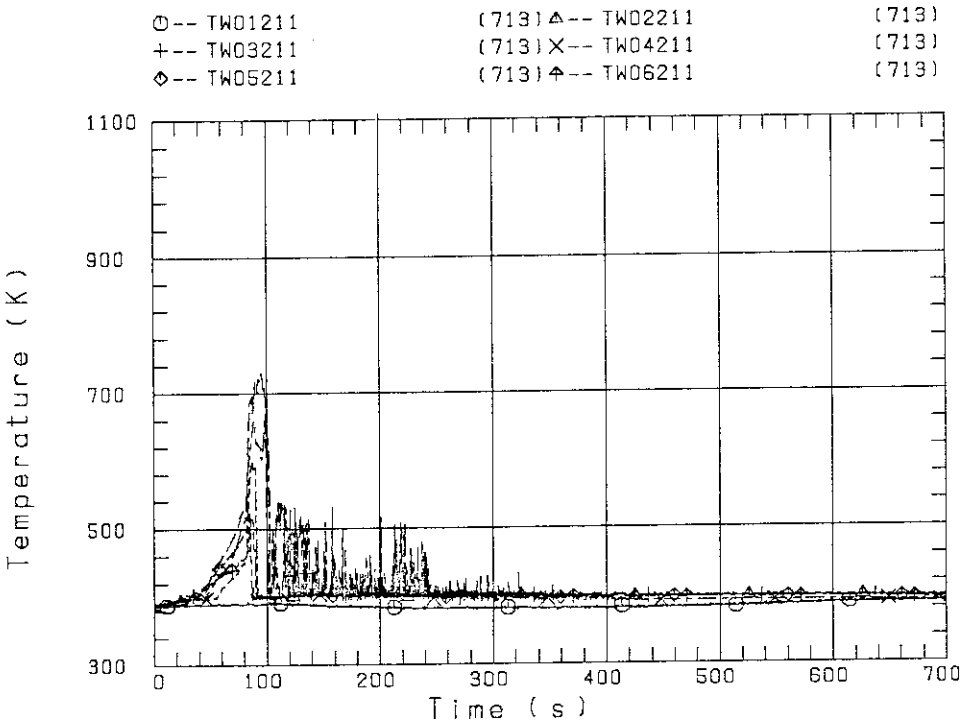

FIG. B-21 TEMPERATURE FOR SPUTTERING DETECTION
BUNDLE 2 , REGION 1 , TYPE 3

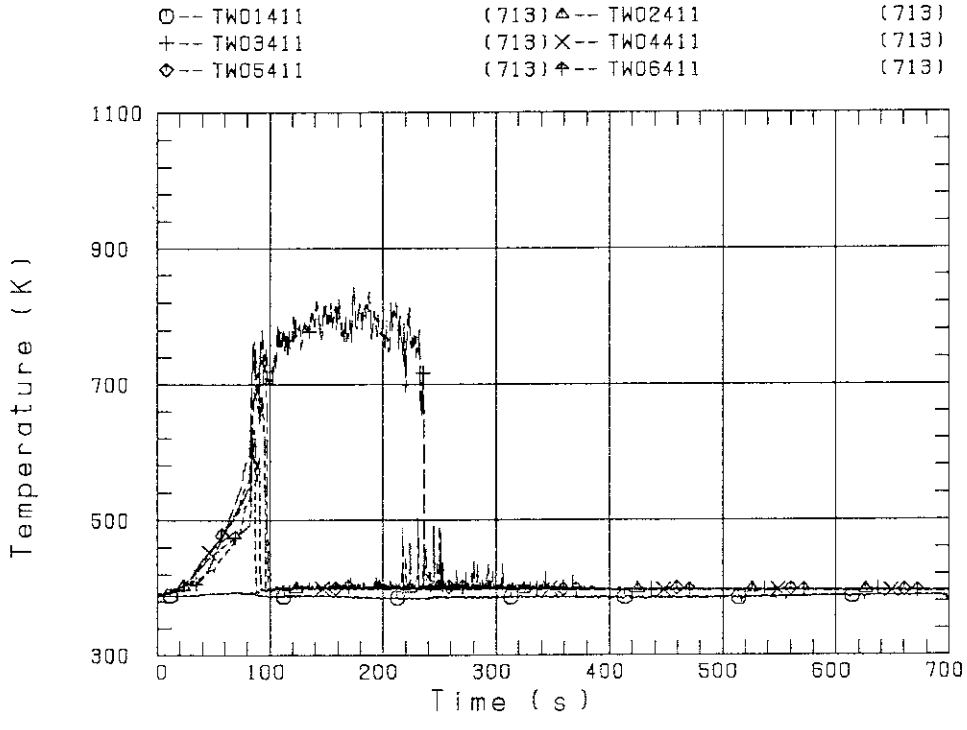

FIG. B-22 TEMPERATURE FOR SPUTTERING DETECTION
BUNDLE 4 , REGION 1 , TYPE 3

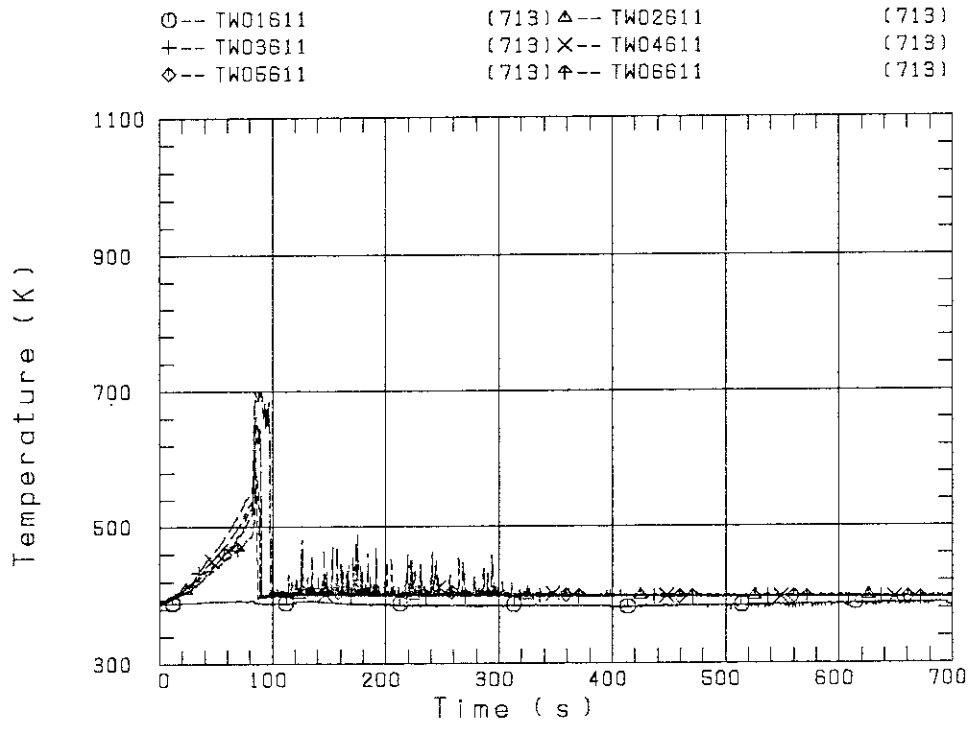

FIG. B-23 TEMPERATURE FOR SPUTTERING DETECTION
BUNDLE 6 , REGION 1 , TYPE 3

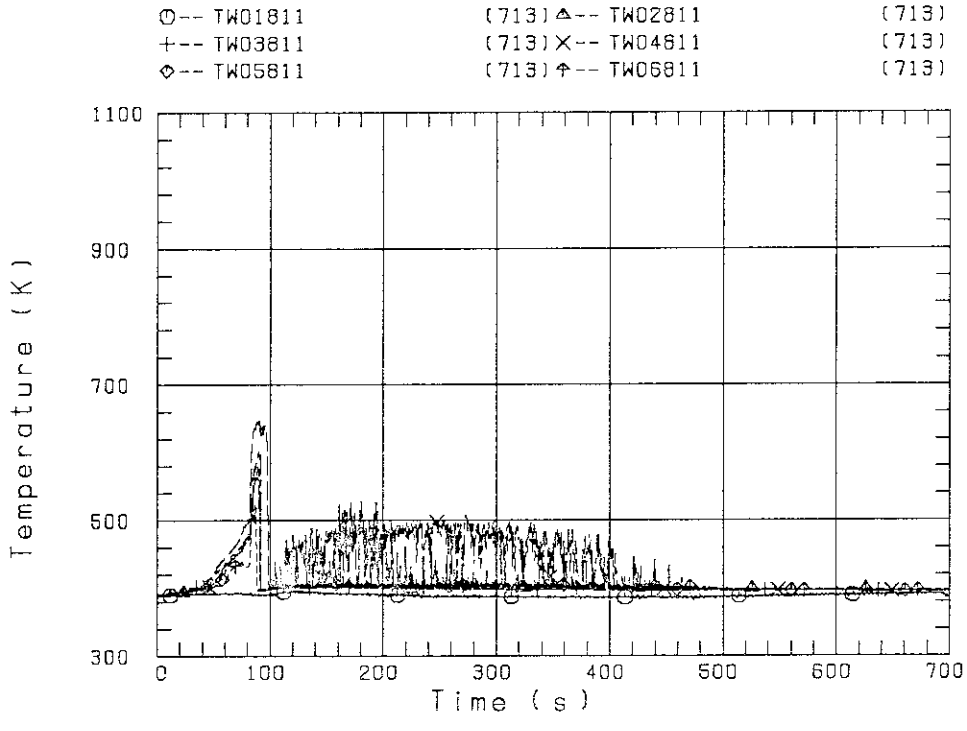

FIG. B-24 TEMPERATURE FOR SPUTTERING DETECTION
BUNDLE 8 , REGION 1 , TYPE 3

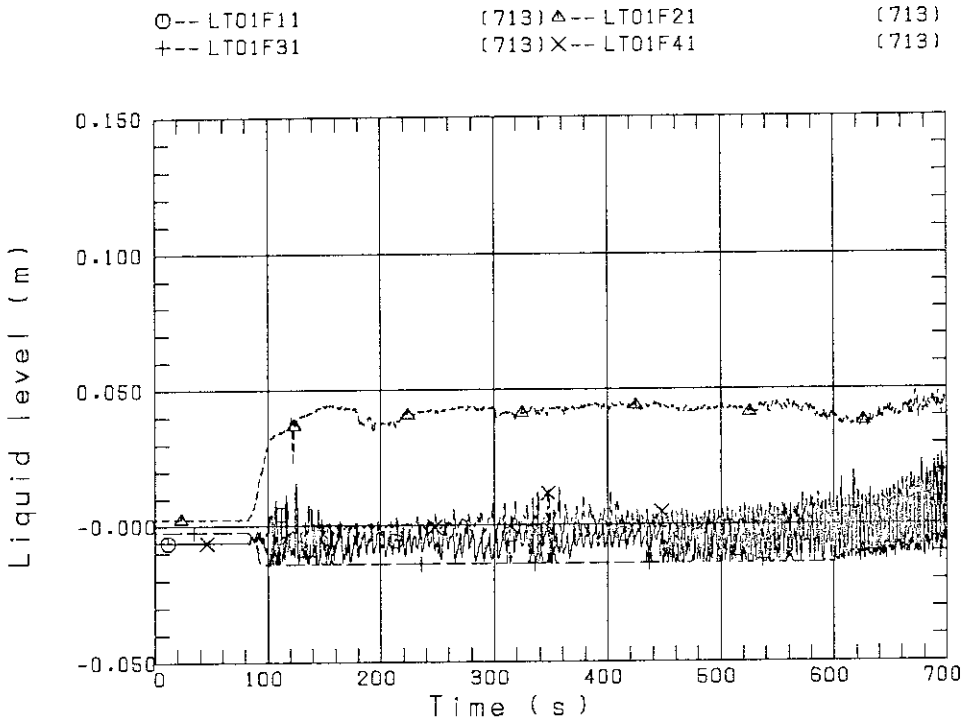

FIG. B-25 LIQUID LEVEL ABOVE END BOX TIE PLATE
(BUNDLE 1,2,3,4)

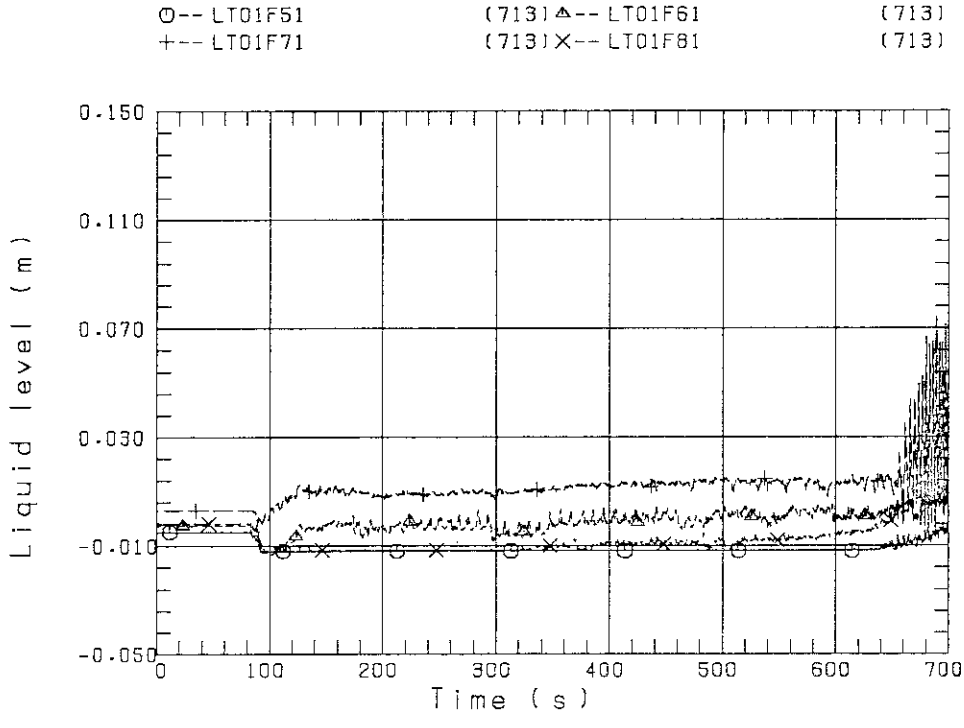

FIG. B-26 LIQUID LEVEL ABOVE END BOX TIE PLATE
(BUNDLE 5,6,7,8)

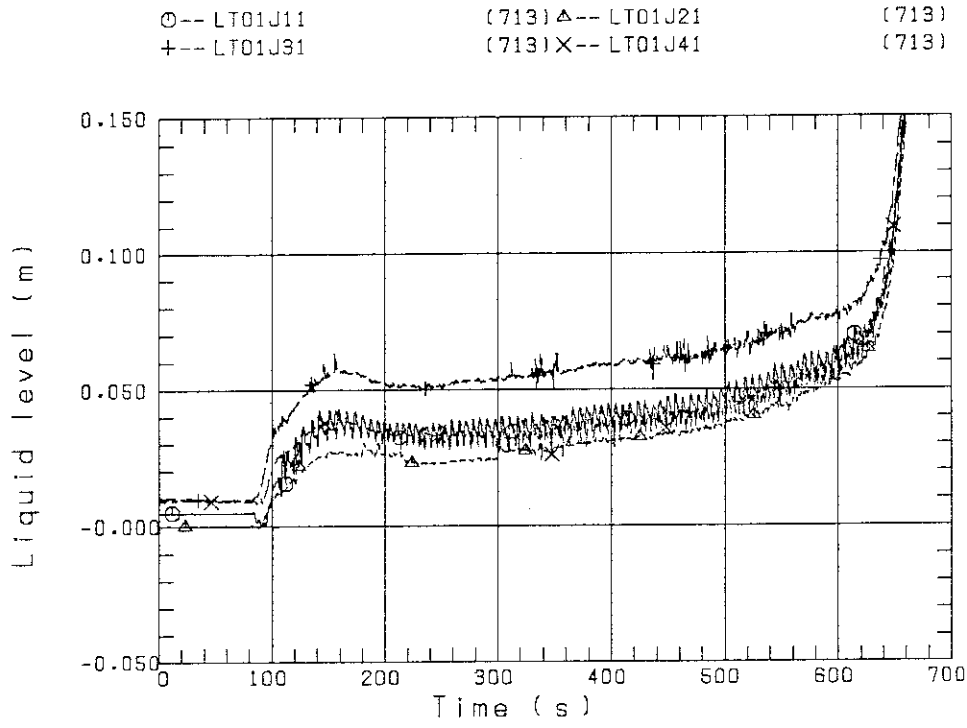

FIG. B-27 LIQUID LEVEL ABOVE UCSP
(BUNDLE 1,2,3,4)

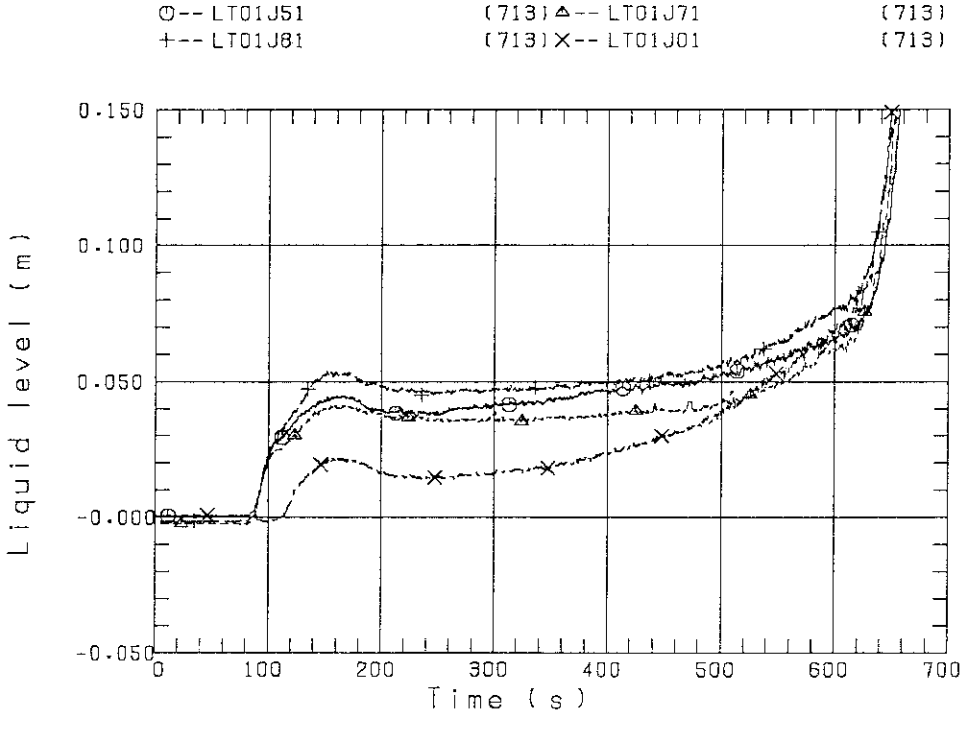

FIG. B-28 LIQUID LEVEL ABOVE UCSP
(BUNDLE 5,6,7,8 AND CORE BUFFLE)

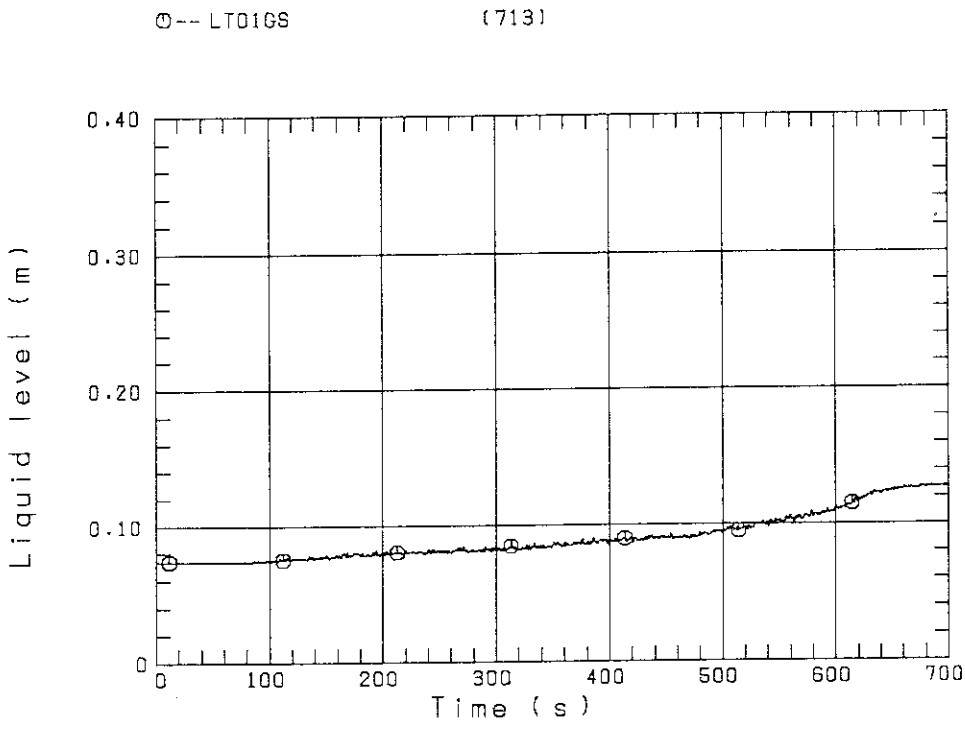

FIG. B-29 LIQUID LEVEL IN STEAM/WATER SEPARATOR

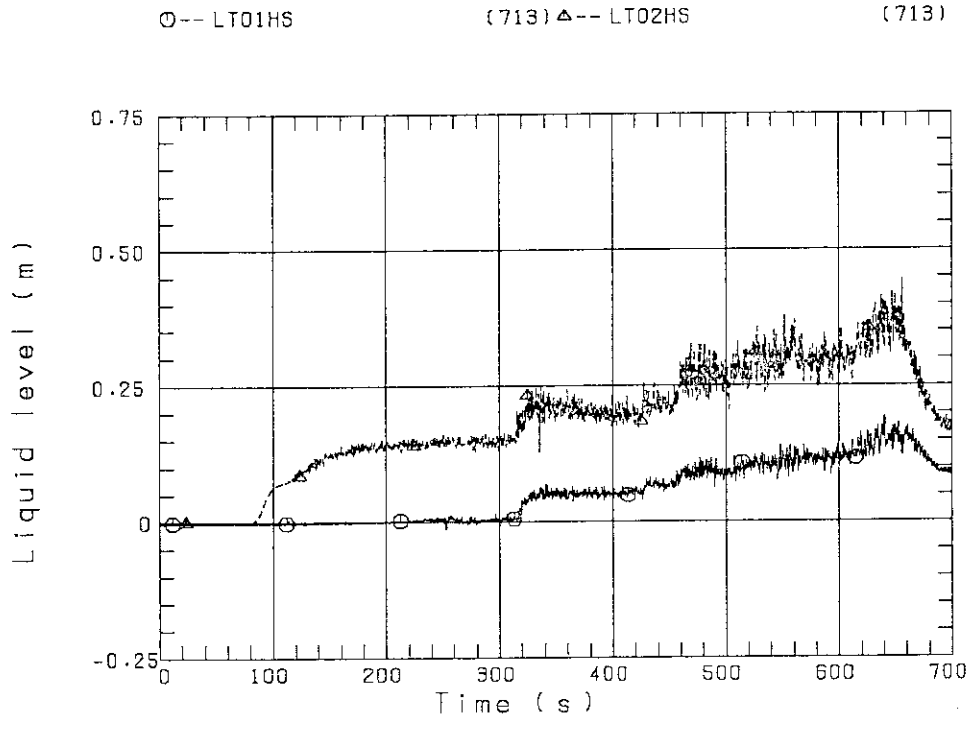

FIG. B-30 LIQUID LEVEL IN HOT LEG
(01HS - PV SIDE, 02HS - STEAM/WATER SEPARATOR SIDE)

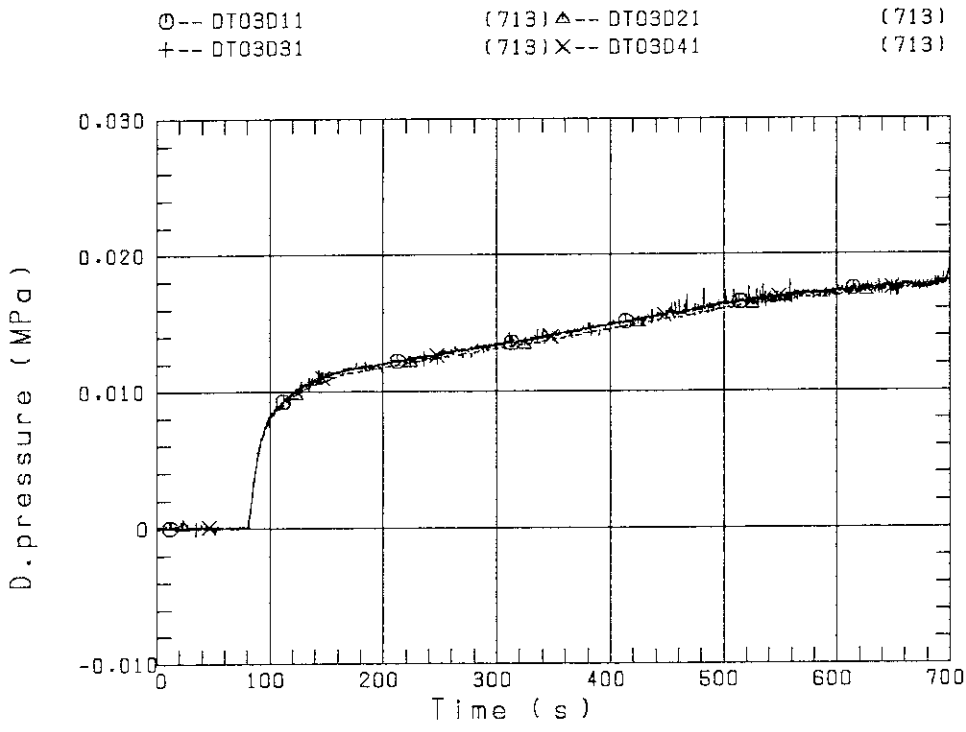

FIG. B-31 DIFFERENTIAL PRESSURE OF CORE FULL HIGHT (BUNDLE 1,2,3,4)

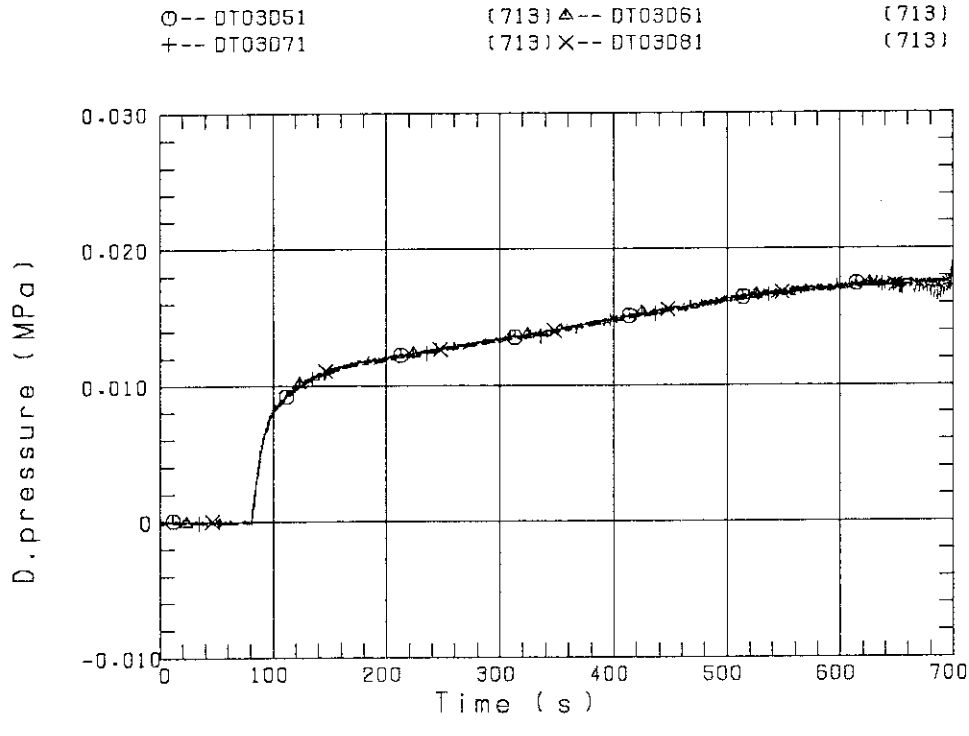

FIG. B-32 DIFFERENTIAL PRESSURE OF CORE FULL HIGHT (BUNDLE 5,6,7,8)

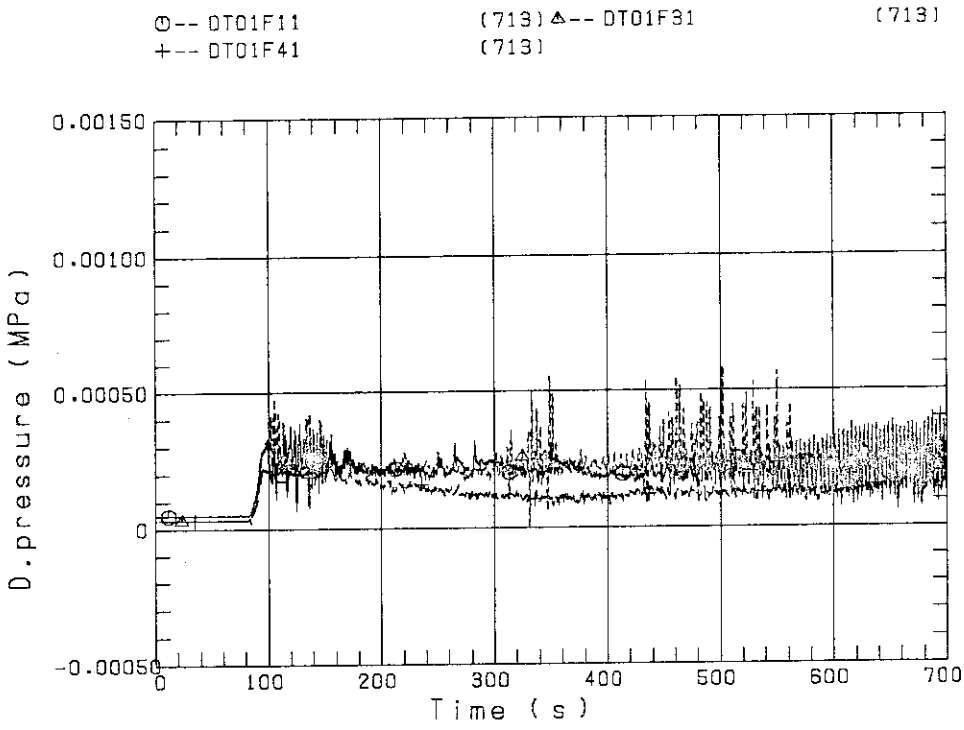

FIG. B-33 DIFFERENTIAL PRESSURE ACROSS END BOX TIE PLATE (BUNDLE 1,3,4)

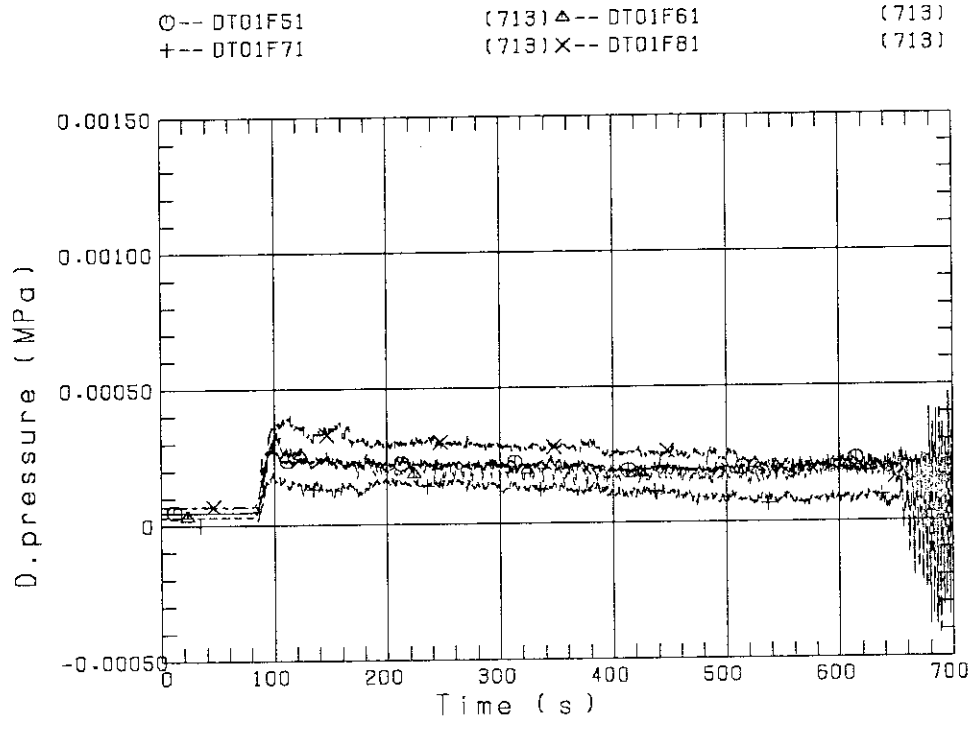

FIG. B-34 DIFFERENTIAL PRESSURE ACROSS END BOX TIE PLATE (BUNDLE 5,6,7,8)

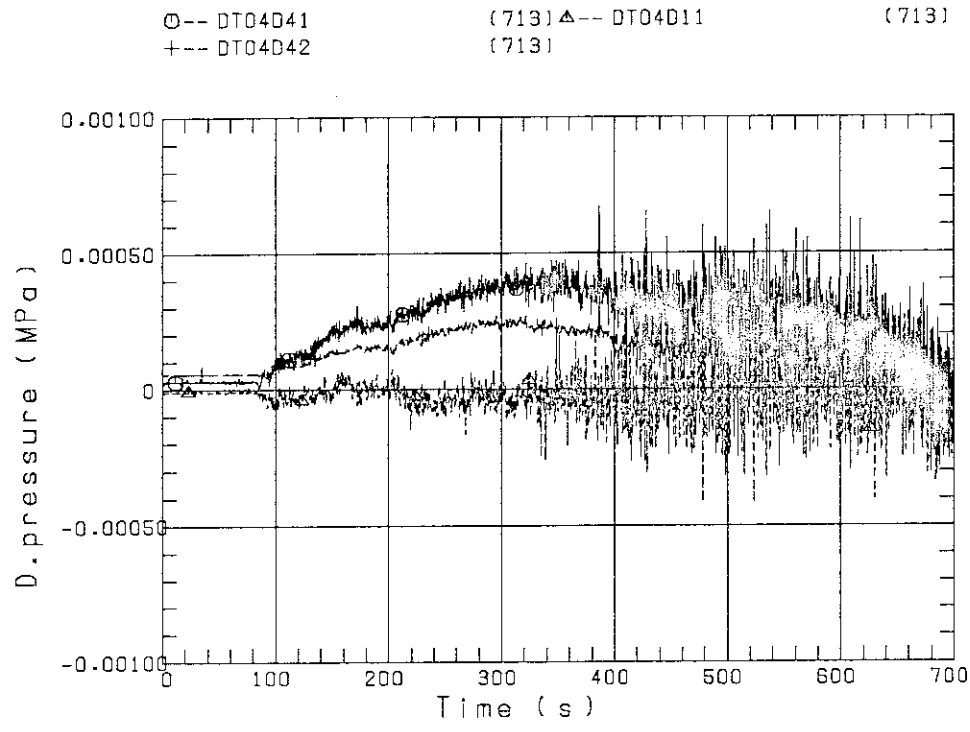

FIG. B-35 DIFFERENTIAL PRESSURE , HORIZONTAL AT 1905 MM
(11-BUNDLE 1-4, 41-BUNDLE 4-8, 42-BUNDLE 4-6)

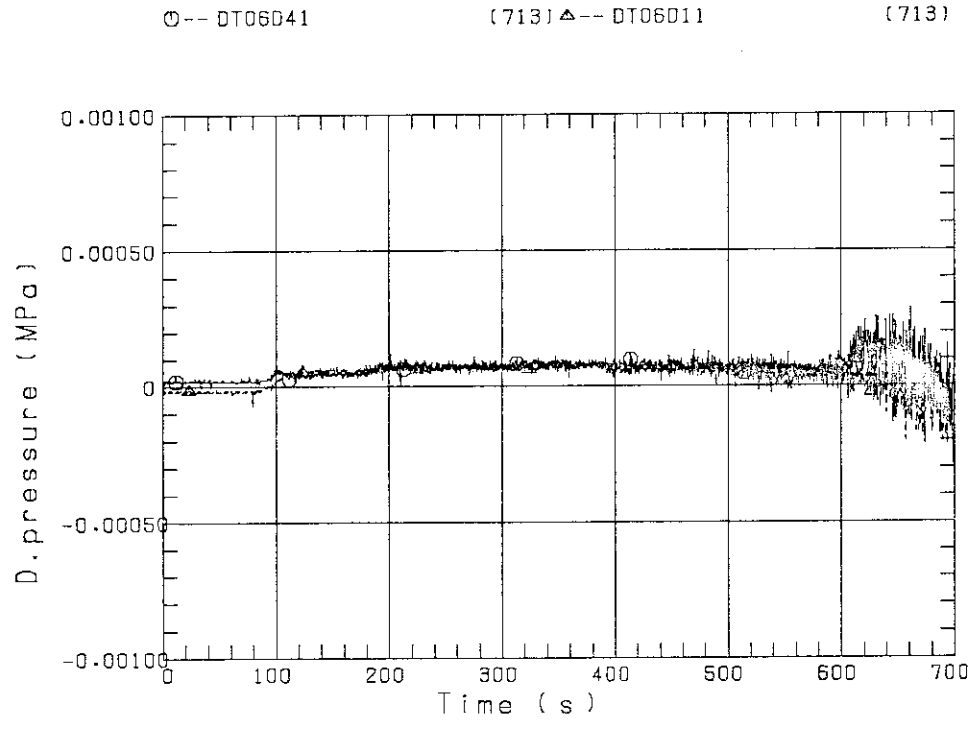

FIG. B-36 DIFFERENTIAL PRESSURE , HORIZONTAL AT 3235 MM
(11-BUNDLE 1-4, 41-BUNDLE 4-8)

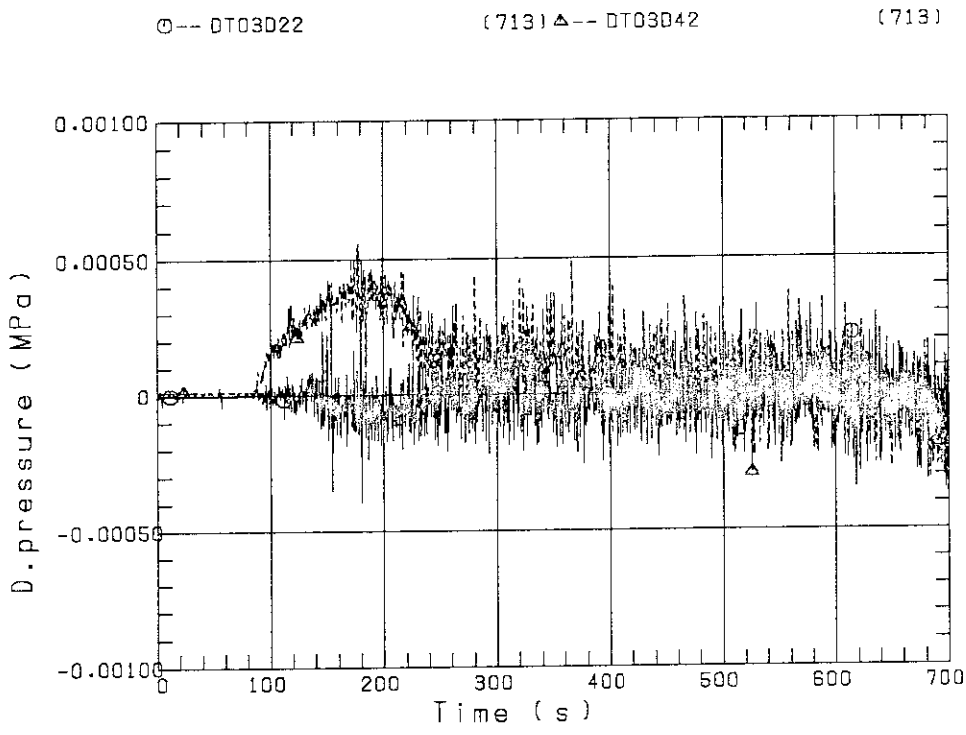

FIG. B-37 DIFFERENTIAL PRESSURE, HORIZONTAL AT 1365 MM (22-BUNDLE 2-4, 42-BUNDLE 4-8)

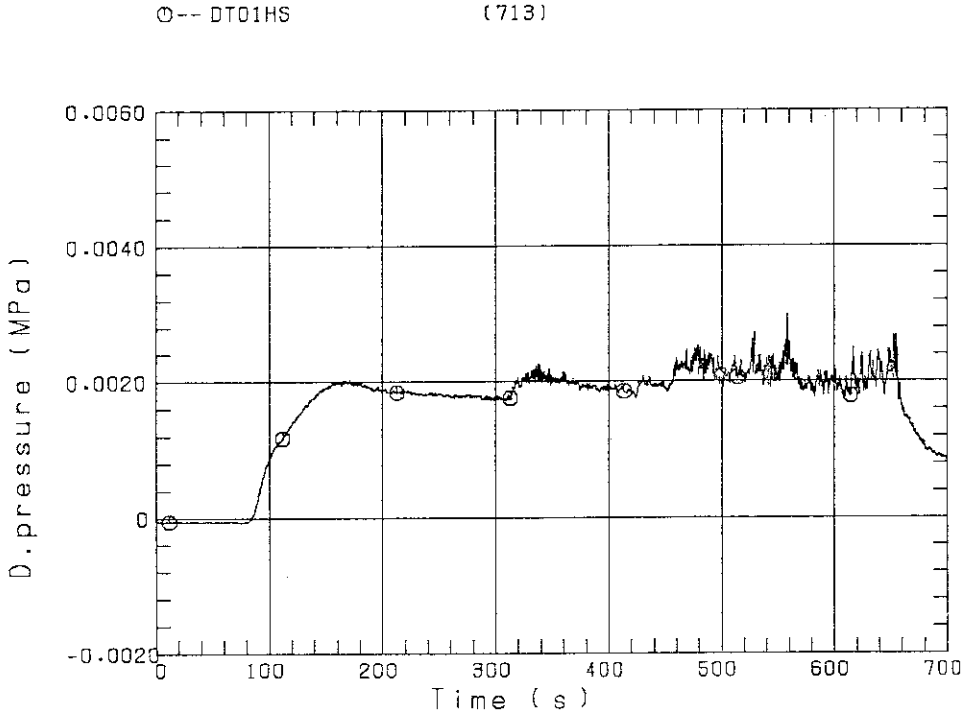

FIG. B-38 DIFFERENTIAL PRESSURE OF HOT LEG HOT LEG INLET - STEAM/WATER SEPARATOR INLET

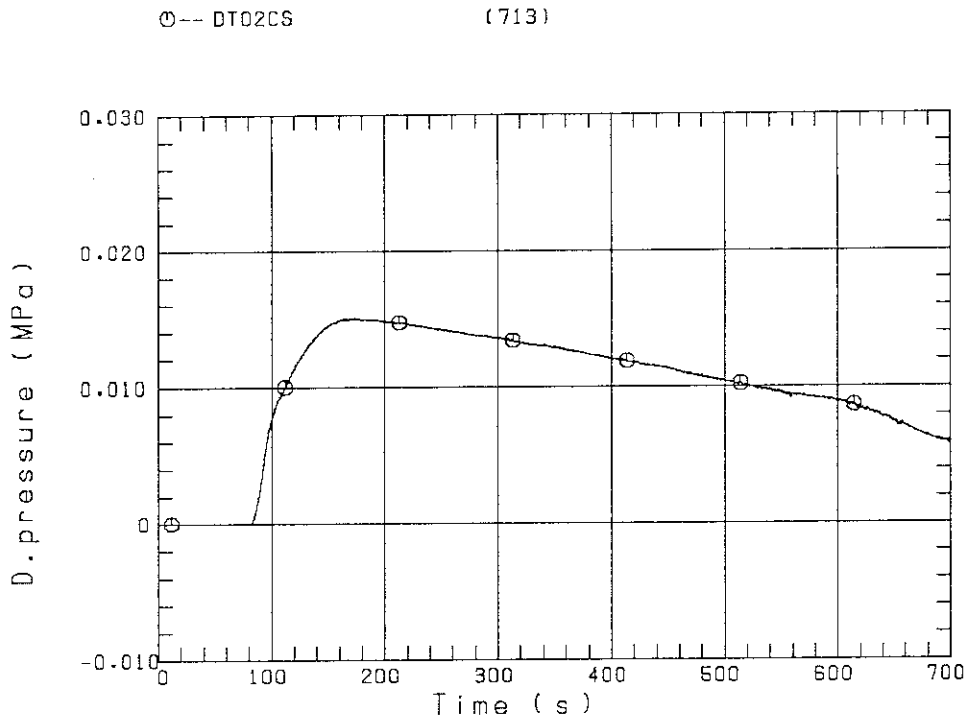

FIG. B-39 DIFFERENTIAL PRESSURE OF INTACT COLD LEG

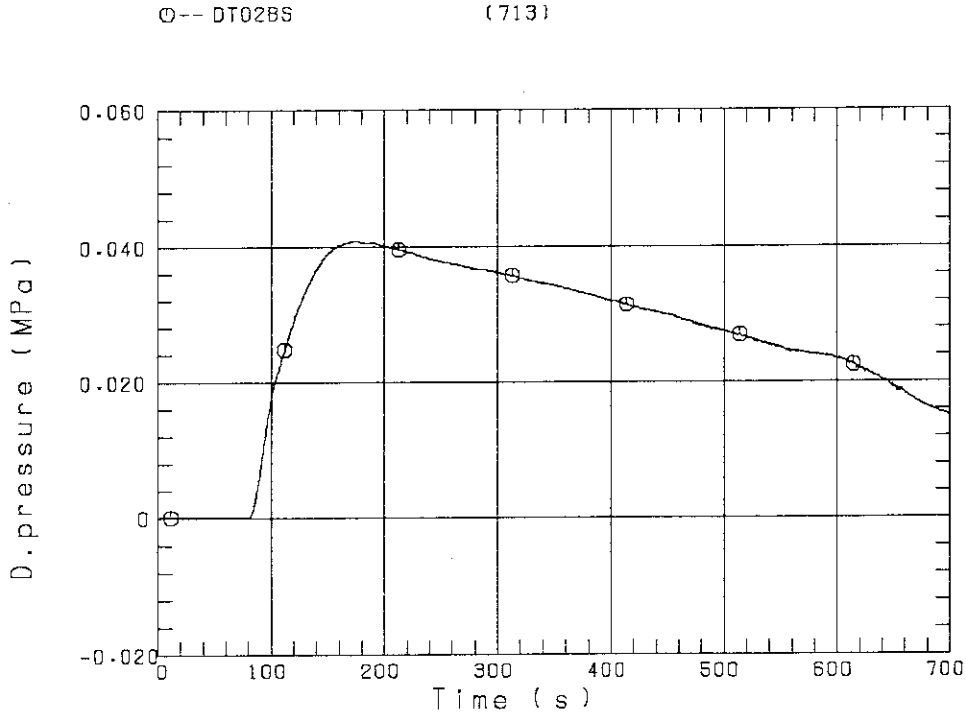

FIG. B-40 DIFFERENTIAL PRESSURE, STEAM/WATER SEPARATOR - CONTAINMENT TANK-II

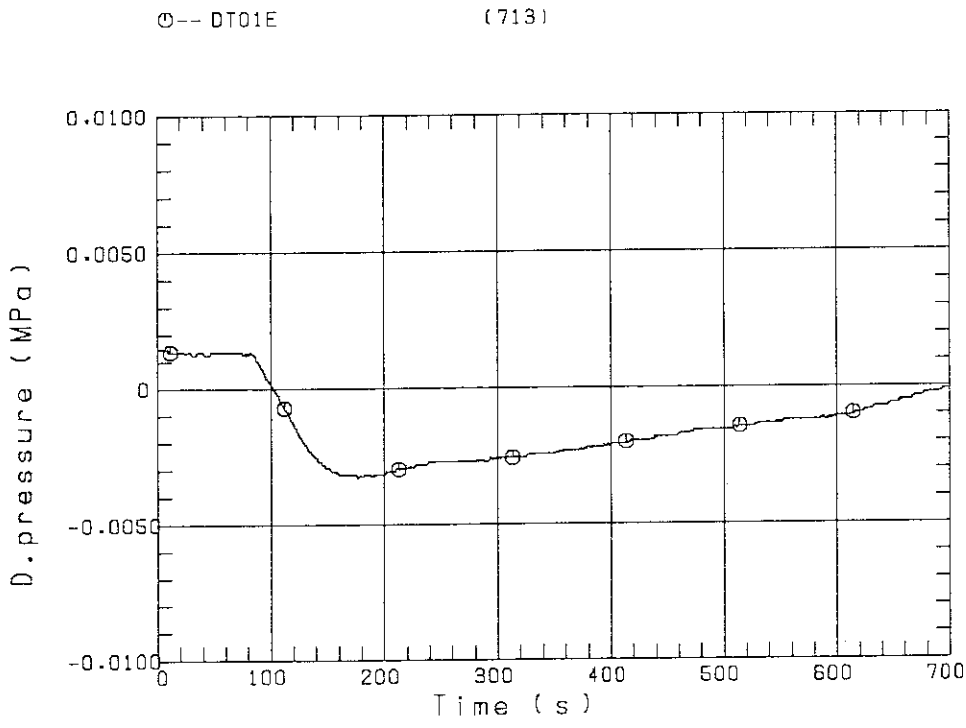

FIG. B-41 DIFFERENTIAL PRESSURE, CONTAINMENT TANK-II - CONTAINMENT TANK-I

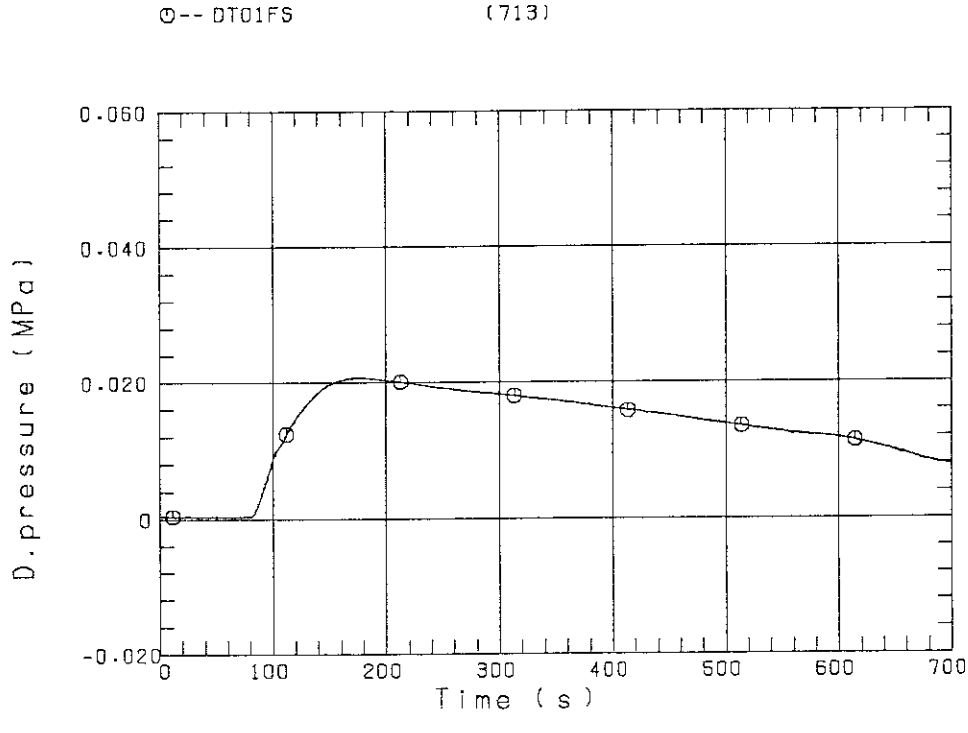

FIG. B-42 DIFFERENTIAL PRESSURE OF BROKEN COLD LEG - PV SIDE, DOWNCOMER - CONTAINMENT TANK-I

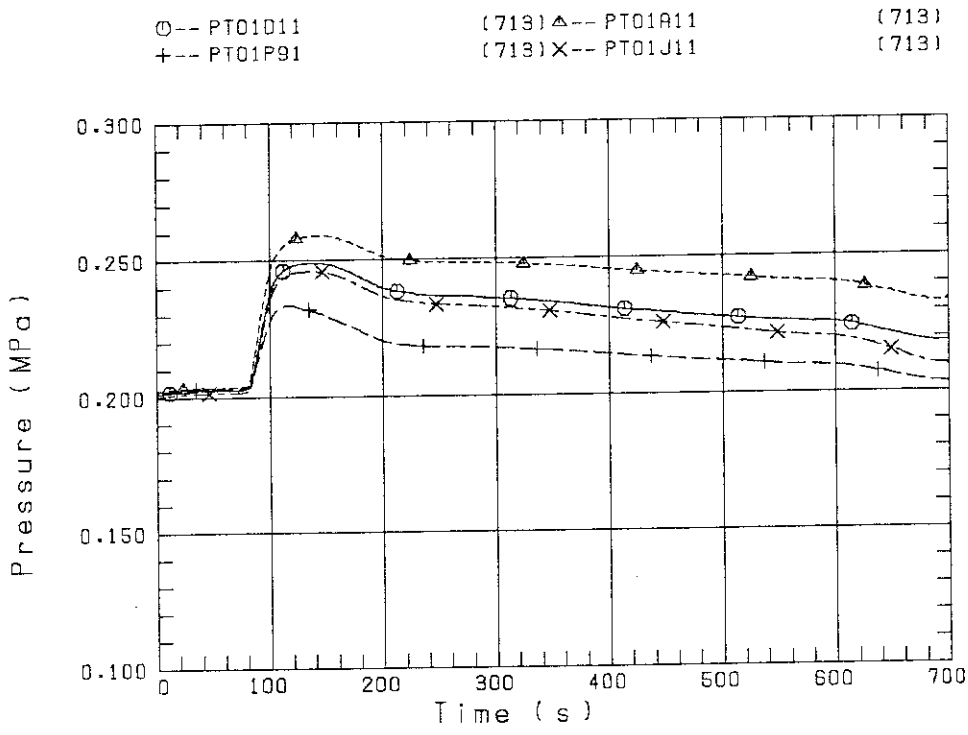

FIG. B-43 PRESSURE IN PV (J - TOP OF PV, D - CORE CENTER, A - CORE INLET, P - BELOW COLD LEG NOZZLE IN DOWNCOMER)

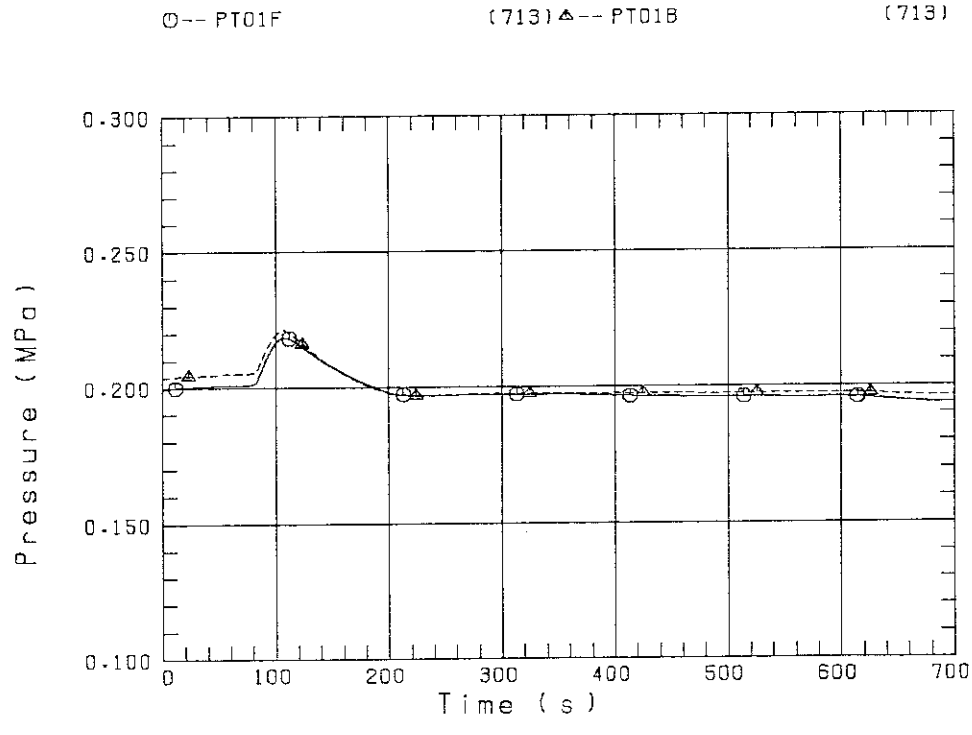

FIG. B-44 PRESSURE AT TOP OF CONTAINMENT TANK-I AND CONTAINMENT TANK-II (F-CONTAINMENT TANK-I, B-CONTAINMENT TANK-II)

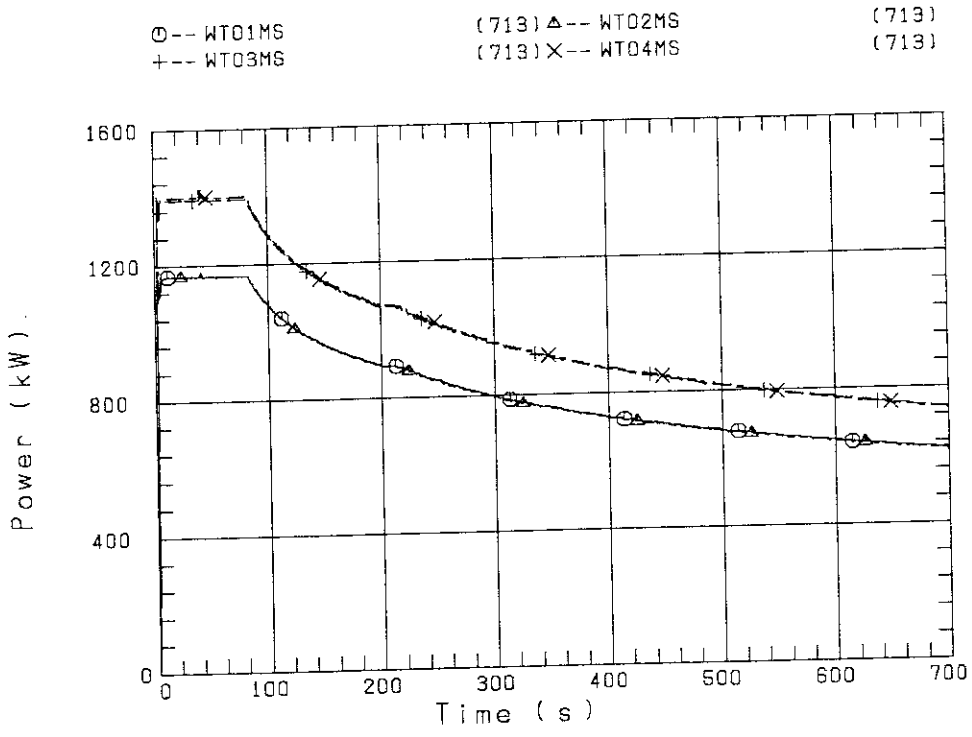

FIG. B-45 BUNDLE POWER
(BUNDLE 1,2,3,4)

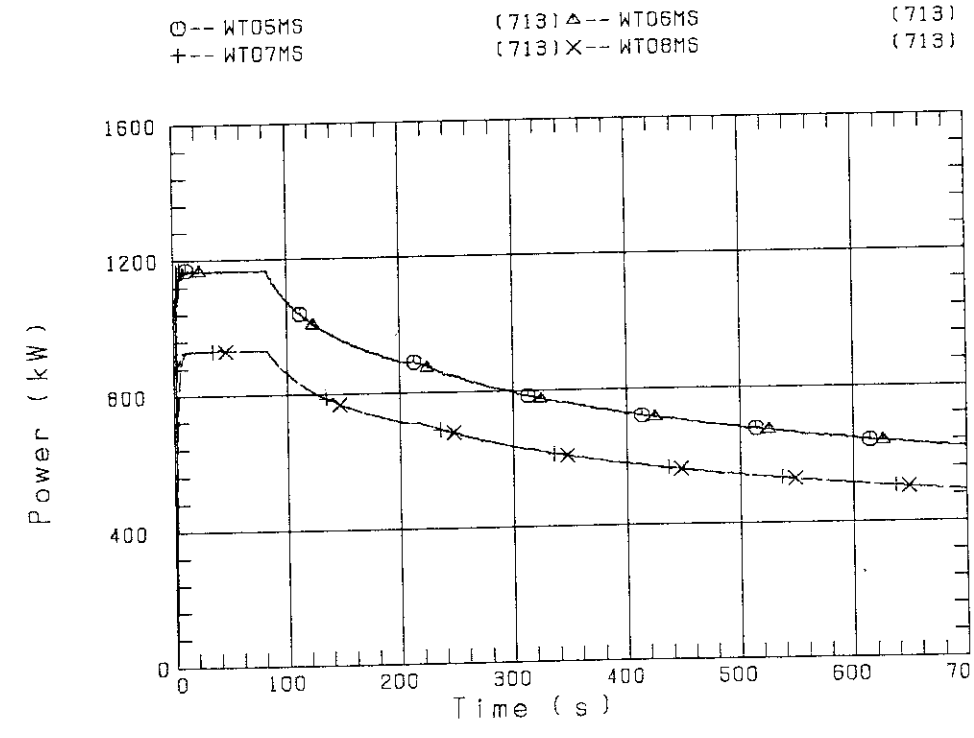

FIG. B-46 BUNDLE POWER
(BUNDLE 5,6,7,8)

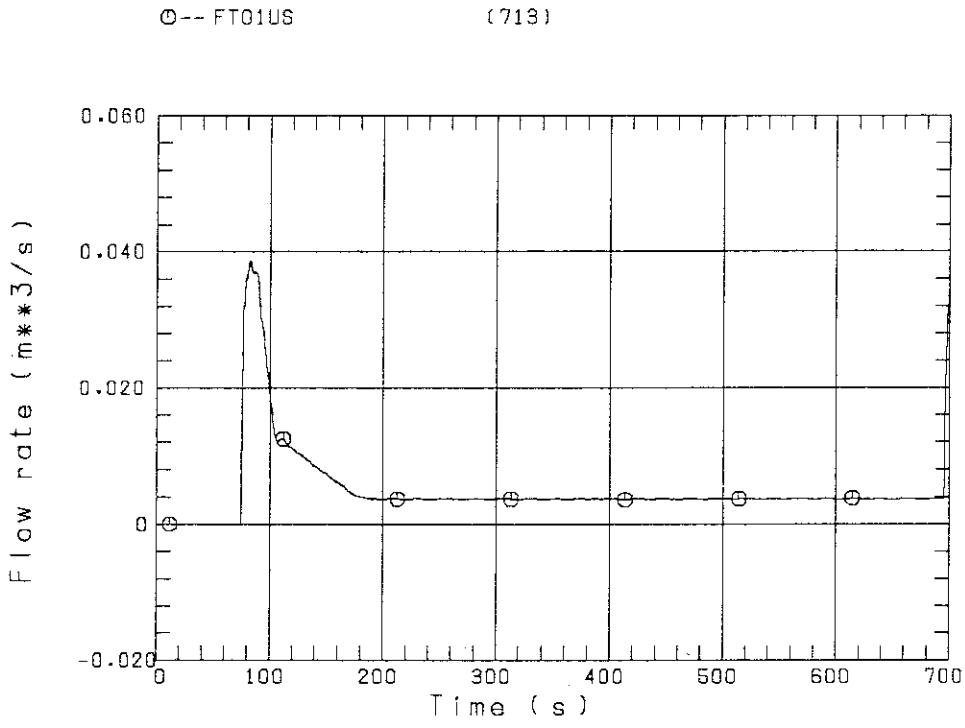

FIG. B-47 FLOW RATE OF LOWER PLENUM INJECTION WATER (ACC HEADER LINE)

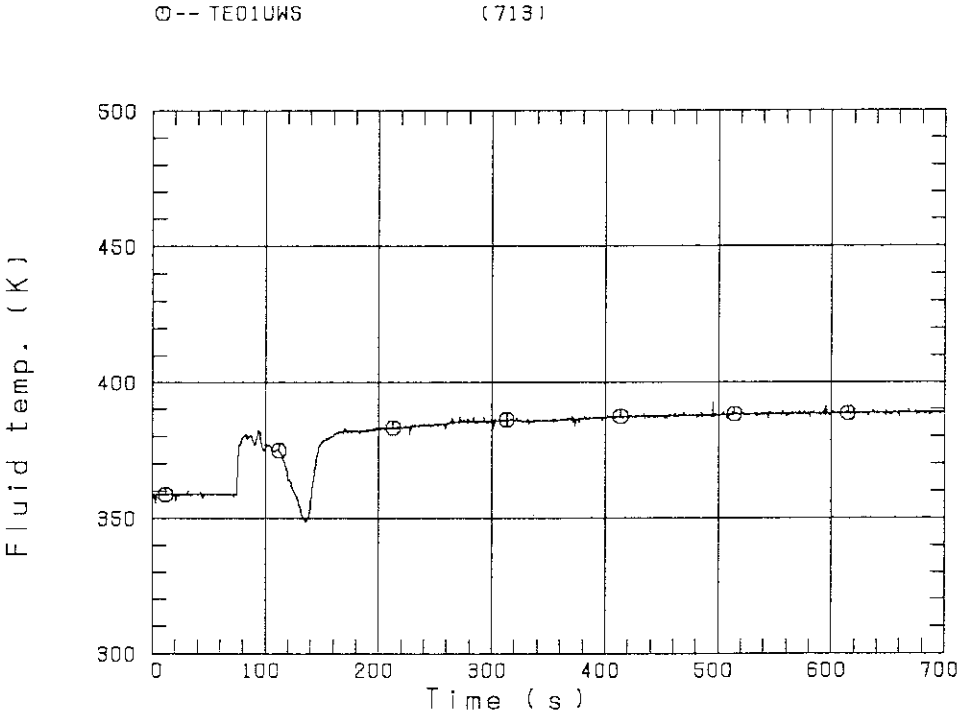

FIG. B-48 FLUID TEMPERATURE IN LOWER PLENUM INJECTION LINE (ACC HEADER LINE)